

# Decentralized CACC controllers for platoons of heterogeneous ve- hicles with uncertain dynamics

Paweł Krzesiński

Master of Science Thesis



# **Decentralized CACC controllers for platoons of heterogeneous vehicles with uncertain dynamics**

MASTER OF SCIENCE THESIS

For the degree of Master of Science in Systems and Control at Delft  
University of Technology

Paweł Krzesiński

7 November 2017

Faculty of Mechanical, Maritime and Materials Engineering (3mE) · Delft University of  
Technology



Copyright © Delft Center for Systems and Control (DCSC)  
All rights reserved.



---

# Abstract

The capacity of public roads has become a serious problem all over the world. The traffic is constantly increasing, while the capacity remains almost the same. This causes traffic jams and road accidents. An effective way to increase the road throughput employs vehicular platoons, which allow to decrease inter-vehicle distances without compromising road safety.

The urgent necessity to increase road capacity has led to the substantial interest in Cooperative Adaptive Cruise Control (CACC), which uses measurements of on-board sensors and inter-vehicle communication to provide safe platooning. Numerous theoretical works and extensive experiments have proved that the possibility to exchange certain parameters via wireless communication allows for a significant decrease of the inter-vehicle distance.

Cooperative Adaptive Cruise Control systems should comply with several requirements. One of the requirements is so-called string stability, which prevents amplification of disturbances, propagating along the string of vehicles. To simplify the design of CACC, vehicles in a platoon are often assumed to have identical and fully known dynamics. These assumptions in practice are too restrictive. The heterogeneity of vehicles increases the complexity of CACC controller design problem.

In this master thesis a decentralized CACC algorithm is implemented based on continuous sliding-mode control and adaptation laws, which estimate uncertain vehicle's parameters. Evaluation of Cooperative Adaptive Cruise Control algorithm has been conducted on a vehicle simulator DYNACAR.



---

# Contents

<b>Acknowledgements</b>	<b>ix</b>
<b>1 Introduction</b>	<b>1</b>
1-1 Advanced Driver Assistance Systems . . . . .	1
1-2 Vehicle longitudinal control systems . . . . .	2
1-2-1 Cruise Control . . . . .	2
1-2-2 Adaptive Cruise Control . . . . .	3
1-2-3 Cooperative Adaptive Cruise Control . . . . .	3
1-3 Aims and Objectives . . . . .	6
1-4 Contribution of Thesis . . . . .	6
1-5 Outline . . . . .	7
<b>2 Cooperative Adaptive Cruise Control - Requirements and Problem Setup</b>	<b>9</b>
2-1 Platoon Heterogeneity . . . . .	9
2-1-1 Model Uncertainties and Parameters Range . . . . .	9
2-2 Spacing Policy . . . . .	9
2-3 String Stability . . . . .	10
2-4 Communication Structures . . . . .	11
2-5 Node Dynamics - Simplified Longitudinal Vehicle Model . . . . .	12
2-6 Performance Specification . . . . .	13
2-7 Problem Formulation . . . . .	14
<b>3 Cooperative Adaptive Cruise Control - Design</b>	<b>15</b>
3-1 Platoon Control Law . . . . .	15
3-1-1 Adaptive Bidirectional Coupled Sliding Mode Control . . . . .	15
3-1-2 Continuous Controller Design . . . . .	17

---

<b>4</b>	<b>Cooperative Adaptive Cruise Control - Experimental Setup and Evaluation</b>	<b>23</b>
4-1	Practical Constraints . . . . .	23
4-2	Vehicle Simulator . . . . .	24
4-3	Dynacar - Vehicle Model . . . . .	25
4-4	Evaluation of Designed Controller . . . . .	26
4-5	Heterogeneous Platoon . . . . .	26
4-6	Simulation Results . . . . .	27
4-6-1	Traffic Scenario Design . . . . .	27
4-6-2	Heterogeneous Platoon Simulation . . . . .	29
4-6-3	Heterogeneous Platoon Simulation with Disturbances . . . . .	38
4-6-4	Heterogeneous Platoon Simulations with Delays . . . . .	43
4-6-5	Simulation Results - Conclusion . . . . .	55
<b>5</b>	<b>Conclusions and Future Works</b>	<b>57</b>
5-1	Conclusions . . . . .	57
5-2	Future Works . . . . .	58
<b>6</b>	<b>Appendix A</b>	<b>59</b>
6-1	Matlab Code . . . . .	59
<b>7</b>	<b>Appendix B</b>	<b>65</b>
7-1	Simulink Overview . . . . .	65
<b>8</b>	<b>Appendix C</b>	<b>71</b>
8-1	Longitudinal Forces . . . . .	71
8-2	Aerodynamic Drag Force . . . . .	72
8-3	Suspension Model . . . . .	72
8-4	Tire Model . . . . .	73
	<b>Bibliography</b>	<b>77</b>

---

# List of Figures

1-1	General hierarchical control structure . . . . .	3
1-2	Aerodynamics drag forces reduction for different inter-vehicle distances [1] . . . . .	4
1-3	Highway capacity for different CACC market penetration . . . . .	6
2-1	Schematic overview of a vehicular platoon, [2] . . . . .	10
2-2	Information flow topologies [3]. a) "everybody knows everything", b) designated platoon leader, c) bidirectional, d) N- vehicles look-ahead, e) directly preceding vehicle, f) mini-platoons with designated platoon leader. Blue arrows indicate wireless communication, while radars or other ranging sensor are denoted with black arrows. . . . .	12
2-3	ISO 22179:2009 deceleration and acceleration standards for FSRA (X is velocity [m/s] and Y is acceleration [ $m/s^2$ ]), [4] . . . . .	14
3-1	Constant spacing policy . . . . .	16
3-2	Comparison of applied wheel torque for continuous control law and discontinuous control law . . . . .	18
3-3	Stable LTI system . . . . .	22
4-1	Schematic overview of connections . . . . .	24
4-2	Wheel dynamics . . . . .	24
4-3	Bidirectional control structure . . . . .	25
4-4	Overview of Dynacar's vehicle model, [5] . . . . .	26
4-5	Scenario 1 - Normal highway scenario . . . . .	27
4-6	Scenario 2 - Stop and Go scenario . . . . .	28
4-7	Scenario 3 - Emergency braking scenario . . . . .	29
4-8	Joining the platoon scenario . . . . .	29
4-9	Scenario 1 - distance error and relative velocity . . . . .	31
4-10	Scenario 1 - vehicles velocity, acceleration and wheel torque . . . . .	32

4-11 Scenario 2 - distance error and relative velocity . . . . .	33
4-12 Scenario 2 - vehicles velocity, acceleration and wheel torque . . . . .	35
4-13 Scenario 3 - distance error and relative velocity . . . . .	36
4-14 Scenario 3 - vehicles velocity, acceleration and wheel torque . . . . .	37
4-15 Join scenario - relative distance and relative velocity . . . . .	39
4-16 Join scenario - vehicles velocity, acceleration and wheel torque . . . . .	40
4-17 Disturbance (light breeze) - relative distance and relative velocity . . . . .	41
4-18 Disturbance (light breeze) - vehicles velocity, acceleration and wheel torque . . . . .	42
4-19 Disturbance (moderate breeze) - relative distance and relative velocity . . . . .	44
4-20 Disturbance (moderate breeze) - vehicles velocity, acceleration and wheel torque . . . . .	45
4-21 Disturbance (strong wind) - relative distance and relative velocity . . . . .	46
4-22 Disturbance (strong wind) - vehicles velocity, acceleration and wheel torque . . . . .	47
4-23 Delay (radar - 0.1 s, wireless - 0.15 s) - relative distance and relative velocity . . . . .	48
4-24 Delay (radar - 0.1s, wireless - 0.15s) - vehicles velocity, acceleration and wheel torque . . . . .	50
4-25 Delay (radar - 0.1s, wireless - 0.3s) - relative distance and relative velocity . . . . .	51
4-26 Delay (radar - 0.1s, wireless - 0.3s) - vehicles velocity, acceleration and wheel torque . . . . .	52
4-27 Delay (radar - 0.1s, wireless - 0.3s, "powertrain" - 0.2s) - relative distance and relative velocity . . . . .	53
4-28 Delay (radar - 0.1s, wireless - 0.3s, "powertrain" - 0.2s) - vehicles velocity, acceleration and wheel torque . . . . .	54
4-29 Decreasing relative distance error . . . . .	55
7-1 Simulink - vehicle platoon overview . . . . .	66
7-2 Simulink - vehicle platoon overview (zoomed) . . . . .	67
7-3 Simulink - vehicle platoon overview (zoomed) . . . . .	68
7-4 Simulink - vehicle platoon overview (zoomed) . . . . .	68
7-5 Simulink - Control and Torque blocks overview . . . . .	69
7-6 Simulink - torque applied to wheels block . . . . .	69
7-7 Simulink - brake torque applied to wheels block . . . . .	70
7-8 Simulink - control block overview . . . . .	70
8-1 Forces acting on a vehicle, [6] . . . . .	71
8-2 Suspension models: a) bicycle model, b) "roll stiffness", c) multi-body, [7] . . . . .	73
8-3 Multi-body suspension design, [5] . . . . .	73
8-4 Tire-road forces, [8] . . . . .	74
8-5 Inputs and outputs of the Magic Formula tire model, [7] . . . . .	75

---

# List of Tables

1-1	Advanced Driver Assistance Systems - Benefits, [1]	2
1-2	Time gap distribution for the ACC	5
1-3	Time gap distribution for the CACC	5
2-1	Range of parameters for a passenger car, [9]	10
4-1	Platoon heterogeneity - uncertain parameters	27
4-2	Scenario 1 - MRV	30
4-3	Scenario 2 - MRV	34
4-4	Scenario 3 - MRV	34
4-5	Wind scenarios	38
4-6	Light wind scenario - MRV	38
4-7	Moderate wind scenario - MRV	43
4-8	High wind scenario - MRV	43
4-9	Radar (0.1 s) and wireless (0.15 s) delay scenario - MRV	49
4-10	Radar (0.1 s) and wireless (0.3 s) delay scenario - MRV	49
4-11	Radar (0.1 s), wireless (0.15 s) and "powertrain" (0.2 s) delay scenario - MRV	49



---

# Acknowledgements

I would like to express my gratitude to my supervisors dr. Anton Proskurnikov and dr. ir. Manuel Mazo Jr. for the meaningful comments, remarks and guidance through the process of writing this master thesis. Furthermore, I would like to extend my gratitude to dr. Barys Shyrokau for support and remarks on my master thesis.

Finally, I would like to express my deepest gratitude to my family and my beloved girlfriend for constant, unconditional support and having faith in me.

Delft, University of Technology  
7 November 2017

Paweł Krzesiński

The research was supported by NWO Domain TTW, The Netherlands, under the project TTW#13712 "From Individual Automated Vehicles to Cooperative Traffic Management - predicting the benefits of automated driving through on-road human behavior assessment and traffic flow models" (IAVTRM).

Master of Science Thesis

Paweł Krzesiński



“In theory, theory and practice are the same. In practice, they are not.”

— *Albert Einstein*



---

# Chapter 1

---

## Introduction

For the last decades a great deal of vehicle control systems have been created by automotive companies and scientific institutes. The invented systems, such as the ABS, ESP or ACC are intended to increase car safety and comfort of its driver and the occupants. The rapid development of computers, sensors and digital technologies has made it possible to create ADAS to enhance not only the car's safety, but also the safety of vulnerable road users, for instance pedestrians, and the occupants of other vehicles.

In this chapter an overview of ADAS is given, followed by an introduction to vehicle longitudinal control systems. The three generations of cruise control systems are described in the order of increasing complexity: the standard Cruise Control (CC), the Adaptive Cruise Control (ACC) and the most advanced Cooperative Adaptive Cruise Control (CACC) system.

### 1-1 Advanced Driver Assistance Systems

According to the Annual Accident Report 2016 compiled by European Road Safety Observatory [10], annually in European Union over one million road accidents take place (statistics for 2014), around 26000 of which are fatal. Data presented in [11] shows that about 90% of those accidents are caused by human errors rather than by vehicles' failures or weather conditions.

Advanced Driver Assistance Systems are primarily intended to improve road safety by providing warnings or even temporarily overriding a driver's input. However, it is equally important to provide a comfortable ride for the driver and the occupants. Systems such as the CC or ACC can increase the driver's comfort by relieving him/her from constant supervision of the vehicle's speed. In case of Adaptive Cruise Control, a driver is also supported in maintaining the right distance between its own and preceding vehicle. This function also positively influences safety on the road. It allows to reduce the driver's workload [1], and the driver can focus on the road situation, while functions such as throttle and distance adjusting are done by an on-board computer. This kind of a human-machine cooperation allows to react faster to various accidental events.

Advanced Driver Assistance Systems				
System	Collision avoid- ance	Comfort work- load	Travel effi- ciency	Fuel effi- ciency
<b>LONGITUDINAL</b>				
Autonomous Emergency Braking	++			
(Cooperative) Adaptive Cruise Control		+	+* <sup>a</sup>	+*
Speed warning/ assistance	+			
Eco Driving Support				+
<b>LATERAL</b>				
Lane Departure Warning	++	+		
Lane Keeping Assistance	++	+		
Automated Lane Keeping	++			
Traffic Jam Assist	+	+		
Blind Spot Warning	++			
Merging Assistance	++	+	+	
<b>Intersection Assist</b>	++	+		
<b>Park Assist</b>	+	++		

<sup>a</sup>\* especially for Cooperative Adaptive Cruise Control

**Table 1-1:** Advanced Driver Assistance Systems - Benefits, [1]

The control functionality of driver support systems can be divided into two groups: (i) longitudinal and (ii) lateral systems. In Table 1-1 other examples of the ADAS with its benefits in a few categories are presented.

In this work only longitudinal vehicle control (primarily, Cooperative Adaptive Cruise Control) systems are considered.

## 1-2 Vehicle longitudinal control systems

The longitudinal controllers play a central role in vehicle control, being responsible for the maintenance of the speed, acceleration and the distance between the consecutive cars on the lane. A control action in the longitudinal controllers is performed by actuation of either a throttle or a brake. We consider first Cruise Control and Adaptive Cruise Control.

### 1-2-1 Cruise Control

The Cruise Control system is one of the basic longitudinal controllers. Its goal is to maintain the speed preset by the driver by adjusting the throttle and the brake pedals' positions. The system does not require any ranging sensors, hence it does not react to the dangerous approach to the preceding vehicle. In such a dangerous situation, the driver is obliged to disengage the system by taking manual control over the brake pedal.

The control system architecture of cruise control consists of the upper-level and lower-level controllers [12]. The general hierarchical control structure is shown in Figure 1-1.

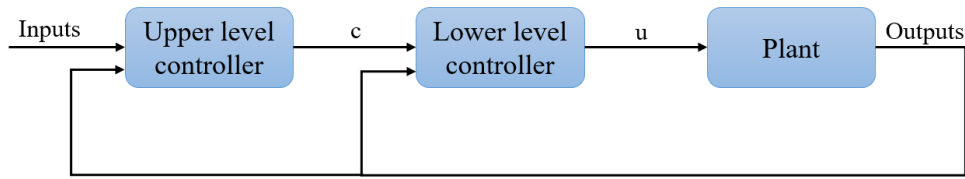


**Figure 1-1:** General hierarchical control structure

The upper level controller is responsible for determining a desired acceleration, denoted by 'c' in Figure 1-1, to achieve the speed preset by the driver. Then the lower level controller is used to control the throttle and brake actuators, denoted as 'u' in Figure 1-1, in such a way as to track the acceleration command, computed by the upper level controller. Usually, the throttle or brake input is calculated based on simplified longitudinal vehicle model, which allows to find the engine torque needed to achieve desired acceleration [12]. Moreover, the controller should satisfy the following performance specifications, (i) zero steady-state error, (ii) preferably zero over-shoot, (iii) reasonably fast rise time and (iv) the comfort constraints [12].

### 1-2-2 Adaptive Cruise Control

An Adaptive Cruise Control system is an extension of the aforementioned Cruise Control system. It employs a radar or other on-board ranging sensor, that is able to measure the relative distance and relative velocity of the preceding vehicle (also often called the host vehicle). The main extension comparing to CC is the ability to adjust the vehicle's speed in such a way as to maintain a desired distance between vehicles by controlling either throttle or brake action. When the car in front exits the lane, an ACC system automatically restores to a reference speed [13].

Adaptive Cruise Control systems can be divided into two major groups: (i) standard ACC and (ii) FSRA, also called Stop&Go system [13].

- According to ISO standard [14], the standard ACC is not able to operate at a very low speed, namely, below speed  $v_{low} \leq 5$  m/s the control is handed over to a driver. Another functional limit of the ISO standard is the minimal preset speed, which has to be above 7 m/s.
- Full-Speed-Range ACC is able to operate in the entire speed range up to 0 m/s [4].

The Adaptive Cruise Control system works in two modes: (i) the speed control mode and (ii) the distance control mode, which is also called time gap control [13]. The transition between those two states takes place automatically, without the driver's influence.

### 1-2-3 Cooperative Adaptive Cruise Control

Nowadays, Adaptive Cruise Control systems are widely available in many commercial vehicles. However, these systems use only on-board sensors, which may be faulty or have measurement

noises and delays. The signal measured for instance by radar is often very noisy and needs to be filtered, what is a cause of aforementioned delays. The appearance of response delays decreases the ability to follow vehicles accurately and force to extend the gap between the two vehicles. Experimental results presented in [15] show that the relative speed measured by radar or other ranging sensors can have 0.5 s delay with comparison to a vehicle with wireless communication, which makes a significant difference. Moreover, without a vehicle-to-vehicle communication it is problematic to detect (quickly) the longitudinal maneuver of the vehicle in front with only on-board sensors. It can cause traffic accidents in extreme situations, like vehicle's heavy braking.

As an improvement of ACC system, Cooperative Adaptive Cruise Control systems have been introduced, which use data exchanged by vehicles via wireless inter-vehicle communication, in addition to on-board sensors. Such an improvement allows to decrease a headway distance between two consecutive vehicles to a few meters [16], which allows to improve traffic throughput of the roads network. Due to vehicle-to-vehicle wireless communication the vehicles can exchange their accelerations and other measurements, which are hard to measure with ranging sensors and are important for ACC/CACC system control [16]. The next important advantage of inter-vehicle communication link is the fact, that it improves string stability in vehicular platoon [17], which in turn enhances safety and throughput. Shrinkage of inter-vehicle distance allows also to decrease fuel consumption [17], due to, among others, a reduction of aerodynamic drag forces (Figure 1-2).

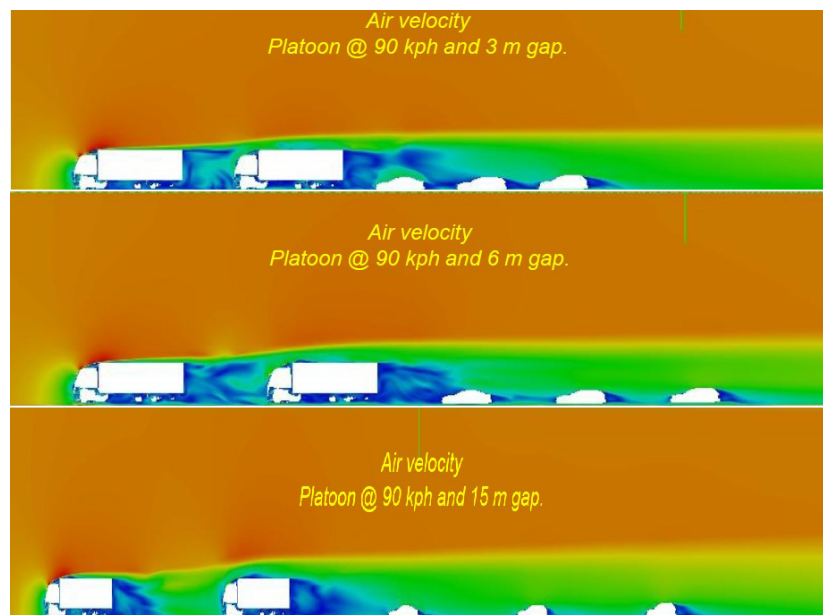


**Figure 1-2:** Aerodynamics drag forces reduction for different inter-vehicle distances [1]

In order to achieve safety and maintain a desired inter-vehicle distance, each vehicle in the interconnected system is equipped with a suitable longitudinal controller. The safety of the vehicle in a platoon is directly related to the inter-vehicle distance and the vehicles' velocity in a string of vehicles. Obviously, when the distance between vehicles in a platoon decreases, the road throughput increases, but safety may be jeopardized, especially during emergency braking. Therefore, there needs to be a trade-off between inter-vehicle distance

and throughput. An important safety factor is also relative velocity, which ideally should be as small as possible and decreasing along the vehicular platoon.

According to a simulation conducted in [18] the throughput with all-manual driving vehicles with a diversity in time gap of  $\pm 10\%$  of 1.64 s allows for an average capacity of 2018 vphpl<sup>1</sup>. When vehicles equipped with the ACC system are incorporated into the traffic stream, the capacities vary between 2030 to 2100 vphpl regardless of the number of cars with the ACC. Such a small improvement is a consequence of the similar driver preferences for time headway (Table 1-2) of ACC system and the time headway for manual-driving. The experiment shows that the ACC is indeed only a comfort system, which does not increase highway capacity.

Percentage	Time headway
31.3 %	2.2 s
18.5 %	1.6 s
50.4 %	1.1 s

**Table 1-2:** Time gap distribution for the ACC

However, in the case of the CACC system, the trend in highway lane capacity increases quadratically with the increase of market penetration of CACC systems (Figure 1-3). The increase of the lane capacity in the first half of the bar plot in Figure 1-3 is not significant, since the vehicle with CACC, which follows a manually-driven vehicle must revert to conventional ACC system. The rapid growth of the lane capacity starts at 60 % of market penetration with vehicles equipped with CACC technology. In a situation of 100 % of the market penetration, the significant improvement from around 2100 vphpl for ACC system to 3970 vphpl (almost double) with the CACC system is observable. In presented example the distribution of the time gaps of the cooperative adaptive cruise control is shown in Table 1-3.

In the Figure 1-3 the improvement of the lane capacity by a so-called Here I Am (HIA) system is also indicated. The HIA system is a short-range radio communication that is used in manually-driven cars [18]. It exchanges its velocity and position with vehicles with CACC technology, which are able to follow such a car with a shorter gap.

Percentage	Time headway
12 %	1.1 s
7 %	0.9 s
24 %	0.7 s
57 %	0.6 s

**Table 1-3:** Time gap distribution for the CACC

Numerous benefits of CACC and development of vehicle-to-vehicle (for example, bidirectional communication, which allows for implementation of constant distance policy) and vehicles-to-infrastructure communication attracted research communities, which have been developing the vehicle platooning technology in the last thirty years. Well-known projects of the vehicle platooning are: SARTRE (Europe), PATH (California), Energy ITS (Japan), SCANIA-platooning (Sweden) and KONVOI (Germany) [19].

<sup>1</sup>vphpl - vehicles per hour per lane

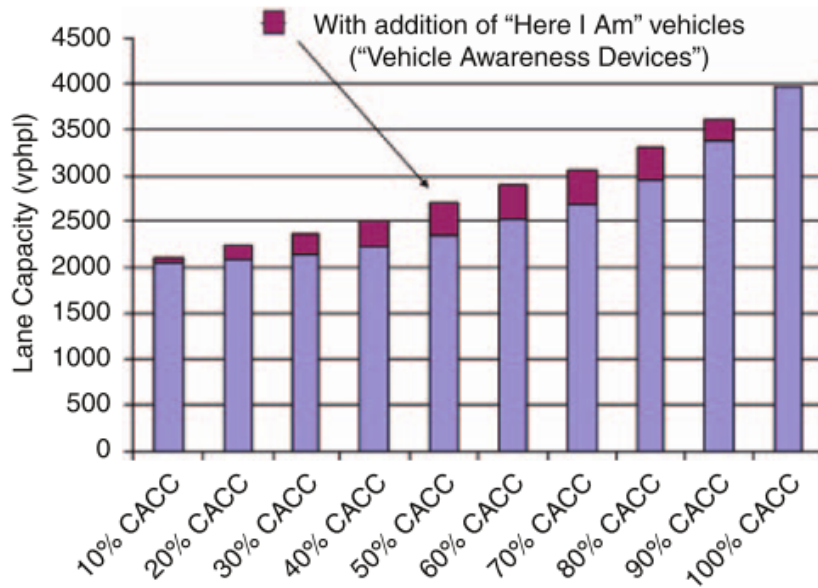


Figure 1-3: Highway capacity for different CACC market penetration

### 1-3 Aims and Objectives

The main aim of this work is to implement a Cooperative Adaptive Cruise Control algorithm, which would be able to control a vehicular platoon with a realistic vehicle model. The main challenges, which need to be faced are as follows:

- A lot of CACC controllers proposed in the literature deal only with a homogeneous vehicle platoon. An improvement of existing CACC algorithms, which are able to deal with the string of heterogeneous vehicles with uncertain parameters is needed.
- Performance evaluation of this control algorithm with real traffic scenarios has to be provided, using a realistic platoon's model.

### 1-4 Contribution of Thesis

The contributions of this master thesis to the Cooperative Adaptive Cruise Control problem are as follows:

- Based on the idea of sliding-mode platooning algorithms from [20], a CACC controller is designed for the platoon of heterogeneous vehicles. Unlike [20], the controller does not involve discontinuous nonlinearities, which simplifies its practical implementation.
- The designed CACC algorithm is tested experimentally by using vehicle simulator Dynacar [21]. The performances of the CACC controller are measured in terms of safety and comfort indicators from ISO 22179 standard and using Maximum Absolute Relative Velocity (MRV), which indicates the error propagation in platoon.

## 1-5 Outline

The remaining chapters are as follows. In Chapter 2, an introduction to the Cooperative Adaptive Cruise Control is given and important features, which are necessary to understand how a CACC works are explained. In Chapter 3, CACC algorithms based on discontinuous and continuous sliding-mode control are presented. In Chapter 4, the implementation of the CACC algorithm with a Dynacar simulator of vehicle is explained and the evaluation of the performances of the designed CACC with realistic vehicle model are presented. The main conclusions and propositions for further work are stated in Chapter 5.



# Cooperative Adaptive Cruise Control - Requirements and Problem Setup

## 2-1 Platoon Heterogeneity

In many works on CACC controllers design, it has been assumed that all the vehicles in the platoon have the same dynamics (the platoon is homogeneous) [22, 23, 24]. In particular, a vehicle's parameters, such as mass or engine time constant are assumed to be known. In practice, CACC algorithms have to deal with platoons of vehicles with different (and partially uncertain) parameters. The platoon dynamics are strongly affected by the heterogeneity of the vehicles and uncertainties of their physical parameters [25]. The CACC controller has to provide the robustness against model uncertainties and disturbances of the closed-loop system.

### 2-1-1 Model Uncertainties and Parameters Range

The uncertainties which affect a vehicle in a platoon are caused by different factors, for instance, by human, environment or ageing of the vehicle. Some examples of parametric uncertainties are: mass of the vehicle, aerodynamic drag and tire rolling friction [25]. A platoon may be also affected by external disturbances such as wind gust or a road slope [9].

The ranges of the parameters for an average passenger car are presented in Table 2-1. Where  $M$  is car mass,  $\eta$  is mechanical efficiency of driveline,  $\tau$  is the time constant of engine dynamics,  $C_w$  stands for coefficient of aerodynamics drag,  $A$  is a frontal cross-area,  $f$  is coefficient of rolling resistance,  $\theta$  denotes a road slop and  $v_w$  is wind speed.

## 2-2 Spacing Policy

Another important factor, which has a great influence on traffic flow and string stability in vehicle platoons is a spacing policy [26], which defines the distance between consecutive

Symbol	Unit	Nominal	Minimum	Maximum
$M$	kg	1400	800	2000
$\eta$	-	0.92	0.86	0.98
$\tau$	s	0.5	0.2	0.8
$C_w$	-	0.34	0.29	0.39
$A$	$m^2$	2.24	1.58	2.9
$f$	-	0.012	0.01	0.014
$\theta$	deg	0	-5.9	5.9
$v_w$	m/s	0	-12.9	12.9

**Table 2-1:** Range of parameters for a passenger car, [9]

vehicles. Most typical, either constant distance or constant time headway policy is used [27].

The constant distance policy leads to a higher throughput, because the distance between vehicles is independent of the vehicles' velocity. The spacing error with a constant distance policy is expressed in the following way:

$$d_i(t) = s_{i-1}(t) - s_i(t) - x_{r,i} - L_i \quad (2-1)$$

where  $s_{i-1}$  and  $s_i$  indicate the absolute position of the two consecutive vehicles,  $x_{r,i}$  is a desired constant spacing distance and  $L_i$  is the length of the i-th car.

The constant headway policy (Figure 2-1), is believed to improve string stability [24] and safety. The desired relative position with constant headway spacing policy is given by

$$x_{r,i}(t) = r_i + h_i v_i(t) \quad (2-2)$$

where,  $r_i$  stands for desired distance at standstill,  $h_i$  is a desired headway time and  $v_i(t)$  is a velocity of the i-th vehicle. The constant headway policy with the headway time  $h_i = 0$  becomes a constant spacing policy.

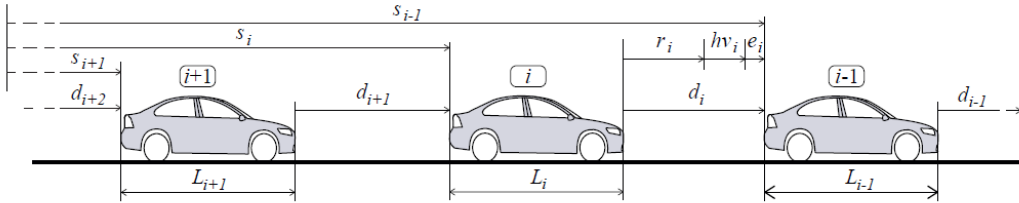


**Figure 2-1:** Schematic overview of a vehicular platoon, [2]

## 2-3 String Stability

The notion of string stability is concerned with the propagation of the disturbances in up-stream direction of the platoon and in the case of bidirectional communication also in down-stream direction [24]. In the case of the string unstable platoon, the oscillatory behaviour of

the leading vehicle may result in so-called "harmonica effect", which may lead to traffic jams or collisions [28].

Frequently adopted description of string stability in literature is a frequency domain approach, in [24] it is called the performance-oriented approach. In this method the amplification of either distance, velocity or acceleration error is measured with the transfer function, for example, from Laplace transform of "input" position error  $E(s)_{i-1}$  to the Laplace transform of "output" position error  $E(s)_i$ , where  $s$  is a complex variable in frequency domain.

$$\Gamma_i(s) = \frac{E_i(s)}{E_{i-1}(s)} \quad (2-3)$$

In case of homogeneous platoon, a transfer function (2-3) is identical for each vehicle in a string  $\Gamma_i(s) = \Gamma(s)$ . In order to assure that the distance error does not amplify among the vehicles, the  $H_\infty$ -norm of the transfer function (2-3) has to satisfy the following condition.

$$\|\Gamma_i(j\omega)\|_{\mathcal{H}_\infty} \leq 1, \quad 1 \leq i \leq m \quad (2-4)$$

A frequency domain is not always suitable, for instance when the platoon is described by a nonlinear system. Then a time-domain approach can be used. For example in [29], it is required that the peak in distance error of each consecutive vehicle is smaller or equal to the error of the predecessor in order to maintain string stability for a platoon of  $N$  vehicles (2-5)

$$\|e_1\|_\infty \leq \|e_2\|_\infty \leq \dots \leq \|e_n\|_\infty \quad (2-5)$$

In this work, we seek for string stability in the following stronger sense [20].

$$|e_{i+1}(t)| \leq |e_i(t)| \quad (2-6)$$

Such a definition of string stability requires that the distance error does not increase as it propagates through the platoon.

## 2-4 Communication Structures

There are many possible communication graphs, which specify the flow of information between vehicles (some of them are shown in Figure 2-2). The communication structure is an important factor, which, in particular, influences string stability [30].

As discussed in [27], the practical implementation of the platooning algorithms require them to be decentralized, that is each vehicle in a platoon gathers the information from neighboring vehicles and decides on its own what should be the vehicle's response to the current road situations.

It is important to mention that not every method of information flow topology is suitable to use in a real traffic scenario. For instance the strategy, in which each vehicle receives data from the platoon leader (designated leader information flow topology) may be difficult to

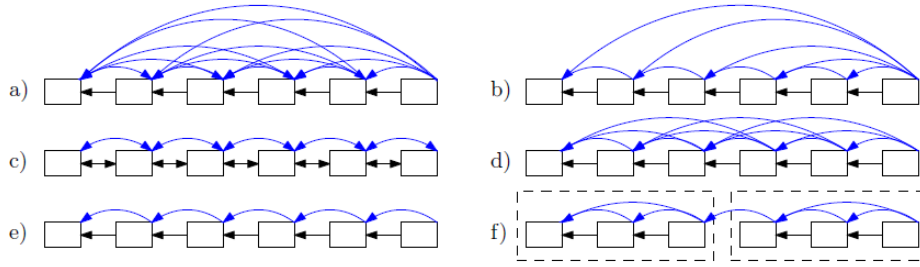


**Figure 2-2:** Information flow topologies [3]. a) "everybody knows everything", b) designated platoon leader, c) bidirectional, d) N- vehicles look-ahead, e) directly preceding vehicle, f) mini-platoons with designated platoon leader. Blue arrows indicate wireless communication, while radars or other ranging sensor are denoted with black arrows.

implement into a platoon with many vehicles, since some of the vehicles may be out of range of wireless communication [20].

In this thesis the control algorithm is based on a bidirectional information flow topology (Figure 2-2c), therefore the data is sent to both the predeceasing and following vehicle. Such a solution is considered to be more feasible, since the vehicles may be always in the range of the wireless network. Another important feature of bidirectional information flow topology is the fact that it can improve string stability with constant inter-vehicle distances [31].

## 2-5 Node Dynamics - Simplified Longitudinal Vehicle Model

For the purpose of the control design simplified and often linear models are frequently used [27]. Most typically, the following four models are used.

The *single-integrator* model is an approach, which can in some specific cases significantly simplify the control design. In this model as an control input the velocity is used and position is the state. The single-integrator model does not map a vehicle dynamics very well and what is more it does not give any information about so-called slinky-type effect or string instability in the platoon [27].

As an improvement of the previously mentioned model, the *double-integrator* model comes along. However, it also has problems with reproducing features of vehicle dynamics, such as internal delay or time constant in powertrain dynamics. However, in overall it mimics a vehicle behaviour satisfactorily and allows to simplify a platooning problem.

$$\ddot{x}_i = \frac{u_i - c_i \dot{x}_i^2 - f_i}{M_i} + \delta_i \quad (2-7)$$

where  $x_i$  is the position of the  $i$ -th vehicle in a platoon, then  $\dot{x}_i$  and  $\ddot{x}_i$  are velocity and acceleration of the  $i$ -th vehicle, respectively. What is more,  $u_i$  is a control input, which is a traction force acting on a vehicle,  $c_i$  stands for the effective aerodynamic drag coefficient,  $f_i$  is the tire rolling resistance friction,  $M_i$  is the vehicle's mass and by  $\delta_i$  the system uncertainties/disturbances are denoted.

Next is the *third-order* model, where dimension of the state vector is increased, which helps to approximate the behaviour of the powertrain.

$$\begin{aligned} \dot{d}_i &= v_{i-1} - v_i \\ \dot{v}_i &= a_i \\ \dot{a}_i &= f_i(v_i, a_i) + g_i(v_i)c_i \end{aligned} \quad (2-8)$$

where  $c_i$  in the third equation stands for the engine input,  $f_i(v_i, a_i)$  and  $g_i(v_i)$  are expressed as

$$f_i(v_i, a_i) = \frac{1}{\tau_i}(\dot{v}_i + \frac{\sigma A_i c_{di}}{2m_i} v_i^2 + \frac{d_{mi}}{m_i}) - \frac{\sigma A_i c_{di} v_i a_i}{m_i} \quad (2-9)$$

$$g_i(v_i) = \frac{1}{\tau_i m_i} \quad (2-10)$$

where,  $i$  is the number of the car in the platoon,  $\tau_i$  is a time constant representing driveline dynamics,  $v_i$  is the vehicle velocity,  $\sigma$  stands for the density of the air,  $A_i$  is cross-sectional area,  $c_{di}$ ,  $d_{mi}$ ,  $m_i$  are drag coefficient, mechanical drag, mass respectively.

In some cases it is easier to analyze certain characteristics of the platoon with frequency domain instead of time domain, hence a vehicle model may be expressed as a *transfer function*. However, for nonlinear vehicular system it may not be the best choice.

Cooperative Adaptive Cruise Control algorithm considered in this work is based on a second-order model (2-7) which is able to provide enough information to perform a desired vehicular platoon's behaviour.

## 2-6 Performance Specification

To be able to evaluate the performances of proposed Cooperative Adaptive Cruise Control algorithm in a vehicular platoon some of the indicators need to be implemented. While choosing CACC performance indicators it is decided to focus on safety and comfort. The comfort and safety performances are assumed to be defined by the ISO 22179:2009 ([4]), where the limits of average deceleration (2-11) and acceleration (2-12) over the time of 2 seconds for different vehicle velocities (Figure 5-1) are specified.

$$\begin{cases} a_i \leq 5, & \text{if } \dot{x}_i \leq 5 \\ a_i \leq -0.1 + 5.5\dot{x}_i, & \text{if } \dot{x}_i \in (5, 20) \\ a_i \leq 3.5, & \text{if } \dot{x}_i \geq 20 \end{cases} \quad (2-11)$$

$$\begin{cases} a_i \leq 4, & \text{if } \dot{x}_i \leq 5 \\ a_i \leq -\frac{2}{15} + \frac{14}{3}\dot{x}_i, & \text{if } \dot{x}_i \in (5, 20) \\ a_i \leq 2, & \text{if } \dot{x}_i \geq 20 \end{cases} \quad (2-12)$$

In addition, a Maximum absolute Relative Velocity (MRV) expressed as  $\|\dot{e}_i\|_\infty$  ([m/s]) is a safety indicator, which allows to measure the error propagation [32]. The string stability requirement (2-6) also has to be satisfied.

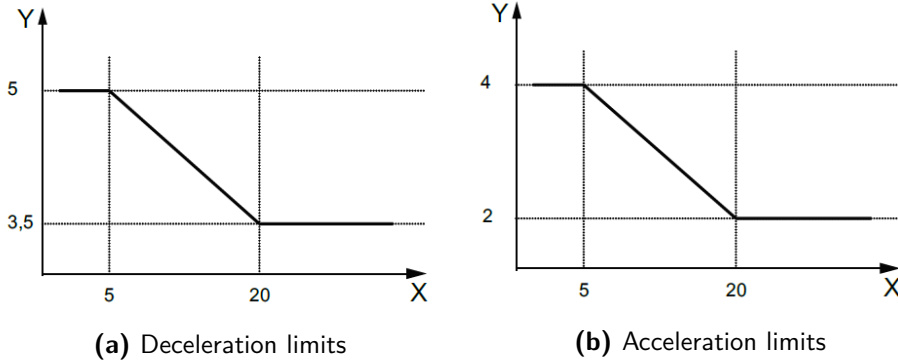


**Figure 2-3:** ISO 22179:2009 deceleration and acceleration standards for FSRA (X is velocity [m/s] and Y is acceleration [ $m/s^2$ ]), [4]

## 2-7 Problem Formulation

Dealing with a longitudinal control algorithm the following longitudinal measurements are taken into account: acceleration, velocity and an absolute distance of each vehicle in a platoon. Control objectives for decentralized CACC algorithm for heterogeneous vehicle platoons are mainly imposed because of the safety issues and are meant to fulfill the following assumptions.

1. The distance error between two consecutive vehicles should converge to zero for all vehicles with uncertain vehicle parameters, such as aerodynamic drag coefficient, rolling resistance friction, vehicle mass.
2. The vehicle platoons should be string stable in distance error sense (2-6) with constant spacing policy for a heterogeneous platoon.
3. The unknown disturbances acting on vehicles in a platoon should be attenuated.
4. The algorithm should satisfy safety and comfort requirements, described in 2-6.

# Cooperative Adaptive Cruise Control - Design

## 3-1 Platoon Control Law

The algorithm of Cooperative Adaptive Cruise Control is based on a sliding mode control combined with adaptive control. Huge advantages of this control approach are robustness and insensitivity to disturbances and model uncertainties [33], which are considered to be two main factors of string instability in vehicle platoon systems [34].

### 3-1-1 Adaptive Bidirectional Coupled Sliding Mode Control

#### Model description

The desired CACC algorithm deals with model (2-7), where the uncertainties and disturbances in (2-7) can result from various sources, like, the additional mass acting on a vehicle (mass of the passengers, load, etc.), the estimation of various vehicle's parameters (i.e aerodynamic drag or tire rolling friction) and for instance wind gust. Those uncertainties and disturbances ( $\delta_i$ ) are assumed to be an unknown time-varying function, which is bounded as  $|M_i\delta_i| \leq D_i$ , where  $D_i$  is unknown positive constant. It is also assumed, that the vehicle's parameters  $c_i$ ,  $f_i$  and  $M_i$  are unknown constants.

#### Sliding mode control

The main aim of the platoon control problem is the ability of each vehicle in a string to be able to keep the desired inter-vehicle distance in a string-stable way, based on the position, velocity and acceleration measurement of both predeceasing and following vehicle (bidirectional flow information topology). It is assumed that the desired distance between two consecutive vehicles is constant (Figure 3-1) and is expressed as follows:

$$e_i = (x_{i-1} - x_i) - x_i^d, \text{ for } i = 1, \dots, n \quad (3-1)$$

where  $x_i^d$  is desired inter-vehicle distance and the leading vehicle is indexed as 0.

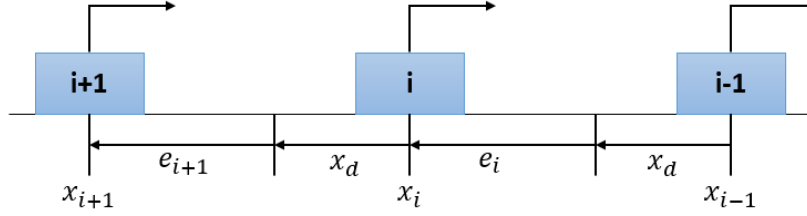


**Figure 3-1:** Constant spacing policy

Having an expression for distance error between the vehicles, the sliding surface of the sliding mode control can be derived. The design of sliding surface is often based on the combination of controlled state and its derivative. Proposed sliding surface in [20] for Cooperative Adaptive Cruise Control used in this master thesis is as follows:

$$s_i = \dot{e}_i + \lambda e_i \quad (3-2)$$

where  $\lambda$  is a positive design constant.

The convergence of (3-2) to zero can guarantee that  $e_i(t)$  goes to 0, however it cannot guarantee string stability in the platoon. Hence, a new sliding surface, which couples the information from both preceding and following vehicle is designed.

$$S_i = \begin{cases} qs_i - s_{i+1}, & i = 1, \dots, n-1 \\ qs_i, & i = n \end{cases} \quad (3-3)$$

where  $q > 0$  is a weighting factor. The last vehicle in a platoon does not have a follower, therefore  $s_{i+1} = 0$ .

In order to guarantee stability of vehicular system an adaptive control law [20] is used and is expressed as follows:

$$u_i = \hat{c}_i \dot{x}_i^2 + \hat{f}_i + \hat{D}_i \operatorname{sgn}(S_i) + \frac{\hat{M}_i}{q+1} A_i + \frac{k}{q+1} S_i + \frac{\bar{k}}{q+1} \operatorname{sgn}(S_i) \quad (3-4)$$

where  $\bar{k}$  and  $k$  are control positive constants,  $\hat{c}_i$ ,  $\hat{f}_i$ ,  $\hat{D}_i$ ,  $\hat{M}_i$  are the estimates of vehicle's unknown parameters  $c_i$ ,  $f_i$ ,  $D_i$ ,  $M_i$  and  $A_i = q\ddot{x}_{i-1} + \ddot{x}_{i+1} + \lambda(q\dot{e}_i - \dot{e}_{i+1})$ .

The control law for the last vehicle in a platoon differs slightly. It is caused by the fact that there is no following vehicle and since it is a bidirectional information flow topology algorithm, a few corrections need to be added.

$$u_n = \hat{c}_n \dot{x}_n^2 + \hat{f}_n + \hat{D}_n \operatorname{sgn}(S_n) + \frac{\hat{M}_n}{q} A_n + \frac{1}{q} (kS_n + \bar{k} \operatorname{sgn}(S_n)) \quad (3-5)$$

where,  $A_n = q(\ddot{x}_{n-1} + \lambda \dot{e}_n)$

The first derivative of  $S_i$  and  $S_n$  from (3-3) are following.

$$\begin{aligned}\dot{S}_i &= q\dot{s}_i - \dot{s}_{i+1} & (3-6) \\ &= q(\ddot{x}_{i-1} - \ddot{x}_i + \lambda \dot{e}_i) - (\ddot{x}_i - \ddot{x}_{i+1} + \lambda \dot{e}_i) \\ &= -\frac{(q+1)}{M_i}(u_i - c_i \dot{x}_i^2 - f_i + \delta'_i) + A_i\end{aligned}$$

where  $\delta'_i = M_i \delta_i$ .

$$\begin{aligned}\dot{S}_n &= q\dot{s}_n & (3-7) \\ &= q(\ddot{e}_n + \lambda \dot{e}_n) \\ &= -\frac{q}{M_n}(u_n - c_n \dot{x}_n^2 - f_n + \delta'_n) + A_n & (3-8)\end{aligned}$$

where,  $\delta'_n = M_n \delta_n$ .

### Adaptation law

In the control law presented in (3-4) the unknown parameters are estimated with adaptation laws and are determined as follows:

$$\dot{\hat{c}}_i = \gamma_i^c (q+1) S_i \dot{x}_i^2 \quad (3-9)$$

$$\dot{\hat{f}}_i = \gamma_i^f (q+1) S_i \quad (3-10)$$

$$\dot{\hat{D}}_i = \gamma_i^D (q+1) |S_i| \quad (3-11)$$

$$\dot{\hat{M}}_i = \gamma_i^M A_i S_i \quad (3-12)$$

where  $\gamma_i^c$ ,  $\gamma_i^f$ ,  $\gamma_i^D$ ,  $\gamma_i^M$  are positive adaptation gains for  $i = 1, \dots, n$ .

For the last vehicle the adaptation laws are as follows:

$$\dot{\hat{c}}_n = \gamma_n^c q S_n \dot{x}_n^2 \quad (3-13)$$

$$\dot{\hat{f}}_n = \gamma_n^f q S_n \quad (3-14)$$

$$\dot{\hat{D}}_n = \gamma_n^D q |S_n| \quad (3-15)$$

$$\dot{\hat{M}}_n = \gamma_n^M A_n S_n \quad (3-16)$$

### 3-1-2 Continuous Controller Design

The control law (3-4) proposed in [20] is a discontinuous function, since it contains a sign function. From a theoretical point of view such a solution may work, however in a practical application, for instance a vehicle control system it may cause serious problems. The main issue is a so-called chattering effect, which causes a rapid change of control input. In order to

avoid this problem a control function is re-designed (3-17), where instead of a discontinuous function a hyperbolic tangent (continuous) function is used.

$$u_i = \hat{c}_i \dot{x}_i^2 + \hat{f}_i + \hat{D}_i \tanh(S_i) + \frac{\hat{M}_i}{q+1} A_i + \frac{k}{q+1} S_i + \frac{\bar{k}}{q+1} \tanh(S_i) \quad (3-17)$$

The control law for the last vehicle, which obviously does not have a following vehicle is expressed as:

$$u_n = \hat{c}_n \dot{x}_n^2 + \hat{f}_n + \hat{D}_n \tanh(S_n) + \frac{\hat{M}_n}{q} A_n + \frac{k}{q} S_n + \frac{\bar{k}}{q} \tanh(S_n) \quad (3-18)$$

The differences in the behaviour of the continuous and discontinuous control laws is presented in Figure 3-2. It is noticeable that for the same traffic scenario the control action of discontinuous controller changes from negative to positive value in a very quick manner. Such an approach is not applicable to the systems, which dynamics are relatively slow (vehicle's dynamic) comparing, for instance to electronic components, like transistors.

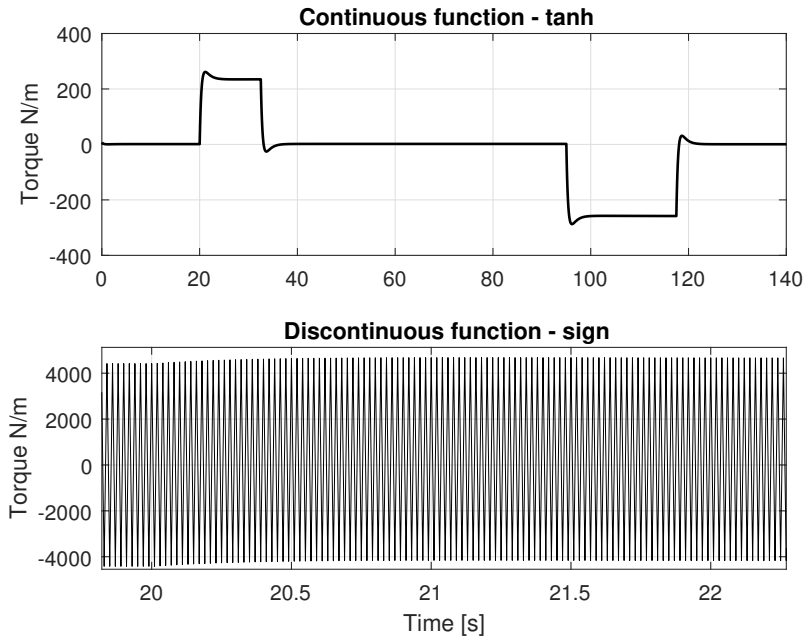


**Figure 3-2:** Comparison of applied wheel torque for continuous control law and discontinuous control law

**Theorem 1.** *Control laws (3-17), (3-18) and adaptive laws for estimation of unknown parameters, where  $q \in (0, 1]$ ,  $\lambda$  is positive constant and vehicle parameters  $c_i$ ,  $f_i$ ,  $M_i$  and  $D_i$  are constants make a vehicle platoon with constant spacing policy stable in sense that  $S_i$ ,  $\tilde{c}_i$ ,  $\tilde{f}_i$ ,  $\tilde{D}_i$  and  $\tilde{M}_i$  are bounded. In addition  $S_i \in L_2$ , hence  $e_i$ ,  $\dot{e}_i \in L_2 \cap L_\infty$ . Therefore, control laws (3-17) and (3-18) guarantee that  $\lim_{t \rightarrow \infty} e_i = 0$ .*

In order to prove the stability of vehicular system the following quadratic Lyapunov function candidate is proposed:

$$V_i = \frac{M_i}{2} S_i^2 + \frac{\tilde{c}_i^2}{2\gamma_i^c} + \frac{\tilde{f}_i^2}{2\gamma_i^f} + \frac{\tilde{D}_i^2}{2\gamma_i^D} + \frac{\tilde{M}_i^2}{2\gamma_i^M} \quad (3-19)$$

and  $\tilde{c}_i$ ,  $\tilde{f}_i$ ,  $\tilde{D}_i$ ,  $\tilde{M}_i$  are the estimations errors defined as  $\tilde{c}_i := c_i - \hat{c}_i$ ,  $\tilde{f}_i := f_i - \hat{f}_i$ ,  $\tilde{D}_i := D_i - \hat{D}_i$ ,  $\tilde{M}_i := M_i - \hat{M}_i$ .

$$\dot{V}_i = M_i S_i \dot{S}_i + \frac{\tilde{c}_i \dot{\tilde{c}}_i}{\gamma_i^c} + \frac{\tilde{f}_i \dot{\tilde{f}}_i}{\gamma_i^f} + \frac{\tilde{D}_i \dot{\tilde{D}}_i}{\gamma_i^D} + \frac{\tilde{M}_i \dot{\tilde{M}}_i}{\gamma_i^M} \quad (3-20)$$

Substituting  $\dot{S}_i$  (3-6) in (3-20) the following is obtained.

$$\dot{V}_i = M_i S_i \left( -\frac{(q+1)}{M_i} (u_i - c_i \dot{x}_i^2 - f_i + \delta'_i) + A_i \right) + \frac{\tilde{c}_i \dot{\tilde{c}}_i}{\gamma_i^c} + \frac{\tilde{f}_i \dot{\tilde{f}}_i}{\gamma_i^f} + \frac{\tilde{D}_i \dot{\tilde{D}}_i}{\gamma_i^D} + \frac{\tilde{M}_i \dot{\tilde{M}}_i}{\gamma_i^M} \quad (3-21)$$

Later substituting control input  $u_i$  with (3-17) in (3-21).

$$\begin{aligned} \dot{V}_i = M_i S_i \left( -\frac{(q+1)}{M_i} (\hat{c}_i \dot{x}_i^2 + \hat{f}_i + \hat{D}_i \tanh(S_i) + \frac{\hat{M}_i}{q+1} A_i + \frac{k}{q+1} S_i + \frac{\bar{k}}{q+1} \tanh(S_i) - c_i \dot{x}_i^2 - f_i \right. \\ \left. + \delta'_i) + A_i \right) + \frac{\tilde{c}_i \dot{\tilde{c}}_i}{\gamma_i^c} + \frac{\tilde{f}_i \dot{\tilde{f}}_i}{\gamma_i^f} + \frac{\tilde{D}_i \dot{\tilde{D}}_i}{\gamma_i^D} + \frac{\tilde{M}_i \dot{\tilde{M}}_i}{\gamma_i^M} \end{aligned} \quad (3-22)$$

Then the constants with a common factor are taken into parenthesis, later an expression for the estimations errors  $\tilde{c}_i := c_i - \hat{c}_i$ ,  $\tilde{f}_i := f_i - \hat{f}_i$  is used.

$$\begin{aligned} \dot{V}_i = M_i S_i \left( -\frac{(q+1)}{M_i} ((\hat{c}_i - c_i) \dot{x}_i^2 + (\hat{f}_i - f_i) + \hat{D}_i \tanh(S_i) + \frac{\hat{M}_i}{q+1} A_i + \frac{k}{q+1} S_i + \frac{\bar{k}}{q+1} \tanh(S_i) \right. \\ \left. + \delta'_i) + A_i \right) + \frac{\tilde{c}_i \dot{\tilde{c}}_i}{\gamma_i^c} + \frac{\tilde{f}_i \dot{\tilde{f}}_i}{\gamma_i^f} + \frac{\tilde{D}_i \dot{\tilde{D}}_i}{\gamma_i^D} + \frac{\tilde{M}_i \dot{\tilde{M}}_i}{\gamma_i^M} \\ = M_i S_i \left( \frac{(q+1)}{M_i} \tilde{c}_i \dot{x}_i^2 + \frac{(q+1)}{M_i} \tilde{f}_i - \frac{(q+1)}{M_i} \hat{D}_i \tanh(S_i) - \frac{\hat{M}_i}{M_i} A_i - \frac{k}{M_i} S_i - \frac{\bar{k}}{M_i} \tanh(S_i) \right. \\ \left. - \frac{(q+1)\delta'_i}{M_i} + A_i \right) + \frac{\tilde{c}_i \dot{\tilde{c}}_i}{\gamma_i^c} + \frac{\tilde{f}_i \dot{\tilde{f}}_i}{\gamma_i^f} + \frac{\tilde{D}_i \dot{\tilde{D}}_i}{\gamma_i^D} + \frac{\tilde{M}_i \dot{\tilde{M}}_i}{\gamma_i^M} \\ = (q+1) \tilde{c}_i \dot{x}_i^2 S_i + (q+1) \tilde{f}_i S_i - (q+1) \hat{D}_i \tanh(S_i) S_i + M_i A_i S_i - \hat{M}_i A_i S_i - k S_i^2 - \bar{k} \tanh(S_i) S_i \\ - (q+1) S_i \delta'_i - \frac{\tilde{c}_i \dot{\tilde{c}}_i}{\gamma_i^c} - \frac{\tilde{f}_i \dot{\tilde{f}}_i}{\gamma_i^f} - \frac{\tilde{D}_i \dot{\tilde{D}}_i}{\gamma_i^D} - \frac{\tilde{M}_i \dot{\tilde{M}}_i}{\gamma_i^M} \end{aligned} \quad (3-23)$$

Substituting  $\hat{c}_i$ ,  $\hat{f}_i$  and  $\hat{M}_i$  with (3-9), (3-10) and (3-12) respectively and (3-11) is substituted with  $\dot{\hat{D}}_i = \gamma_i^D (q+1) \tanh(S_i) S_i$  in (3-23) the following is obtained.

$$\begin{aligned}\dot{V}_i &= -(q+1)\hat{D}_i \tanh(S_i)S_i - kS_i^2 - \bar{k} \tanh(S_i)S_i - (q+1)M_i\delta_i S_i - (q+1)\tilde{D}_i \tanh(S_i)S_i \\ &= -(q+1)(\hat{D}_i + \tilde{D}_i) \tanh(S_i)S_i - kS_i^2 - \bar{k} \tanh(S_i)S_i - (q+1)M_i\delta_i S_i\end{aligned}\quad (3-24)$$

Using the property that  $\tilde{D}_i := D_i - \hat{D}_i$  in (3-24) the (3-25) is obtained.

$$\begin{aligned}\dot{V}_i &= -(q+1)D_i \tanh(S_i)S_i - kS_i^2 - \bar{k} \tanh(S_i)S_i - (q+1)M_i\delta_i S_i \\ &\leq -kS_i^2 - \bar{k} \tanh(S_i)S_i \\ &\leq 0\end{aligned}\quad (3-25)$$

Hence,  $V_i(t)$  is bounded for all  $t \geq 0$  and also  $S_i, \tilde{c}_i, \tilde{f}_i, \tilde{D}_i, \tilde{M}_i \in L_\infty(0, \infty)$ . Therefore it is also true that  $\hat{c}_i, \hat{f}_i, \hat{D}_i, \hat{M}_i \in L_\infty(0, \infty)$ . We know that  $V_i(0)$  is bounded and  $V_i(t)$  is non-increasing and bounded.

Boundness of  $S_n, \tilde{c}_n, \tilde{f}_n, \tilde{D}_n$  and  $\tilde{M}_n$  is proved with the same quadratic Lyapunov function candidate (3-19) as for vehicles from 1 to  $n-1$ . The time derivative of Lyapunov function candidate for the last vehicle is the following:

$$\dot{V}_n = M_n S_n \dot{S}_n + \frac{\tilde{c}_n \dot{\tilde{c}}_n}{\gamma_n^c} + \frac{\tilde{f}_n \dot{\tilde{f}}_n}{\gamma_n^f} + \frac{\tilde{D}_n \dot{\tilde{D}}_n}{\gamma_n^D} + \frac{\tilde{M}_n \dot{\tilde{M}}_n}{\gamma_n^M}\quad (3-26)$$

Substituting  $\dot{S}_n$  in (3-26) gives the following:

$$\begin{aligned}\dot{V}_n &= M_n S_n \left( -\frac{q}{M_n} (u_n - c_n \dot{x}_n^2 - f_n + \delta'_n) + A_n \right) + \frac{\tilde{c}_n \dot{\tilde{c}}_n}{\gamma_n^c} + \frac{\tilde{f}_n \dot{\tilde{f}}_n}{\gamma_n^f} \\ &\quad + \frac{\tilde{D}_n \dot{\tilde{D}}_n}{\gamma_n^D} + \frac{\tilde{M}_n \dot{\tilde{M}}_n}{\gamma_n^M}\end{aligned}\quad (3-27)$$

Applying control input  $u_n$  (3-18) in (3-27) gives:

$$\begin{aligned}\dot{V}_n &= M_n S_n \left( -\frac{q}{M_n} (\hat{c}_n \dot{x}_n^2 + \hat{f}_n + \hat{D}_n \tanh(S_n) + \frac{\tilde{M}_n}{q} A_n + \frac{k}{q} S_n \right. \\ &\quad \left. + \frac{\bar{k}}{q} \tanh(S_n) - c_n \dot{x}_n^2 - f_n + \delta'_n) + A_n \right) + \frac{\tilde{c}_n \dot{\tilde{c}}_n}{\gamma_n^c} + \frac{\tilde{f}_n \dot{\tilde{f}}_n}{\gamma_n^f} + \frac{\tilde{D}_n \dot{\tilde{D}}_n}{\gamma_n^D} + \frac{\tilde{M}_n \dot{\tilde{M}}_n}{\gamma_n^M}\end{aligned}\quad (3-28)$$

In (3-28) parameters with a common factor are taken into parenthesis and expression for the estimation errors  $\tilde{c}_i := c_i - \hat{c}_i, \tilde{f}_i := f_i - \hat{f}_i$  are applied.

$$\dot{V}_n = M_n S_n \left( -\frac{q}{M_n} ((\hat{c}_n - c_n) \dot{x}_n^2 + (\hat{f}_n - f_n) + \hat{D}_n \tanh(S_n) + \frac{\hat{M}_n}{q} A_n \right. \quad (3-29)$$

$$\left. + \frac{\bar{k}}{q} S_n + \frac{\bar{k}}{q} \tanh(S_n) + \delta'_n) + A_n \right) + \frac{\tilde{c}_n \dot{\tilde{c}}_n}{\gamma_n^c} + \frac{\tilde{f}_n \dot{\tilde{f}}_n}{\gamma_n^f} + \frac{\tilde{D}_n \dot{\tilde{D}}_n}{\gamma_n^D} + \frac{\tilde{M}_n \dot{\tilde{M}}_n}{\gamma_n^M}$$

$$= M_n S_n \left( \frac{q}{M_n} \tilde{c}_n \dot{x}_n^2 + \frac{q}{M_n} \tilde{f}_n - \frac{q}{M_n} \hat{D}_n \tanh(S_n) - \frac{\hat{M}_n}{M_n} A_n - \frac{k}{M_n} S_n \right. \quad (3-30)$$

$$\left. - \frac{\bar{k}}{M_n} \tanh(S_n) - \frac{q}{\delta'_n} M_n + A_n \right) + \frac{\tilde{c}_n \dot{\tilde{c}}_n}{\gamma_n^c} + \frac{\tilde{f}_n \dot{\tilde{f}}_n}{\gamma_n^f} + \frac{\tilde{D}_n \dot{\tilde{D}}_n}{\gamma_n^D} + \frac{\tilde{M}_n \dot{\tilde{M}}_n}{\gamma_n^M}$$

$$= q \tilde{c}_n \dot{x}_n^2 S_n + q \tilde{f}_n S_n - q \hat{D}_n \tanh(S_n) S_n + M_n A_n S_n - \hat{M}_n A_n S_n - k S_n^2 \quad (3-31)$$

$$- \bar{k} \tanh(S_n) S_n - q S_n \delta'_n - \frac{\tilde{c}_n \dot{\tilde{c}}_n}{\gamma_n^c} - \frac{\tilde{f}_n \dot{\tilde{f}}_n}{\gamma_n^f} - \frac{\tilde{D}_n \dot{\tilde{D}}_n}{\gamma_n^D} - \frac{\tilde{M}_n \dot{\tilde{M}}_n}{\gamma_n^M}$$

Substituting  $\dot{\hat{c}}_n$ ,  $\dot{\hat{f}}_n$  and  $\dot{\hat{M}}_n$  with (3-13), (3-14) and (3-16) respectively. Adaption law (3-15) is substituted with  $\dot{\hat{D}}_n = \gamma_n^D(q) \tanh(S_n) S_n$  in (3-29). It gives the following expression.

$$\begin{aligned} \dot{V}_n &= -q \hat{D}_n \tanh(S_n) S_n - k S_n^2 - \bar{k} \tanh(S_n) S_n - q M_n \delta_n S_n - q \tilde{D}_n \tanh(S_n) S_n \\ &= -q (\hat{D}_n + \tilde{D}_n) \tanh(S_n) S_n - k S_n^2 - \bar{k} \tanh(S_n) S_n - q M_n \delta_n S_n \end{aligned} \quad (3-32)$$

Using the property that  $\tilde{D}_i := D_i - \hat{D}_i$  in (3-32) the (3-33) is obtained.

$$\begin{aligned} \dot{V}_n &= -q D_n \tanh(S_n) S_n - k S_n^2 - \bar{k} \tanh(S_n) S_n - q M_n \delta_n S_n \\ &\leq -k S_n^2 - \bar{k} \tanh(S_n) S_n \\ &\leq 0 \end{aligned} \quad (3-33)$$

Therefore,  $V_n(t)$  is bounded for all  $t \geq 0$  and also  $S_n, \tilde{c}_n, \tilde{f}_n, \tilde{D}_n, \tilde{M}_n \in L_\infty(0, \infty)$ . Hence, it is also true that  $\hat{c}_n, \hat{f}_n, \hat{D}_n, \hat{M}_n \in L_\infty(0, \infty)$ . We know that  $V_n(0)$  is bounded and  $V_n(t)$  is non-increasing and bounded.

Taking the integral of both sides of (3-25) and (3-33) it can be proved that  $S_i, S_n \in L_2(0, \infty)$ .

$$- \int_0^t \dot{V}_i d\tau \geq \int_0^t (k S_i^2 + \bar{k} \tanh(S_i) S_i) d\tau$$

$$V_i(0) - V_i(t) \geq \int_0^t k S_i^2 d\tau \quad (3-34)$$

Therefore, as  $t \rightarrow \infty$  in (3-34), hence  $S_i \in L_2(0, \infty)$ .

Starting from the  $n$ -th vehicle (last in a platoon), it can be proven that  $e_n$  is also bounded and in  $L_2$ -norm, by taking (3-3) expressed with velocity and distance errors.

$$S_n = q(\dot{e}_n + \lambda e_n) \quad (3-35)$$

Since, (3-35) is stable LTI system, with input  $S_n$  and output  $e_n$  (Figure 3-3) and  $S_n \in L_2(0, \infty) \cap L_\infty(0, \infty)$  it is also true that  $e_n \in L_2(0, \infty) \cap L_\infty(0, \infty)$ .

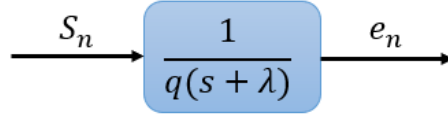


**Figure 3-3:** Stable LTI system

From (3-35) it also can be concluded that  $\dot{e}_n \in L_2(0, \infty) \cap L_\infty(0, \infty)$ , since  $S_n$  and  $e_n$  are in the same  $L$  spaces.

Taking (3-3) expressed in velocity and distance error for vehicle from  $n - 1$  to 1 it can be further proven that  $e_i$  and  $\dot{e}_i$  are bounded and in  $L_2$ -norm.

$$S_{n-1} = \underbrace{\frac{d}{dt}(qe_{n-1} - e_n)}_{\dot{g}(t)} + \underbrace{\lambda(e_{n-1} - e_n)}_{g(t)} \quad (3-36)$$

Since, (3-36) is LTI stable system with input  $S_{n-1}$  and output  $g(t)$  and  $S_{n-1} \in L_2(0, \infty) \cap L_\infty(0, \infty)$  then also  $g(t) \in L_2(0, \infty) \cap L_\infty(0, \infty)$ . Hence,  $\dot{g}(t) \in L_2(0, \infty) \cap L_\infty(0, \infty)$ .

From (3-35),  $e_n$  and  $\dot{e}_n$  are bounded and in  $L_2$ -norm, therefore from (3-36) it can be proven that  $e_{n-1}, \dot{e}_{n-1} \in L_2(0, \infty) \cap L_\infty(0, \infty)$ .

**Lemma 1** (Barbalat). *If  $f(t)$  is uniformly continuous for all  $t \geq 0$ , and if the limit of the integral*

$$\lim_{t \rightarrow \infty} \int_0^t f(\tau) d\tau$$

*exists and finite, then*

$$\lim_{t \rightarrow \infty} f(t) = 0$$

**Corollary 1.** *If  $g(t), \dot{g}(t) \in L_\infty$  and  $g(t) \in L_p$ , for some  $p = [1, \infty)$ , then  $\lim_{t \rightarrow \infty} g(t) = 0$ .*

Hence, it can be proven that  $e_i \rightarrow 0$  as time tends to infinity.

# Cooperative Adaptive Cruise Control - Experimental Setup and Evaluation

During the design process of an advanced longitudinal controller, for instance a Cooperative Adaptive Cruise Control system it is necessary to conduct a series of experiments, which should always show the results highly comparable to reality. Hence, it is necessary to introduce a vehicle's dynamics model, which is sophisticated and trustworthy.

In this chapter the implementation of the designed CACC algorithm is presented. Moreover, limitations and constraints which need to be taken into consideration to make the simulation as realistic as possible are discussed. Lastly, the vehicle model used in the experiments is explained.

## 4-1 Practical Constraints

One of the practical limitations, which have been taken into account is the data transmission among the controllers. Since modern vehicles are equipped with a lot of control systems, like ABS or ACC, there is a necessity to exchange the crucial information between those systems and electronic control units. What is more, those systems need also to receive data from different kinds of sensors. In order to limit the number of electrical wire connections among various types of systems, a CAN bus became an automotive standard. Thanks to the communication bus the number of electrical wires can be reduced. However, such a solution has a limitation concerning the rate of transmission.

It is assumed that the rate of data exchange among decentralized controllers of CACC system is set to be 100 Hz and is a constant value. The schematic connection between a CACC controller and a vehicle model is presented in Figure 4-1, where it can be noticed that the vehicle model is computed with a frequency of 1000 Hz. The rate of vehicle parameters transmission is down-rated to 100 Hz, which is also the rate of CACC controller's data exchange.

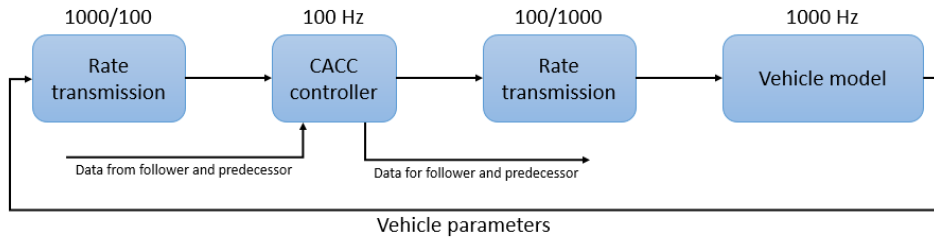


Figure 4-1: Schematic overview of connections

## 4-2 Vehicle Simulator

In this master thesis great attention is paid to the reality of the experiments of the vehicle platoon with CACC. Therefore, a realistic vehicle simulator Dynacar provided by Tecnia company is used in this project. It is a parametric vehicle dynamics simulator, which is based on Matlab/Simulink software that allows to generate different kinds of road arrangements and conduct desired traffic maneuver scenarios. Dynacar is also adapted to simulate multiple vehicles in one simulation, hence a vehicle platoon can be created. Since the software is an advanced parametric vehicle simulator, it allows to change various vehicle parameters, therefore each vehicle can have a different dynamics, hence a platoon can be heterogeneous.

In Figure 4-3 an overview of the decentralized controllers is presented. It can be noticed that each CACC controller exchanges data with its predecessor and follower, since it is the bidirectional communication structure. Each vehicle, except the platoon leader, obtains data about position, velocity and acceleration of its predecessor. The two first parameters can be measured with a radar or other type of a ranging sensor, while the acceleration is transmitted by the wireless network. The data is also transmitted from the follower to the predecessor and it is  $\dot{e}_i$ ,  $s_i$  and acceleration. Those parameters are necessary to compute  $S_i$  and a control law (3-17).

The output of the CACC controller  $u_i$  is a longitudinal traction force ( $F_x$ ) Figure 8-4, which needs to be applied to the wheels. It is so because presented continuous control law (3-17) is a model-based control based on a second order vehicle model (2-7). Hence, it is assumed that the traction force can be directly delivered to the driven wheels omitting the powertrain, throttle and brake pedals (lower level controller). The leading vehicle is following a specified velocity profile (Cruise Control), which is controlled by a PID controller.

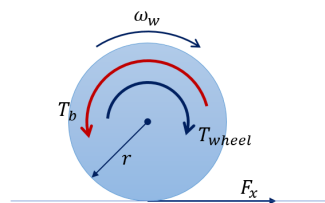


Figure 4-2: Wheel dynamics

Since the input to Dynacar simulator is a torque applied to the wheels, the traction force

$(F_x)$  needs to be converted into a torque and it can be expressed as:

$$T_{wheel, b} = rF_x \quad (4-1)$$

where  $T_{wheel, b}$  is a total desired traction or braking torque, which should be applied to the wheels,  $r$  is a radius of a wheel, which is assumed to be known and the same for each vehicle. It is also assumed that each vehicle in a platoon is front wheel driven. Since only a longitudinal direction is considered the total torque is simply divided by two and applied only to the front wheels. The braking torque is applied both to the driven and non-driven wheels with 60% of desired braking torque on front wheels and 40% on rear wheels.

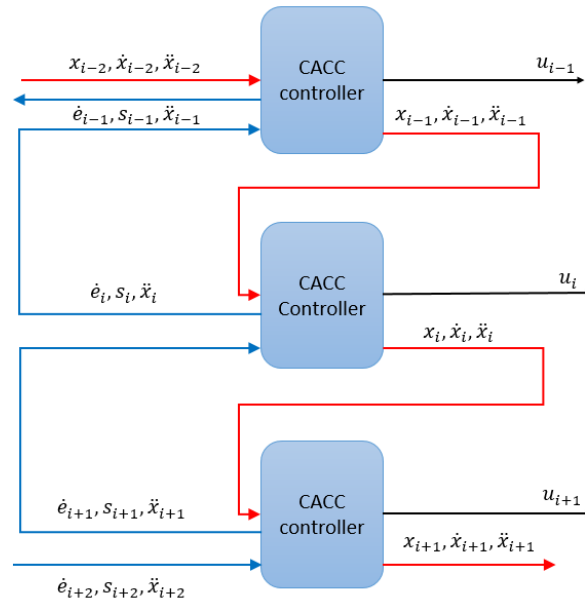


**Figure 4-3:** Bidirectional control structure

## 4-3 Dynacar - Vehicle Model

Since Cooperative Adaptive Cruise Control is a longitudinal controller, the main focus in the description of Dynacar's vehicle model is put on the longitudinal features and parameters of a car.

There is a great deal of methods to represent a longitudinal vehicle dynamics with different kinds of approaches. The complexity of the developed vehicle model depends on the purpose of usage and needed accuracy. There are quite a few aims of usage of a developed model, for instance it can be employed to study a load transfer between front and rear axle while braking or accelerating, or it can be used to verify how a suspension influences the vehicle body while hitting a bump. Therefore, a few standard practised approaches exist, such as quarter car model, half car model (bicycle model) or full car model.

The Dynacar's vehicle model is an advanced physical model based on multi-body formulation, where relative coordinates and semi-recursive equations of motion are used. The suspension

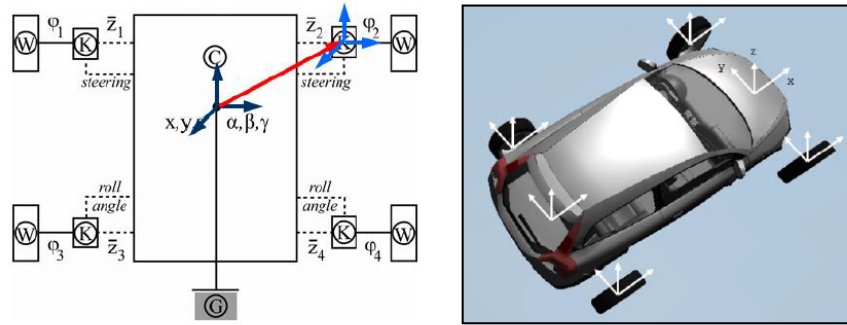


Figure 4-4: Overview of Dynacar's vehicle model, [5]

system of vehicle model is considered as macro-joints and the behaviour of each suspension system is modelled with usage of look-up tables.

In Figure 4-4 an overview of Dynacar vehicle model is presented. A local Cartesian coordinates of a point in the chassis reference frame and a Cardan angles, which provides an orientation with respect to the chassis reference frame are shown in the picture on the left. In the picture on the right an axis convention is presented. The X, Y and Z axis represent the longitudinal, lateral and vertical directions, respectively. Also in the model the roll, pitch and yaw rotations are considered around X, Y and Z axis, respectively.

To see in details vehicle dynamics model see 8.

#### 4-4 Evaluation of Designed Controller

The evaluations of the conducted simulation of the designed Cooperative Adaptive Cruise Control are presented in this section. All of the presented simulations are conducted in Matlab/Simulink with continuous control law (3-17) explained in the CACC design chapter (3). Since an important factor is reality of the experiments, all the simulations are conducted with Dynacar vehicle simulator in order to provide results as realistic as possible. Also each simulation is evaluated with comfort and safety indicators presented in 2-6.

#### 4-5 Heterogeneous Platoon

All the simulations presented in this chapter are conducted for a platoon of seven vehicles. Since the heterogeneity of the vehicles in realistic environment is something obvious, the simulations are also carried on with a heterogeneous platoon, where all the vehicles in a platoon are assumed to be passenger cars and the parameters of a vehicle are uncertain. Table 4-1 presents the uncertain parameters of each vehicle in a platoon. It can be seen that it is assumed, that the vehicular platoon is heterogeneous in sense of the vehicles' mass, frontal cross area and aero drag coefficient.

Vehicle number	1	2	3	4	5	6	7
Mass [kg]	1100	1800	1750	1500	1200	1350	1600
Frontal cross area [m <sup>2</sup> ]	1.78	2.18	2.15	2.01	1.84	1.92	2.06
Aero drag coefficient [-]	0.3	0.2	0.25	0.32	0.4	0.28	0.21

**Table 4-1:** Platoon heterogeneity - uncertain parameters

In all those simulations the desired inter-vehicle distance is assumed to be constant and is 20 meters for each vehicle.

## 4-6 Simulation Results

In this section the results of simulations with realistic vehicle models (Dynacar) for a heterogeneous vehicular platoon are presented. The simulations are conducted for different traffic scenarios. Later on simulation results with disturbances and system delays are shown.

### 4-6-1 Traffic Scenario Design

The performances of designed CACC algorithm are tested in different highway scenarios [32]. In the paper specific velocity profiles are proposed, which the leading vehicle, equipped with Cruise Control system is suppose to follow.

#### 1. Normal scenario

This scenario mimics the typical highway traffic motion and its main purpose is to check how the vehicular platoon performs with some gentle accelerating and decelerating. All the vehicles start with zero distance error and the same velocity of 20 m/s. After 20 seconds the velocity increases to 25 m/s in 10 seconds. In 95-th second the velocity decreases to 15 m/s and stays constant till the end.

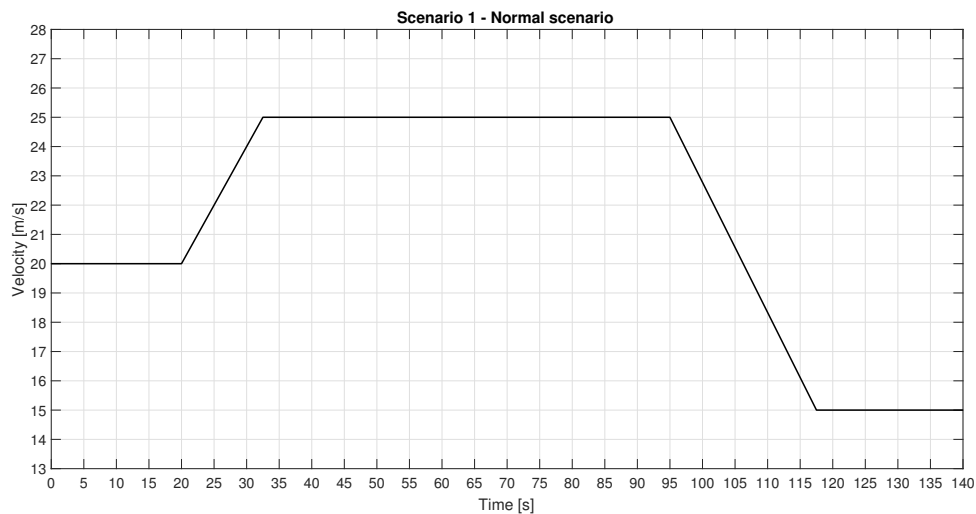


**Figure 4-5:** Scenario 1 - Normal highway scenario

## 2. Stop and Go scenario

In this scenario a traffic jam is simulated. It provides a possibility to check the behaviour of the platoon after a total stop. Similarly as in normal scenario all the vehicles start with zero distance error and the same velocity of 10 m/s. In 5-th second the braking action is applied till total stop, which lasts 20 seconds. Next, within 42 seconds the leading vehicle accelerates up to 15.6 m/s. In 130-th second the vehicle again decelerates gently to 0 m/s and stays until the end of simulation.

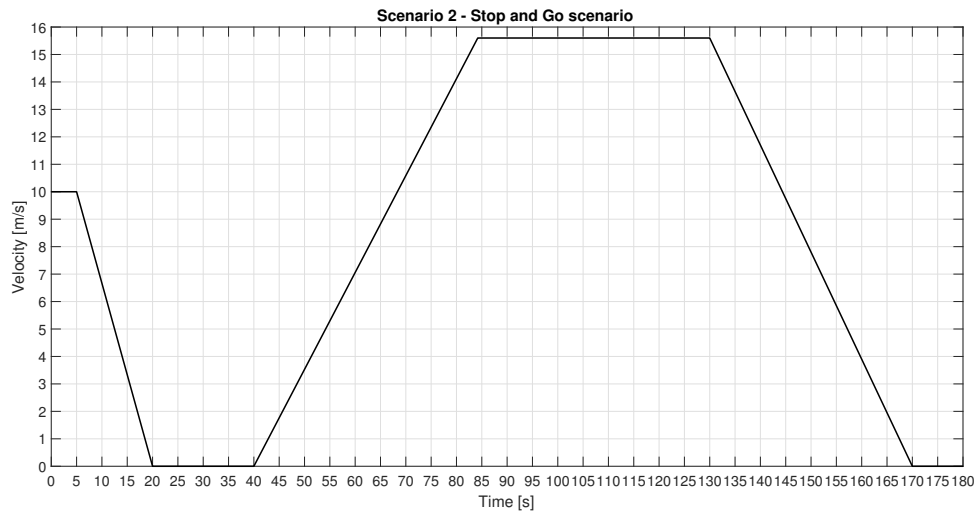


Figure 4-6: Scenario 2 - Stop and Go scenario

## 3. Emergency braking scenario

The scenario mimics a heavy braking action, which may occur in a highway traffic, for instance a sudden break down of the vehicle in front of the vehicular platoon. All the vehicles travel with zero distance error with the speed of 25 m/s. In 10-th second a sudden braking action is applied by a leading vehicle, which lasts 5 seconds until total stop.

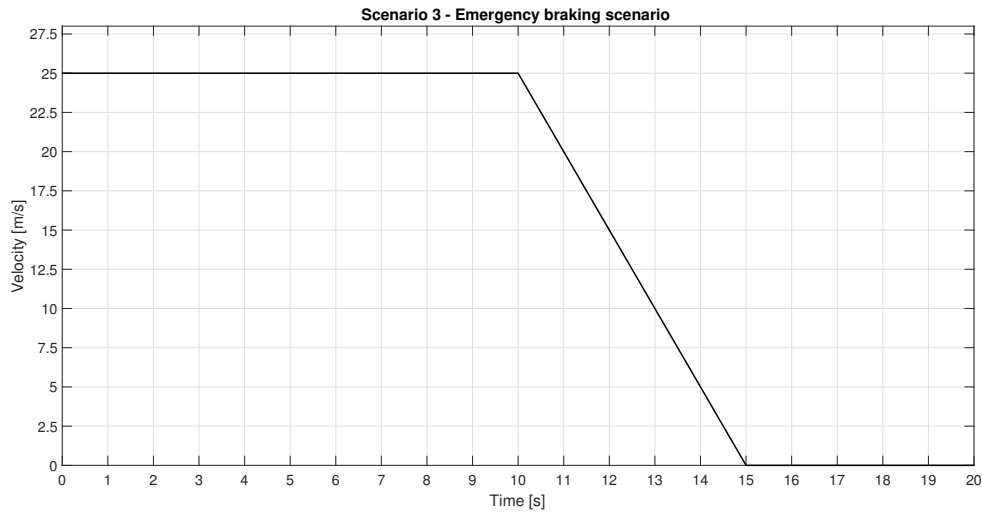


Figure 4-7: Scenario 3 - Emergency braking scenario

#### 4. Joining the platoon scenario

In this scenario a platoon leader travels the whole time with constant speed of 27.7 m/s and the starting distance error is zero, except the last vehicle, which is joining the platoon. The last vehicle is assumed to be 50 meters behind the predeceasing vehicle and is approaching the platoon with the speed of 36.1 m/s. It is assumed that the approaching vehicle is from the very beginning already in the range of wireless communication network and radar network with the predeceasing vehicle.

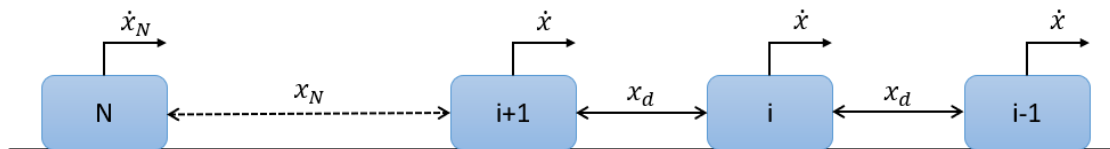


Figure 4-8: Joining the platoon scenario

### 4-6-2 Heterogeneous Platoon Simulation

The first series of simulations are conducted for the heterogeneous (Table 4-1) platoon. In this section the behaviour of the vehicular string is tested with all 4 traffic scenarios explained above. In all of the presented scenarios the vehicles in a platoon begin with zero distance error and the same longitudinal velocity, except the joining scenario.

#### Scenario 1 - Normal Scenario

As it can be observed, for a normal highway scenario the behaviour of the vehicular platoon performs the string stability in sense of relative distance. The acceleration action applied by

the leading vehicle in 20-th second is  $0.4 \text{ m/s}^2$  and as it can be seen the rest of the platoon also achieves the same acceleration with small oscillation at the beginning and at the end of this acceleration maneuver. The biggest overshoot in the acceleration in 20-th second is achieved by the 5-th vehicle and is equal to  $0.6 \text{ m/s}^2$  and  $-0.22 \text{ m/s}^2$  in 33-rd second. Later on the platoon travels with constant speed and each vehicle achieves zero acceleration, as can be expected. During the braking action, which starts in 95-th second the achieved deceleration by the leader is  $-0.44 \text{ m/s}^2$  with small overshoot at the beginning. The platoon followers decelerate with gently oscillatory behaviour, but finally achieve the deceleration value of the leader vehicle. The recovery from the braking action in 117-th second causes a small acceleration peak for the following vehicles (maximum acceleration value for 5-th vehicle is  $0.64 \text{ m/s}^2$ ). This acceleration peak is caused by a sudden torque applied to the wheels by the platoon followers. However, after 124-th second the acceleration converges to zero.

The acceleration and deceleration values fulfill the limits stated in ISO 22179 standard (Figure 2-3b, Figure 2-3a).

The error propagation indicator (MRV) shown in Table 4-2 confirms that the platoon error is attenuated along the vehicular string. The relative velocity performs a small amplitude oscillatory behaviour, which finally stabilizes at zero.

Vehicle number (i)	1	n
MRV ( $\ \dot{e}_i\ _{\infty}$ , [m/s])	0.23	0.05

**Table 4-2:** Scenario 1 - MRV

## Scenario 2 - Stop and Go scenario

In a Stop and Go scenario the vehicular platoon is tested in terms of recovery from full stop and behaviour of the vehicles at relatively low speeds. As it can be noticed the platoon performs also string stably in sense of the relative distance errors for the whole time of simulation (Figure 4-12). Similarly as in the first scenario during the braking action the platoon braking input is oscillatory, but after some time it converges to the acceleration value of the leader. The first deceleration begins in 5-th second and the value of deceleration of the leader is  $-0.67 \text{ m/s}^2$ , while the overshoot of the last vehicle achieves  $-1.02 \text{ m/s}^2$ . The same as in scenario 1 after acceleration action the torque applied to the wheels performs a sudden peak, what causes an acceleration peak, which is maximal for the 6-th vehicle and is equal  $1.15 \text{ m/s}^2$ , while the leader's acceleration value is  $0.35 \text{ m/s}^2$ , however after 4 seconds the acceleration of the following vehicles reaches the constant value of  $0.35 \text{ m/s}^2$ . Later on in 130-th second another braking action occurs, although this time it is gentle and the deceleration oscillations are not as big as in the beginning. Achieved acceleration values are also satisfactory according to the ISO 22179 standard.

Similarly, as in the first scenario the propagation of error is diminished along the end of the platoon. The highest peak in the relative vehicles occurs around 8-th second and the values of MRV are smaller for each pair of vehicles moving to the end of the string.

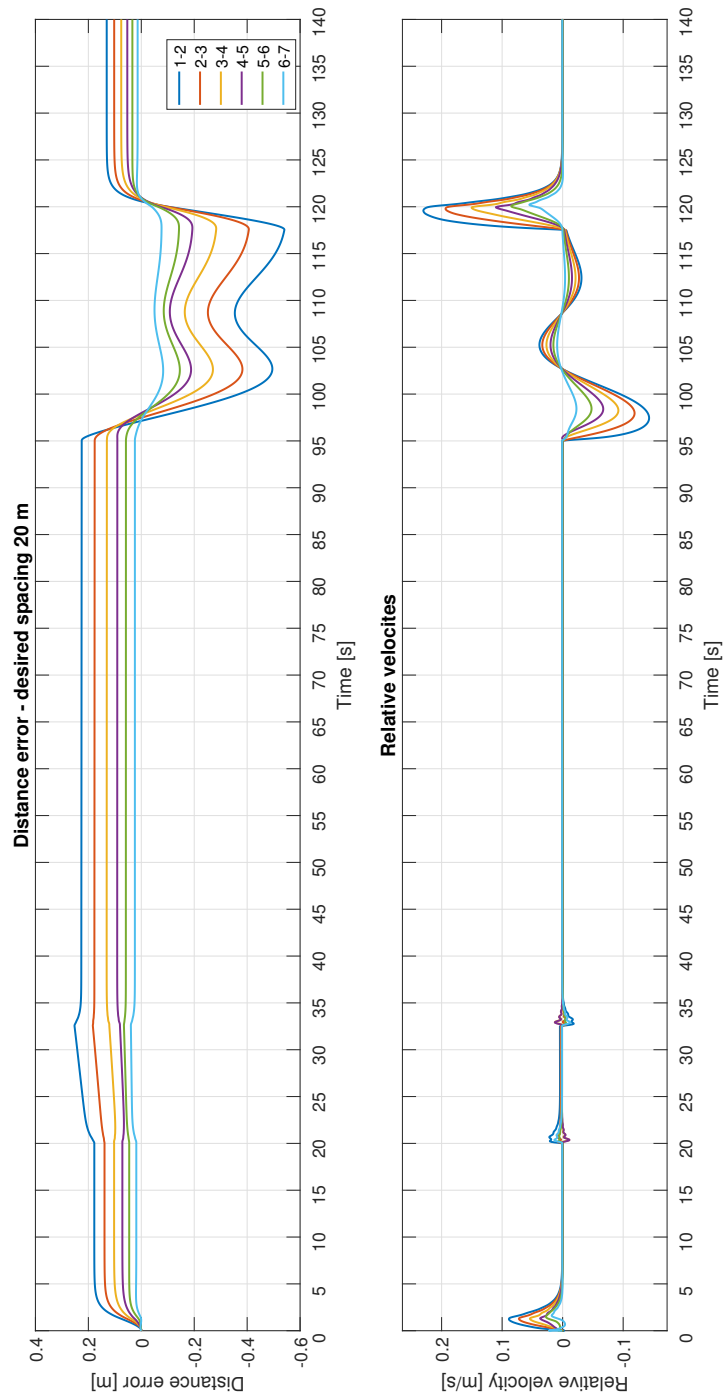


**Figure 4-9:** Scenario 1 - distance error and relative velocity

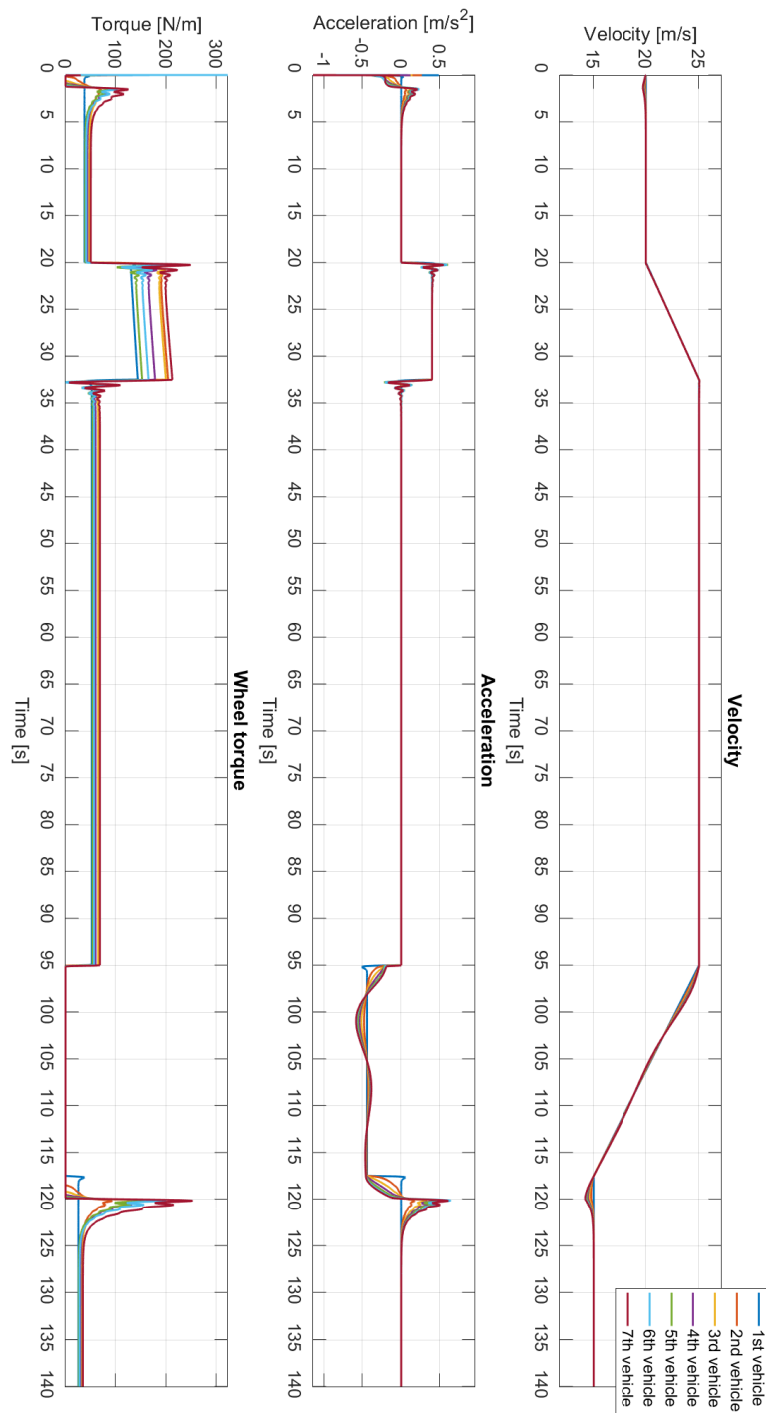


Figure 4-10: Scenario 1 - vehicles velocity, acceleration and wheel torque

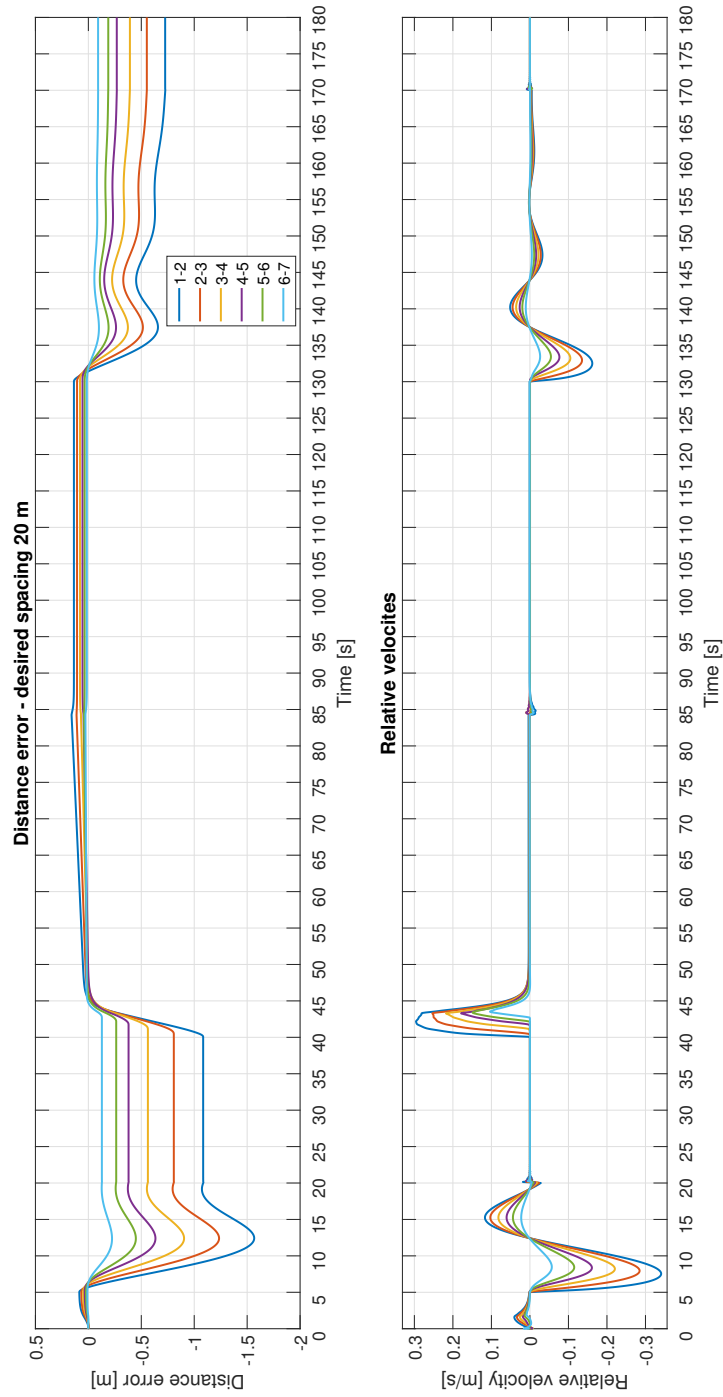


Figure 4-11: Scenario 2 - distance error and relative velocity

Vehicle number (i)	1	n
MRV ( $\ \dot{e}_i\ _\infty$ , [m/s])	0.34	0.056

**Table 4-3:** Scenario 2 - MRV

### Scenario 3 - Emergency braking scenario

In emergency braking scenario the behaviour of the platoon in an emergency situation is checked. The heavy braking action starts at 10-th second and lasts 5 seconds, as it can be seen in Figure 4-14 the deceleration applied by the leading vehicle is  $-5 m/s^2$  with an overshoot ( $-5.6 m/s^2$ ). The following vehicles apply a braking action, where for almost 3.2 seconds the deceleration of each vehicle is smaller than the leader's. However, after that time the followers' deceleration overpasses  $-5m/s^2$  and for the 7-th vehicle it achieves  $7.2 m/s^2$ . After the velocity of a vehicle reaches  $0 m/s$  the oscillatory behaviour of acceleration appears. This phenomenon lasts for around 1.5 seconds or less, depending on the index number of the vehicle in a platoon. Those values of deceleration do not fulfill requirements stated in ISO standard for FSRA, however such a situation is exceptional and unusual. Thanks to such big deceleration values the rear-end collision is avoided, what is shown in Figure 4-13, where it can be noticed that the string stability is maintained.

As shown in Figure 4-13 the maximum peak of each pair of the vehicles in the platoon is smaller toward the end of the string. It can be stated that the error propagation is also attenuated, even for such an unusual scenario as emergency braking.

Vehicle number (i)	1	n
MRV ( $\ \dot{e}_i\ _\infty$ , [m/s])	2.93	0.44

**Table 4-4:** Scenario 3 - MRV

### Scenario 4 - Joining the platoon scenario

In this scenario a new vehicle is joining the platoon, where vehicles travel with constant speed. The aim of this experiment is to check how the string of vehicles behaves in such a situation. It is assumed that from the very beginning the approaching vehicle is already connected in a wireless way with the platoon (it is able to exchange data with other vehicles). Since the simulation is conducted for bidirectional information flow topology platoon structure it can be seen that the behaviour of the vehicle at the back can influence the behaviour of the leading vehicles. In Figure 4-15 it can be seen that the approaching vehicle causes the distance error to increase (the gap is bigger) between the vehicles up to  $1.2 m$ . Then when the approaching vehicle reaches the desired inter-vehicle distance of  $20 m$  the whole platoon stabilizes. It is explicitly visible in the velocity plot (Figure 4-16) how the approaching vehicle influences the whole platoon. It can be seen that the platoon at the beginning tries to "wait" for an approaching vehicle, but after it tries to correct the desired platoon velocity. It causes a small oscillatory behaviour around the velocity of the leader (the deviation from leader's velocity is  $[-1.7 1.1] m/s$ ). Unfortunately, this behaviour causes a sudden wheel torque action, what

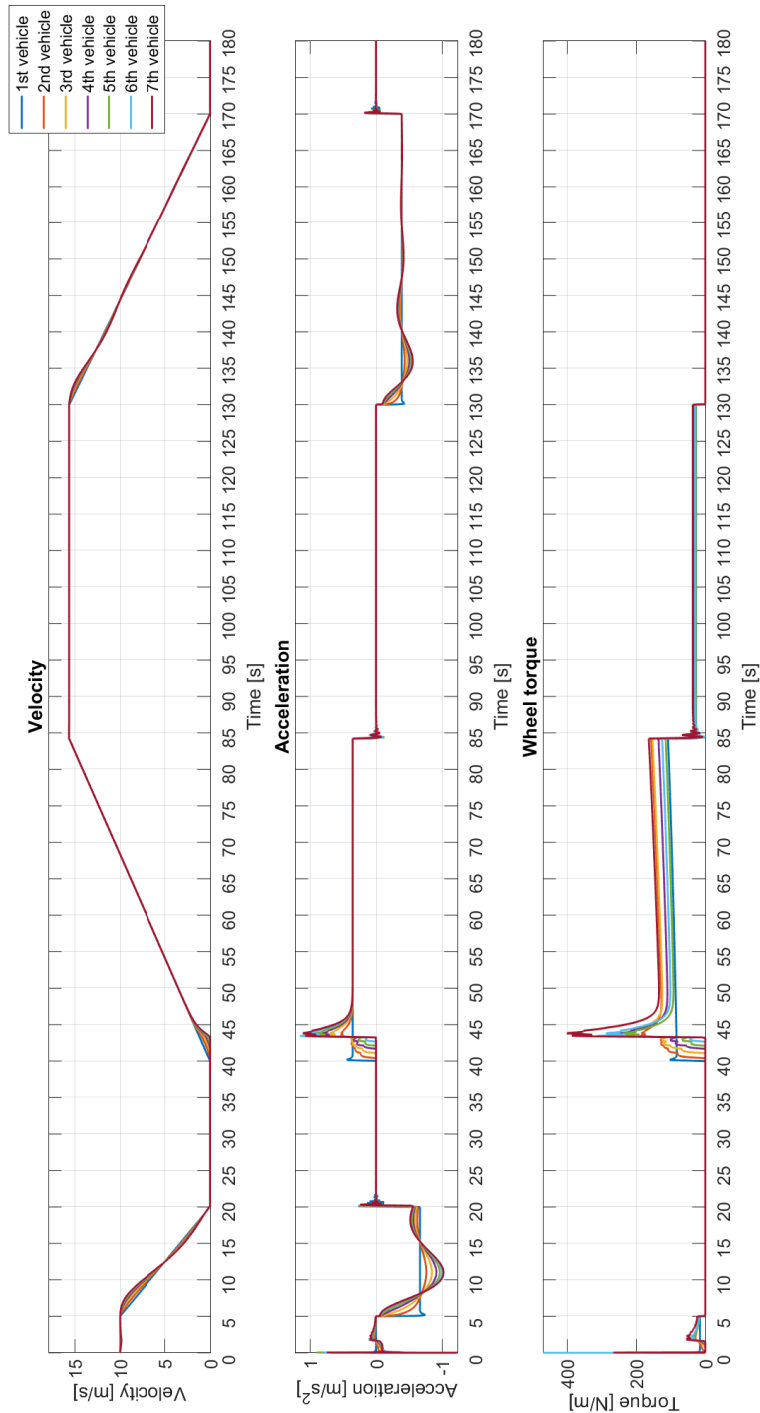
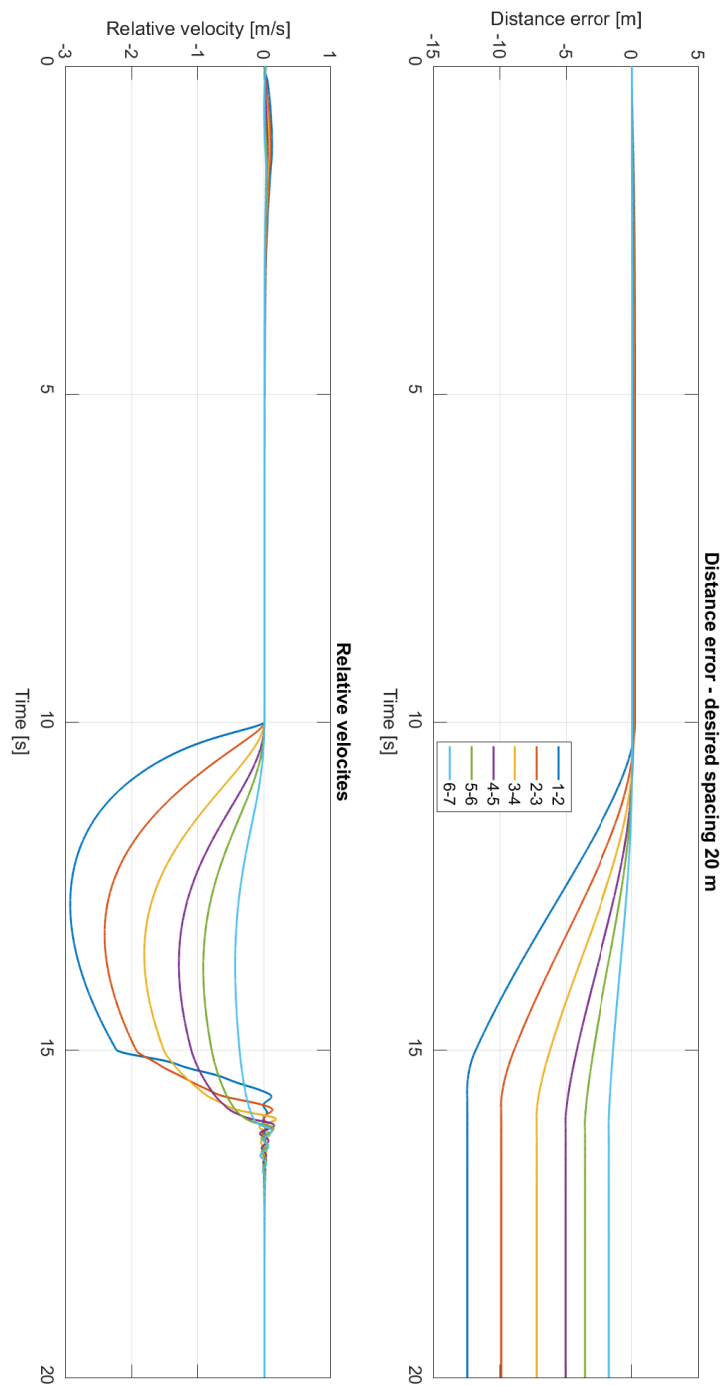


Figure 4-12: Scenario 2 - vehicles velocity, acceleration and wheel torque



**Figure 4-13:** Scenario 3 - distance error and relative velocity

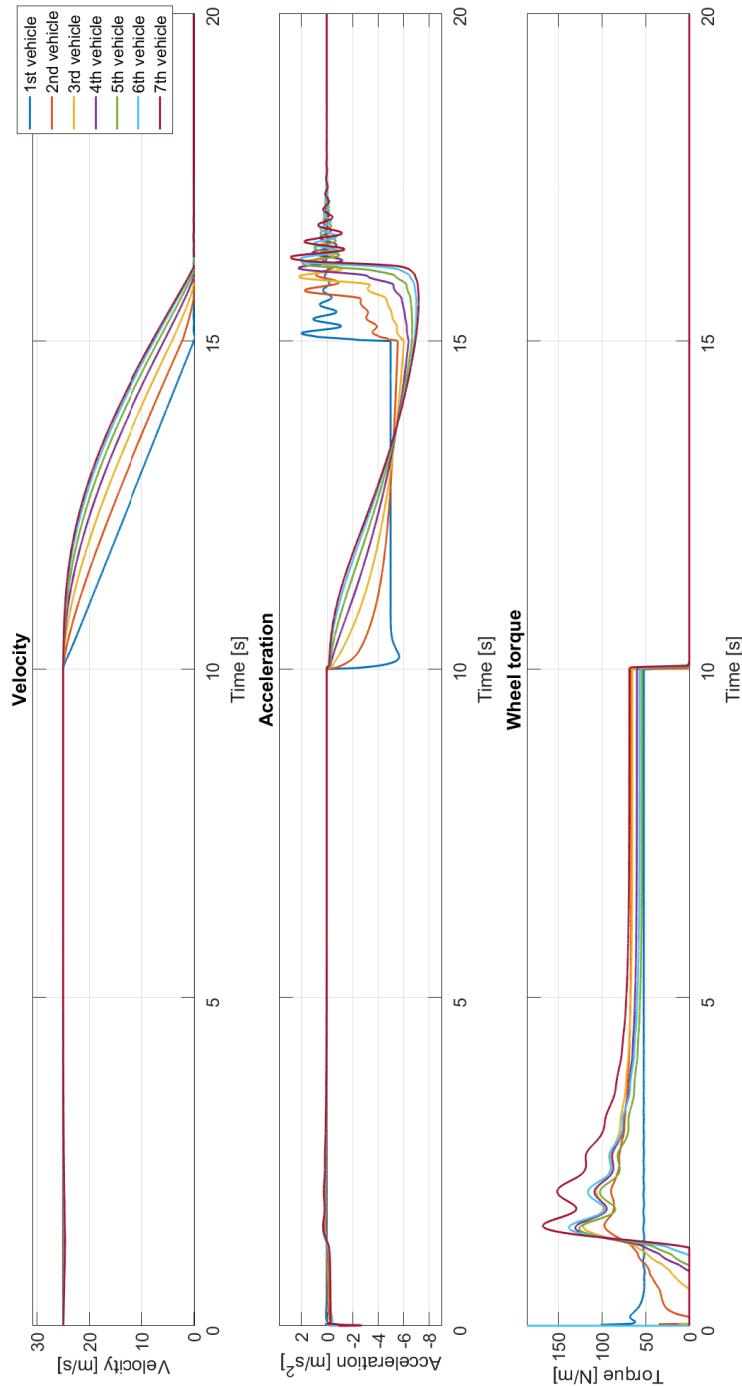


Figure 4-14: Scenario 3 - vehicles velocity, acceleration and wheel torque

in effect causes an acceleration peak, which reaches even  $3 \text{ m/s}^2$  for the 6-th vehicle in 5-th second. Such an acceleration is still compliant with ISO standard, since above the velocity of  $20 \text{ m/s}$  the average acceleration over 2 seconds cannot be bigger than  $2 \text{ m/s}^2$ . The average acceleration of 6-th vehicle in period of time from 4.5-th to 6.5-th second is equal  $1.37 \text{ m/s}^2$ .

In this scenario also a string stability is maintained since for all times the distance error is being attenuated toward the end of the platoon.

### 4-6-3 Heterogeneous Platoon Simulation with Disturbances

In this section, the simulations of a heterogeneous platoon with disturbances are presented. The disturbances are assumed to be a headwind, which affects the whole platoon. There are three scenarios, where the varying function is a wind amplitude. The chosen wind speed can be expressed in a Beaufort scale, which is a 12-level scale. The wind speed is presented in Table 4-5. All of those simulations are based on scenario 1 - Normal highway traffic.

Wind scenario	1	2	3
Wind speed [m/s]	2.5	6.67	15.6
Beaufort scale	2	4	7

**Table 4-5:** Wind scenarios

#### Light breeze

In the case of a platoon on which a headwind is acting with Beaufort scale 2 wind, it is observable that the platoon in behaviour resembles the situation from 4-6-2. It is so, because the wind is very light and does not influence the motion of the vehicles significantly. The string stability in sense of distance error is maintained and the acceleration profiles of each vehicle in a string are almost identical to the mentioned scenario 1 in 4-6-2.

The propagation error indicator (MRV) is also almost identical to the values shown in Table 4-2.

Vehicle number (i)	1	n
MRV ( $\ \dot{e}_i\ _\infty$ , [m/s])	0.22	0.05

**Table 4-6:** Light wind scenario - MRV

#### Moderate breeze

Unlike in the first wind scenario, in the case of a stronger wind (4 in Beaufort scale) it is visible that the headwind influences the behavior of the vehicular platoon, which is expected. First of all, the applied wheel torque is bigger, however the acceleration and deceleration of the leading vehicle stays at the same level as in 4-6-2 ( $0.4 \text{ m/s}^2$  and  $-0.44 \text{ m/s}^2$ ). Due to the additional aero force (headwind) the oscillatory behaviour damps slightly. However, again the recovery from braking action causes the same peak in wheel torque, hence there is also a peak in acceleration.

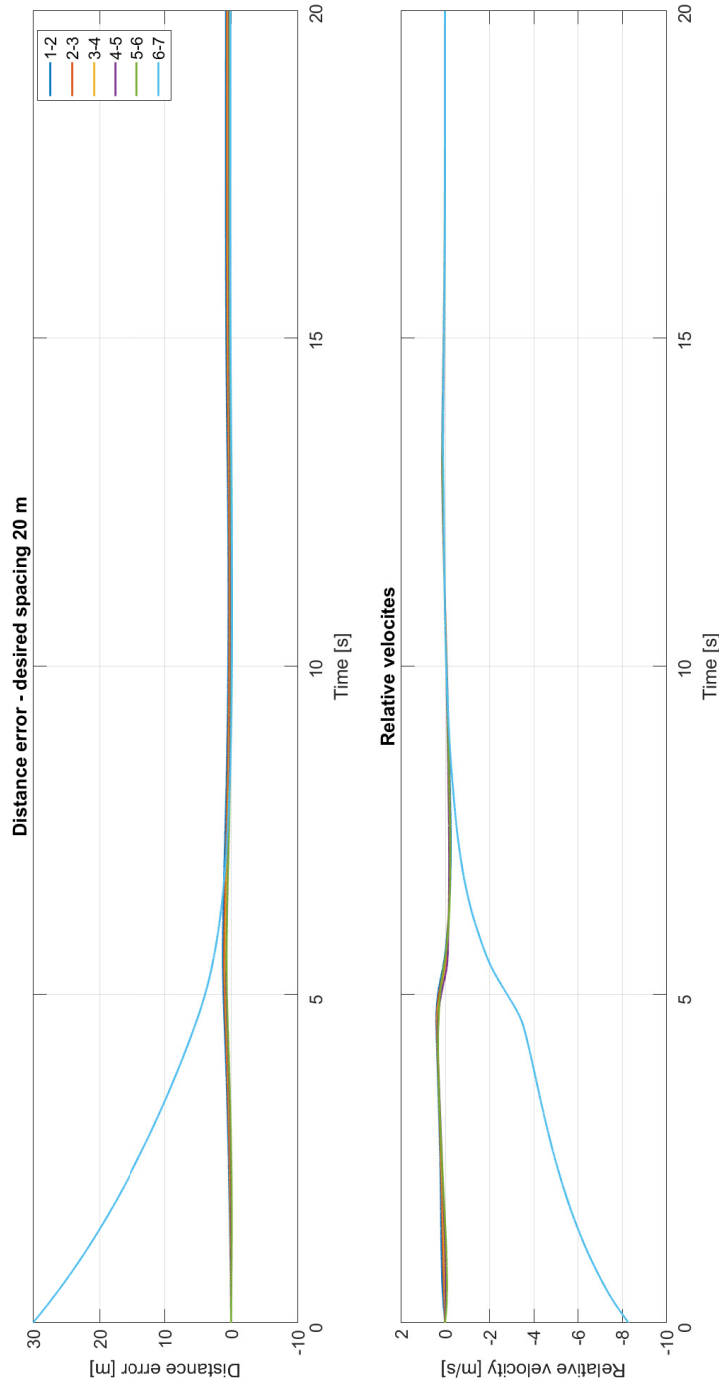


Figure 4-15: Join scenario - relative distance and relative velocity

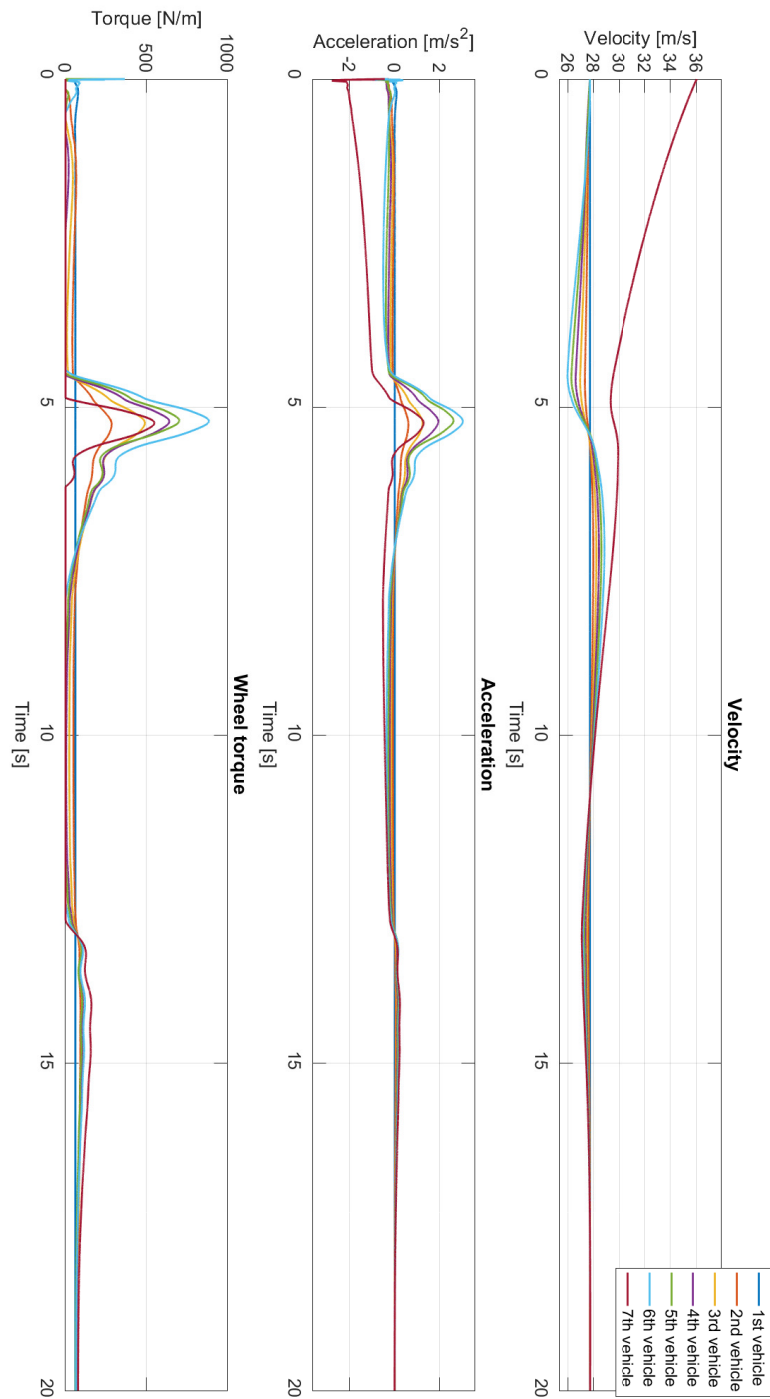
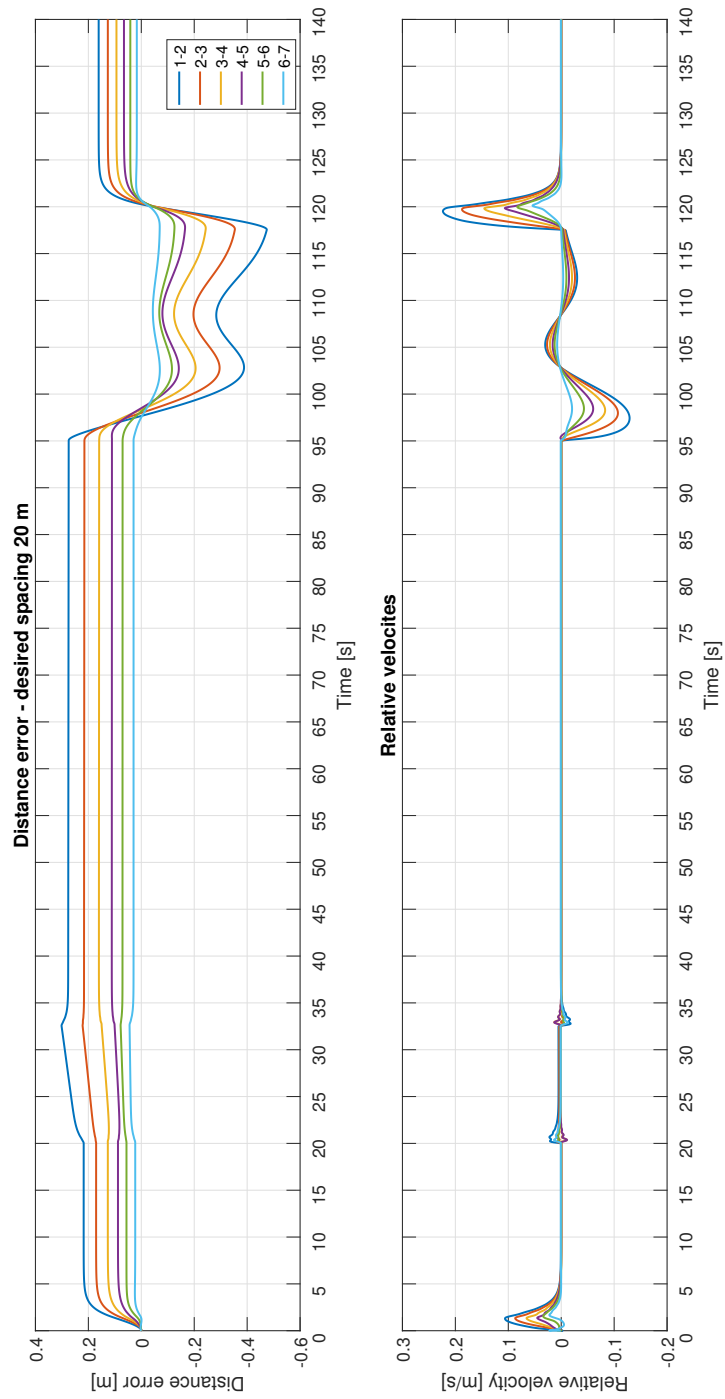
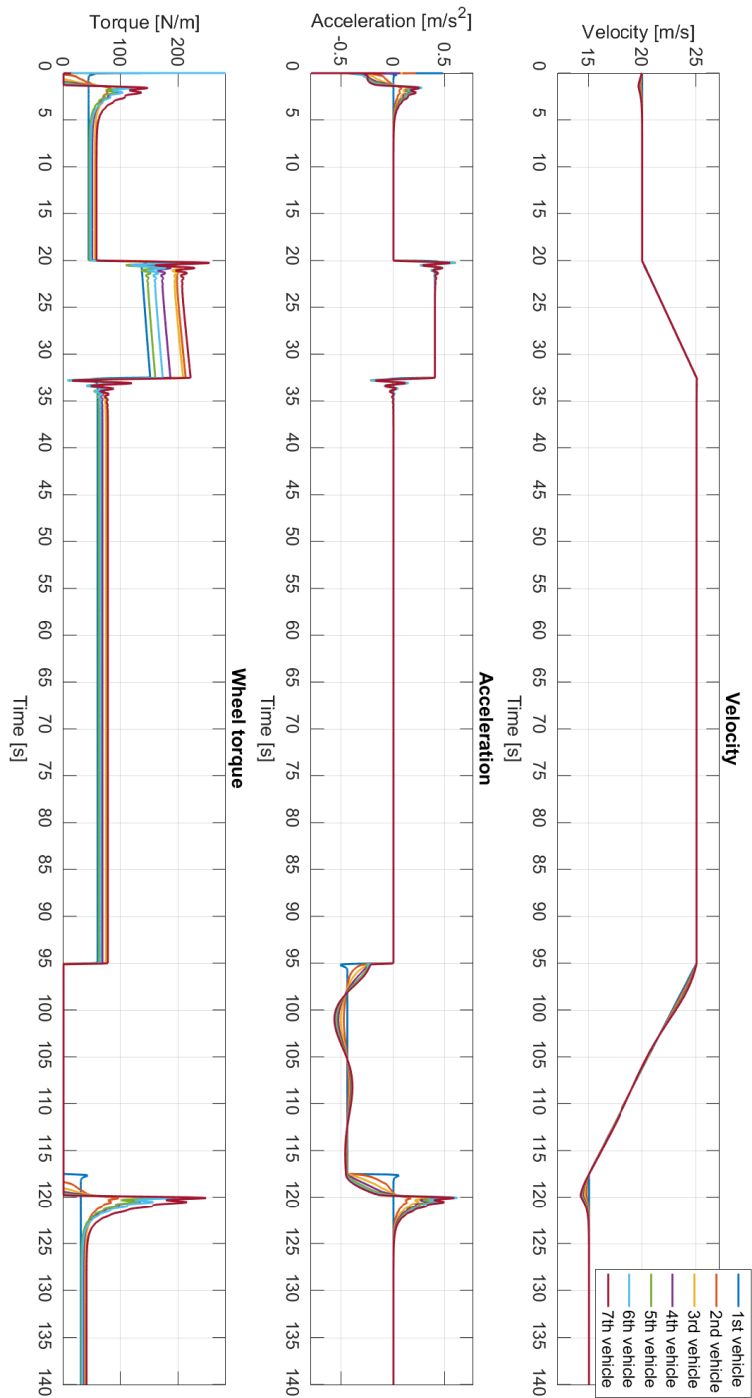


Figure 4-16: Join scenario - vehicles velocity, acceleration and wheel torque



**Figure 4-17:** Disturbance (light breeze) - relative distance and relative velocity



**Figure 4-18:** Disturbance (light breeze) - vehicles velocity, acceleration and wheel torque

The relative distance plot (Figure 4-19) indicates that in the platoon a string stability is achieved.

Again, as previously there is no error propagation as the relative velocity decreases towards the end of the platoon.

Vehicle number (i)	1	n
MRV ( $\ \dot{e}_i\ _\infty$ , [m/s])	0.35	0.11

**Table 4-7:** Moderate wind scenario - MRV

### Strong wind

In the case of the strong wind (7 in a Beaufort scale) it is instantly visible that a platoon becomes locally string instable. In 117-th second the relative distance between first and second pair of vehicles becomes smaller than the relative distance between the other vehicles in the platoon. However, it almost instantly recovered and the platoon becomes again string stable. It is also obvious that the torque applied to the wheels increases with the stronger wind (Figure 4-22). It can be observed that the acceleration of the vehicles is damped and the oscillation is smaller than it was in the previous simulations results. The achieved accelerations and decelerations are in compliance with ISO 22179 standard.

The relative velocities, which are assumed to be a propagation of error indicator are indicating that the errors in the platoon are attenuated.

Vehicle number (i)	1	n
MRV ( $\ \dot{e}_i\ _\infty$ , [m/s])	0.27	0.1

**Table 4-8:** High wind scenario - MRV

### 4-6-4 Heterogeneous Platoon Simulations with Delays

In this section in the heterogeneous platoon the delays are introduced. Two first experiments are conducted with the radar and wireless network delay, while in the third experiment also a "powertrain" delay is added. It is assumed that all the delays are constant and in case of radar the delay is equal 0.1 s and for the wireless network the delays are 0.15 s and 0.3 s.

The simulations of the vehicular platoon are conducted for the scenario 1 - normal highway scenario.

#### Radar delay of 0.1 s and wireless delay of 0.15 s

In the case when the radar and wireless network delays are 0.1 s and 0.15 s respectively, the behaviour of the platoon is comparable to the simulations from 4-6-2. The acceleration and the deceleration profiles are of the same values, however the small oscillations after the

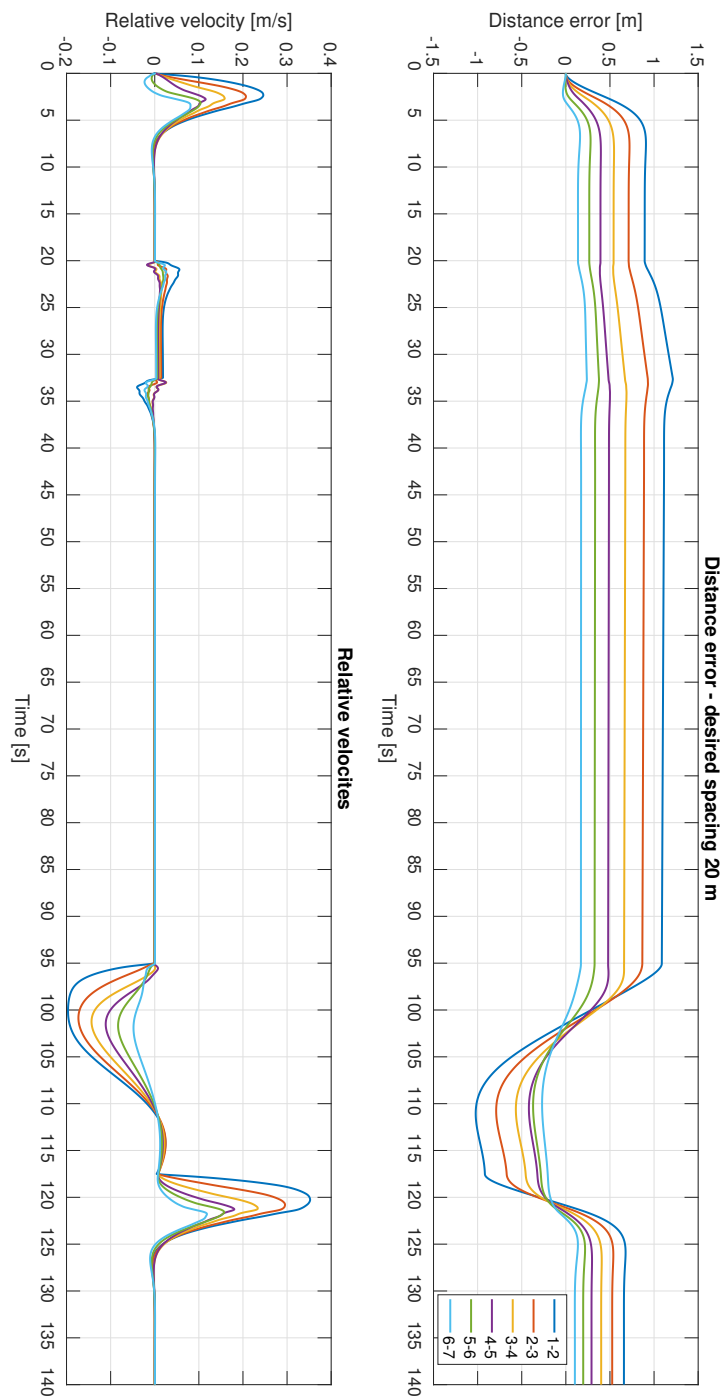


**Figure 4-19:** Disturbance (moderate breeze) - relative distance and relative velocity

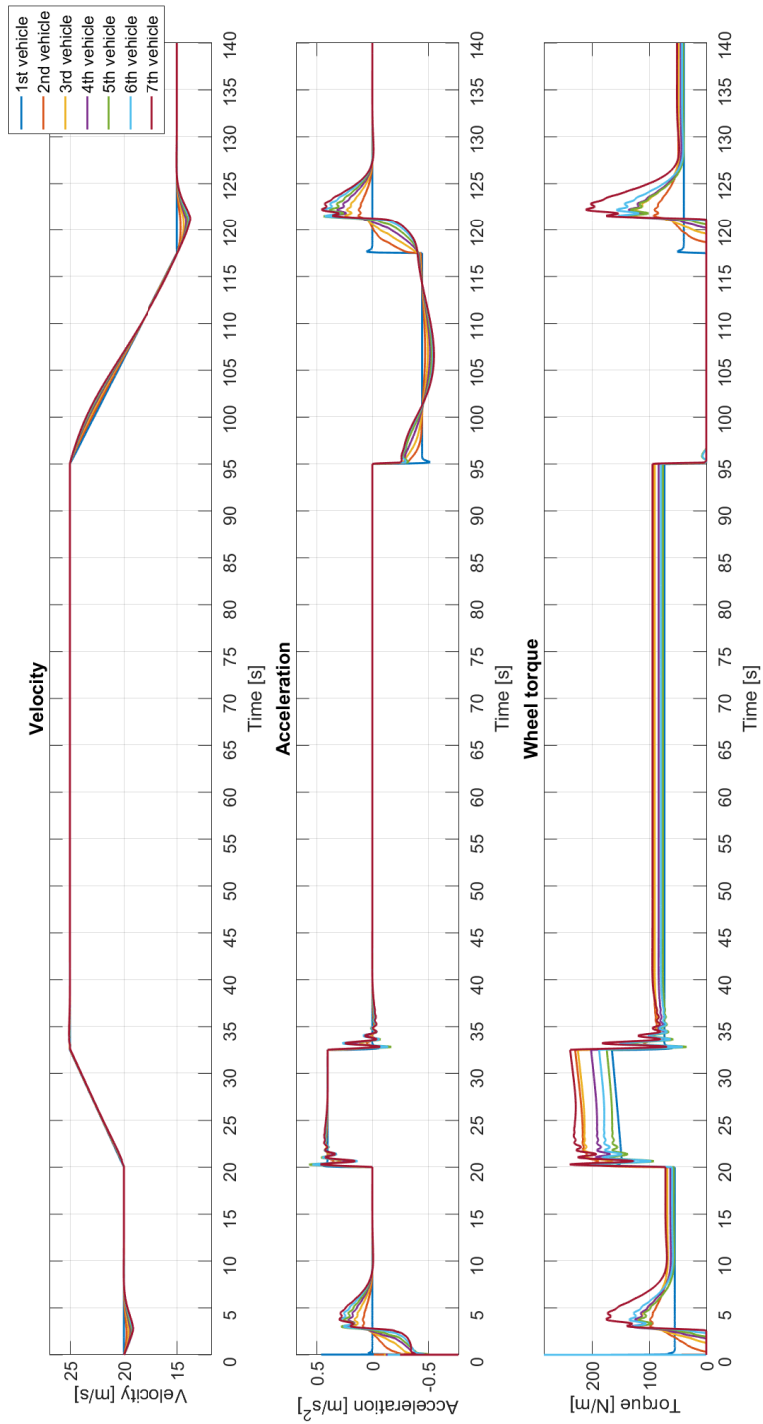


**Figure 4-20:** Disturbance (moderate breeze) – vehicles velocity, acceleration and wheel torque

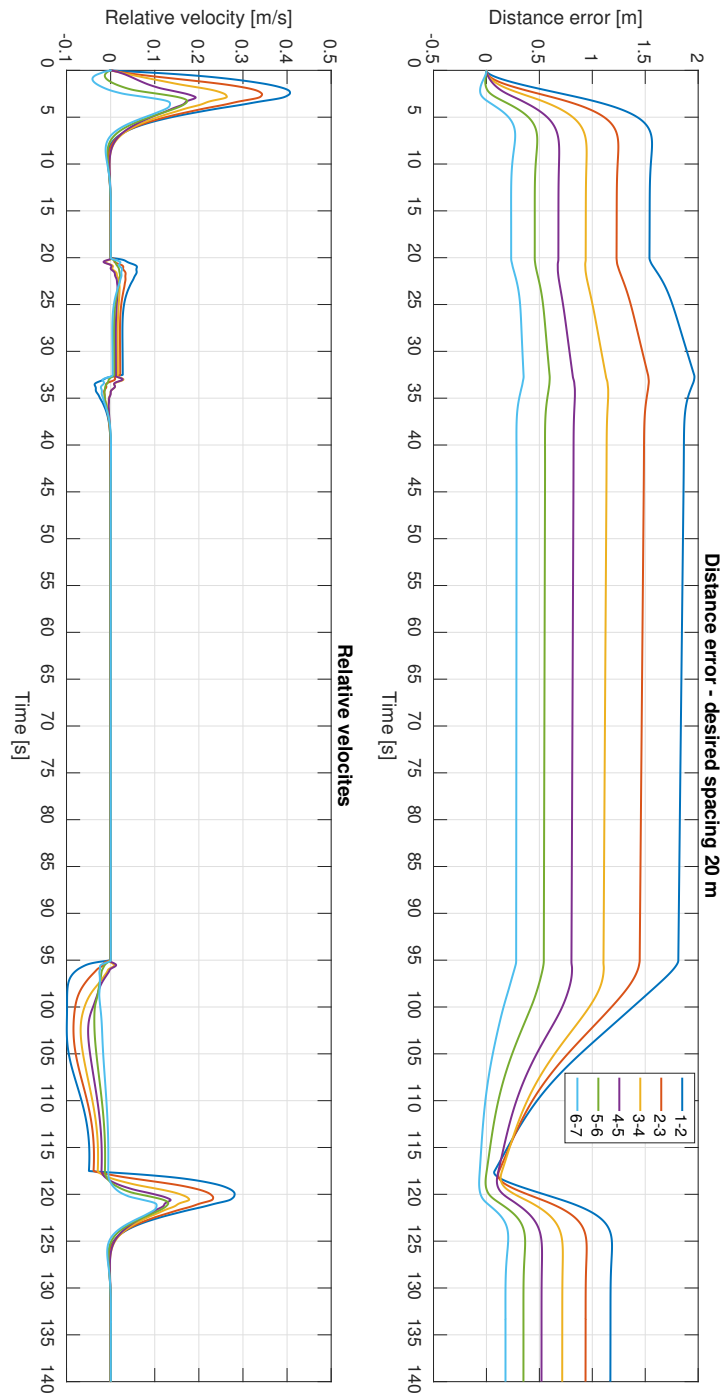
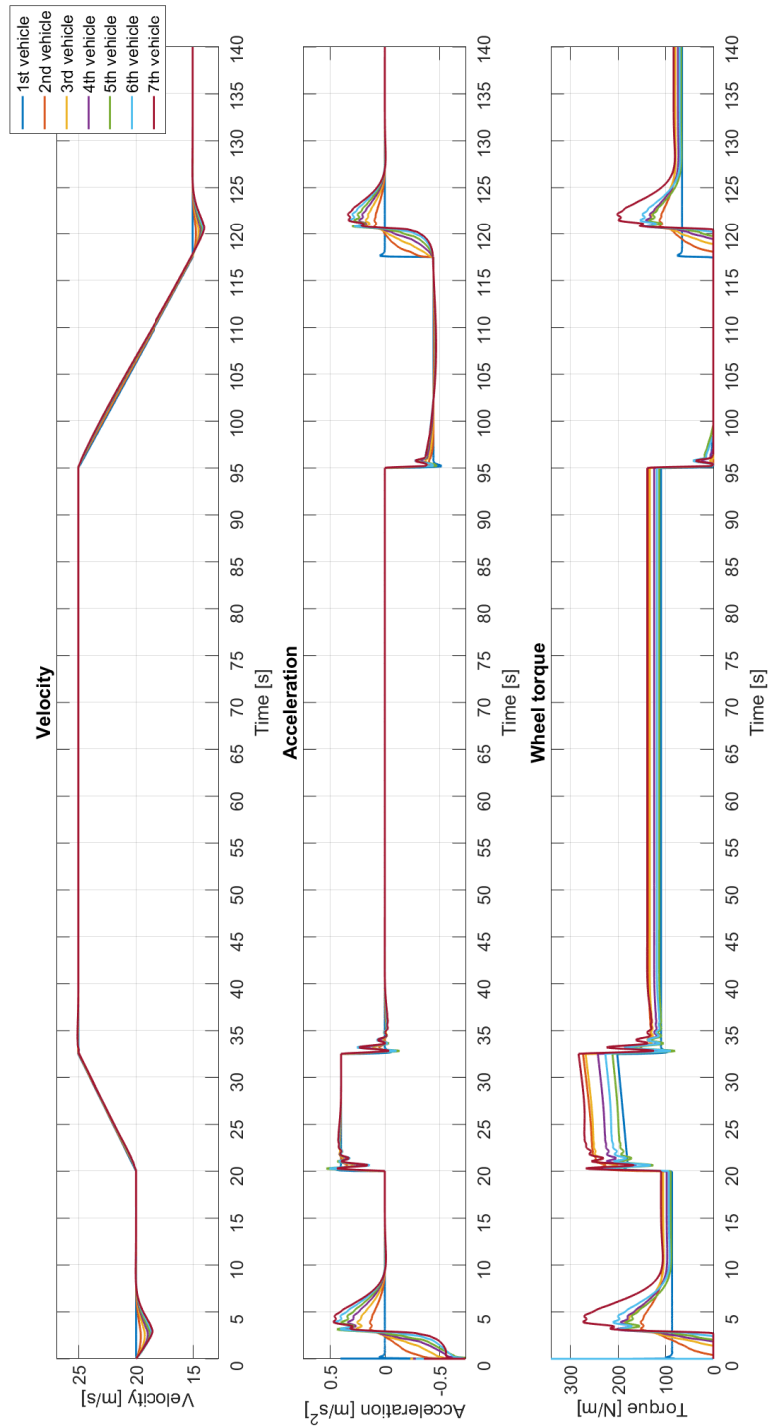
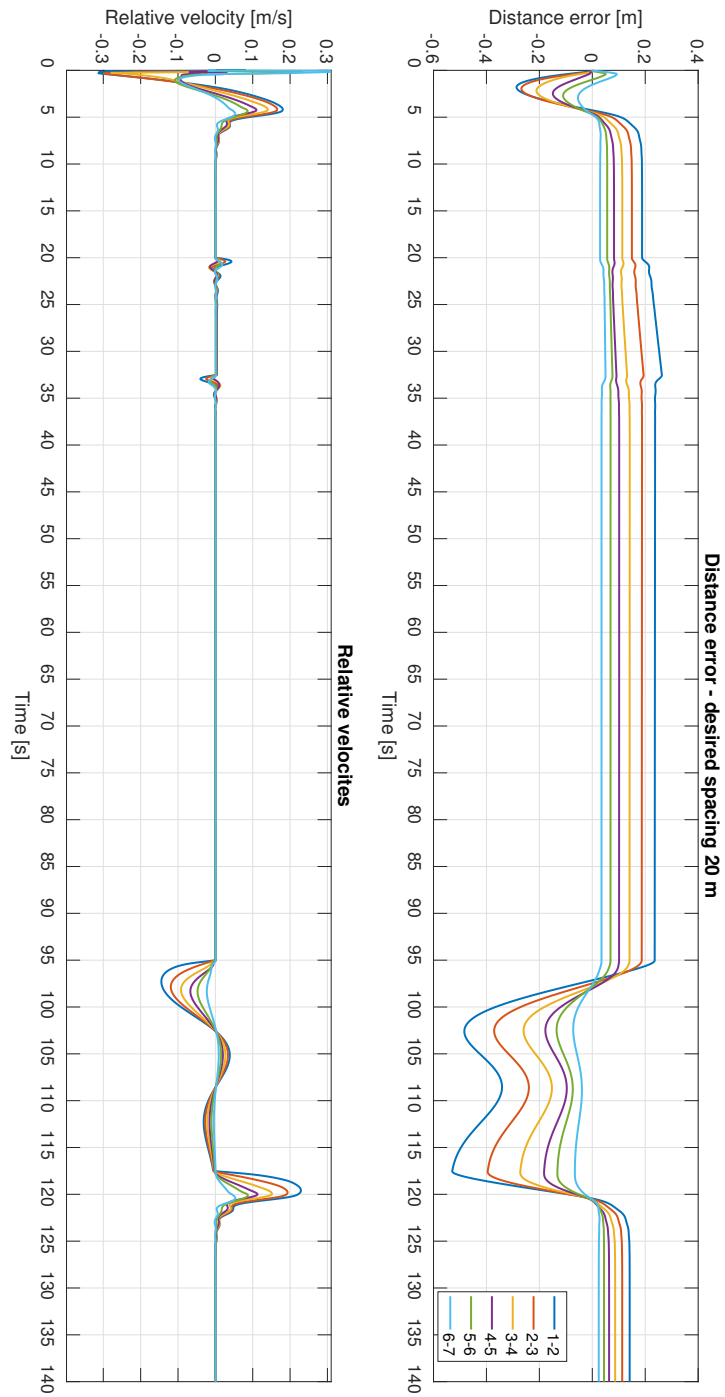


Figure 4-21: Disturbance (strong wind) - relative distance and relative velocity



**Figure 4-22:** Disturbance (strong wind) - vehicles velocity, acceleration and wheel torque



**Figure 4-23:** Delay (radar - 0.1 s, wireless - 0.15 s) - relative distance and relative velocity

transient action last longer. One can also observe that the applied wheel torque is smoother, nonetheless the peak values are bigger.

Both the string stability and propagation error indicator (relative velocity) are satisfying, meaning the platoon is string stable, hence the errors are attenuated. Also similar to the scenario from 4-6-2 the ISO standards are fulfilled.

Vehicle number (i)	1	n
MRV ( $\ \dot{e}_i\ _\infty$ , [m/s])	0.23	0.05

**Table 4-9:** Radar (0.1 s) and wireless (0.15 s) delay scenario - MRV

### Radar delay of 0.1s and wireless delay of 0.3s

At first, it can be seen that increasing the delay (0.3 s of wireless communication delay) the oscillations after a transient action last longer than before 4-6-4 and the amplitude of the acceleration is also higher (with wireless delay of 0.3 s an acceleration peak in 21-st second is  $0.76 \text{ m/s}^2$ , while with a delay of 0.15 s the peak is equal to  $0.69 \text{ m/s}^2$ ). However it can be seen that the sting stability in sense of relative distance is maintained.

The maximal values of relative velocities are the same as in the case of the previous experiment, however the peaks are shifted relative to each other.

Vehicle number (i)	1	n
MRV ( $\ \dot{e}_i\ _\infty$ , [m/s])	0.23	0.05

**Table 4-10:** Radar (0.1 s) and wireless (0.3 s) delay scenario - MRV

### Radar delay of 0.1s, wireless delay of 0.15s and "powertrain" delay of 0.2s

In the last scenario with heterogeneous platoon with delays a "powertrain" delay of 0.2 s is applied. By the "powertrain" delay it is meant that the control signal is applied with certain time constant. It can be noticed instantly that the next delay in a system causes even bigger oscillation than in two previous examples. The oscillations of applied wheel torque cause the acceleration to also be oscillating. The amplitude of the acceleration oscillation is in value similar to the example with wireless network delay of 0.3 s, however the duration is extended. Proposed CACC algorithm is able to maintain the string stability of a platoon, nonetheless the comfort of such a travel would be significantly be decreased.

It can be noticed that for maximal relative velocity the propagation error attenuated even with a "powertrain" delay of 0.2 s.

Vehicle number (i)	1	n
MRV ( $\ \dot{e}_i\ _\infty$ , [m/s])	0.23	0.05

**Table 4-11:** Radar (0.1 s), wireless (0.15 s) and "powertrain" (0.2 s) delay scenario - MRV

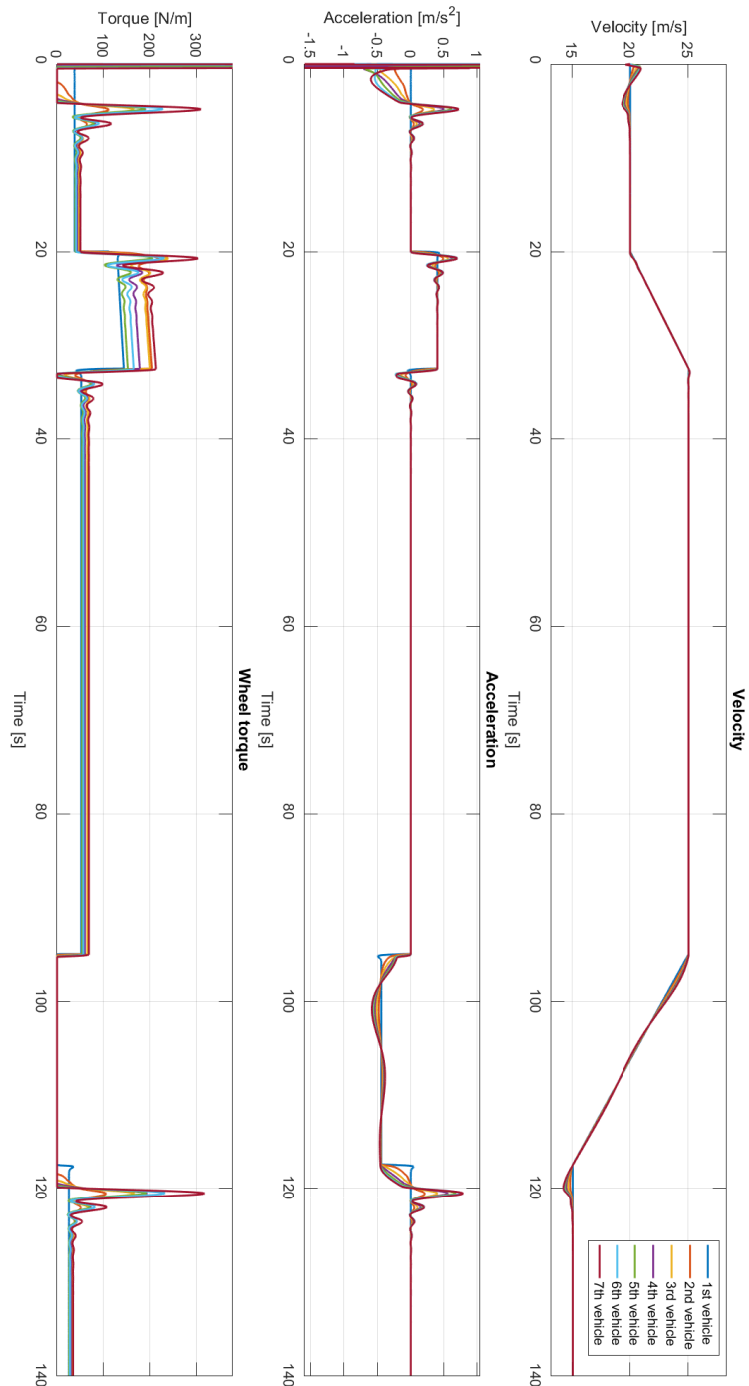


**Figure 4-24:** Delay (radar - 0.1s, wireless - 0.15s) - vehicles velocity, acceleration and wheel torque

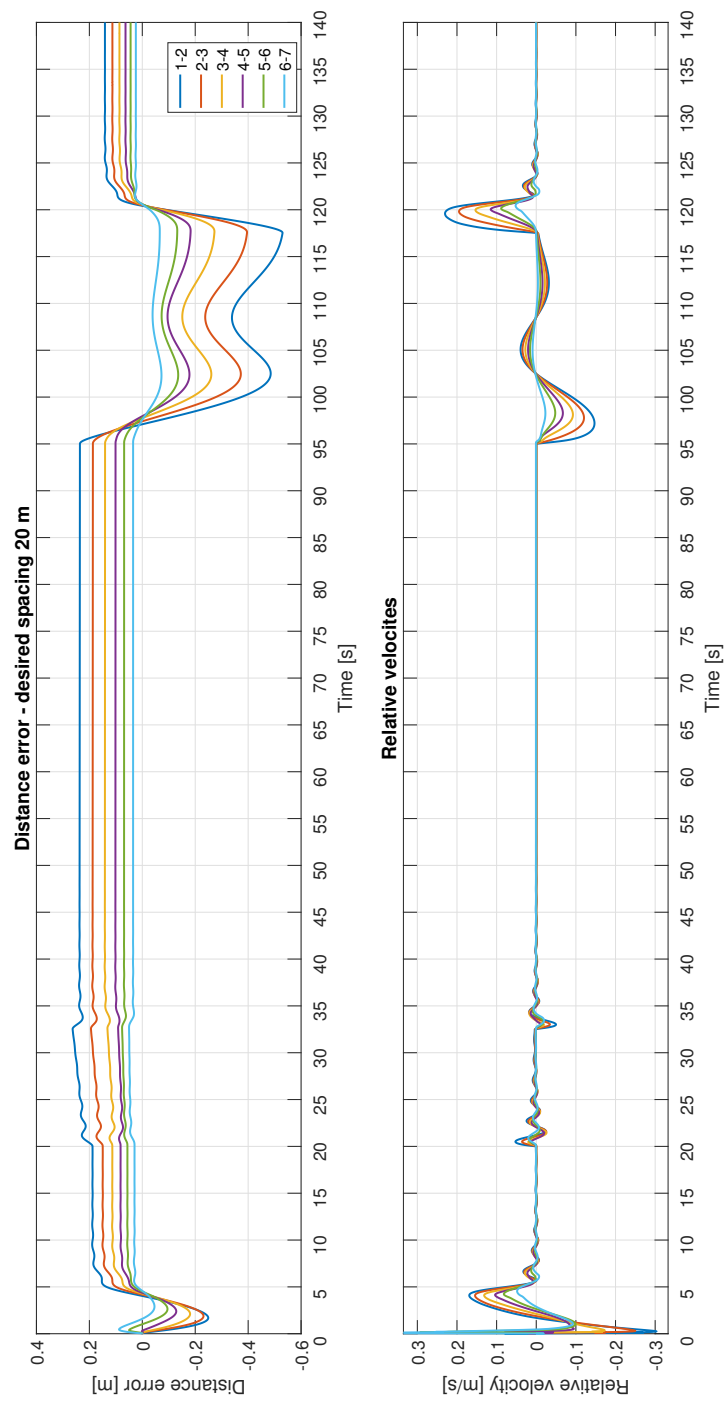


**Figure 4-25:** Delay (radar - 0.1s, wireless - 0.3s) - relative distance and relative velocity

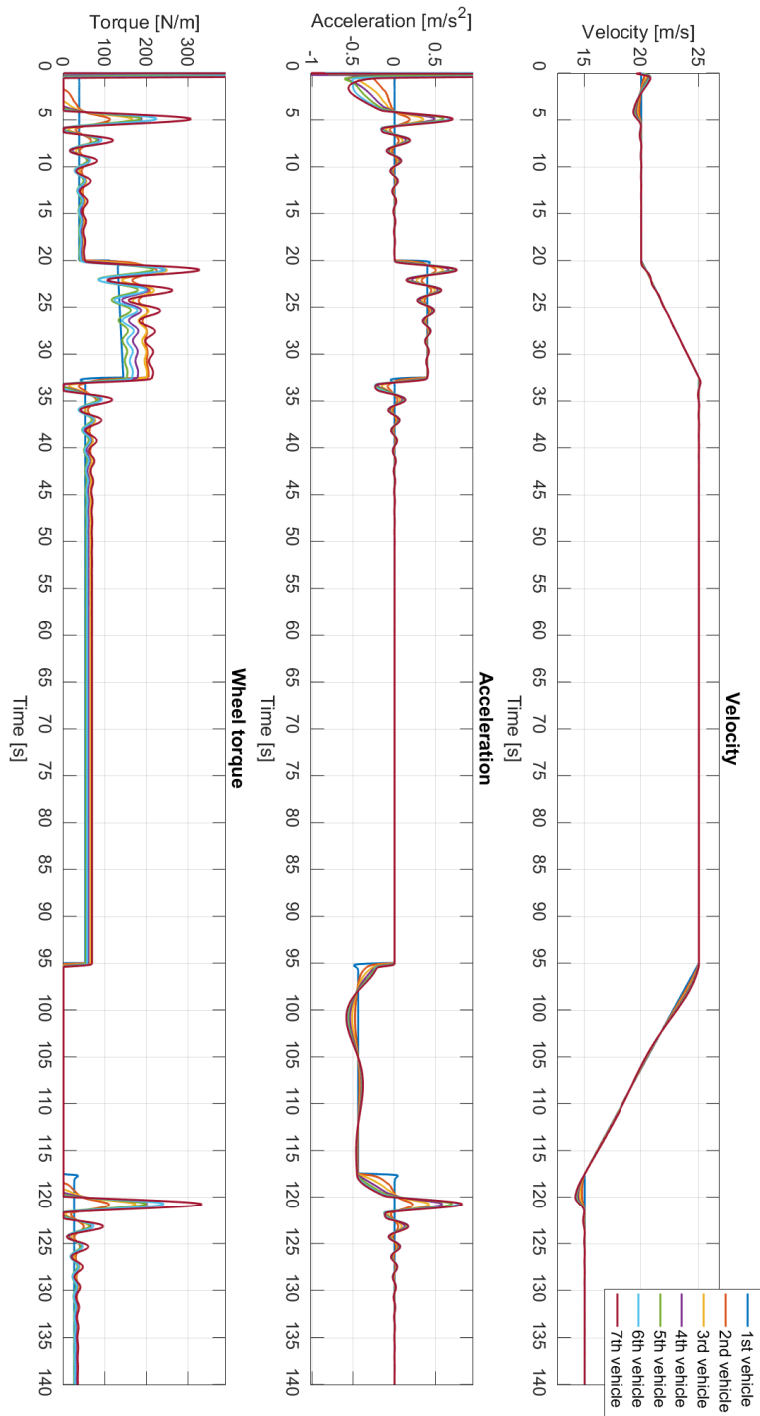


**Figure 4-26:** Delay (radar - 0.1s, wireless - 0.3s) - vehicles velocity, acceleration and wheel torque

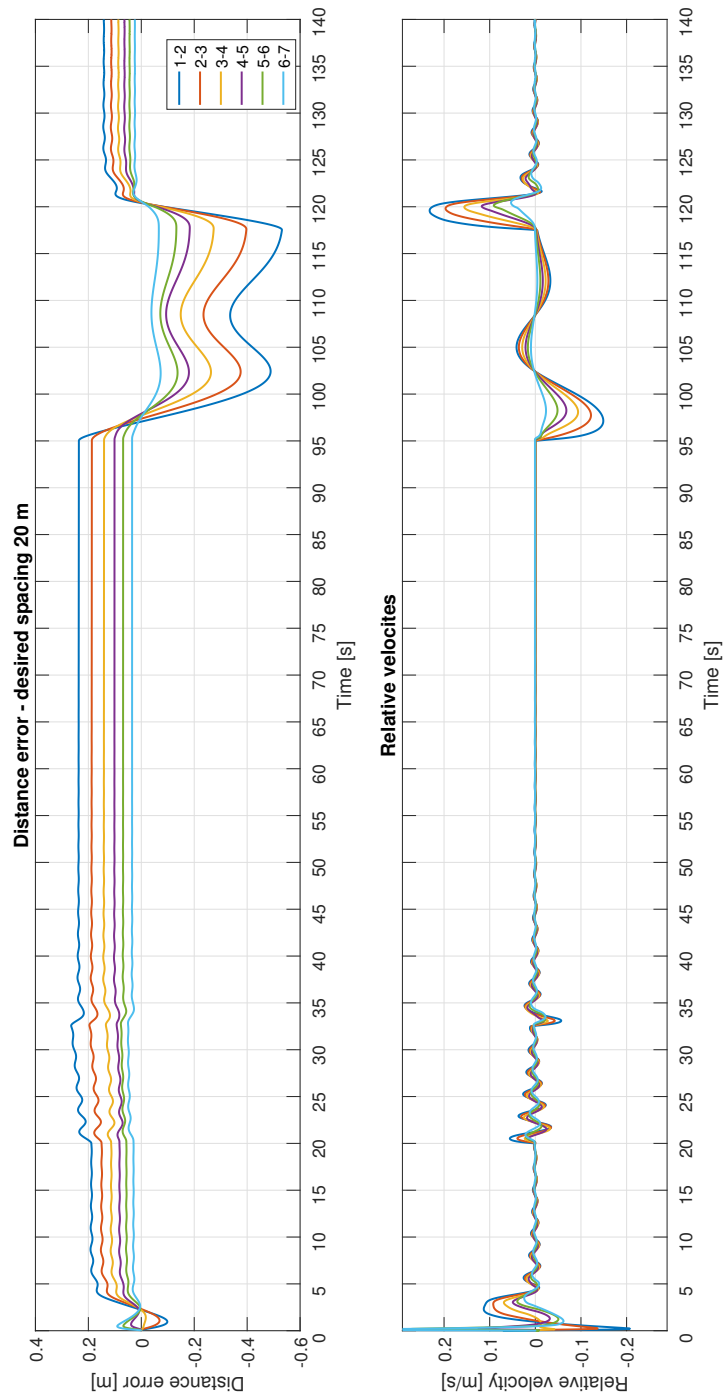


**Figure 4-27:** Delay (radar - 0.1s, wireless - 0.3s, "powertrain" - 0.2s) - relative distance and relative velocity

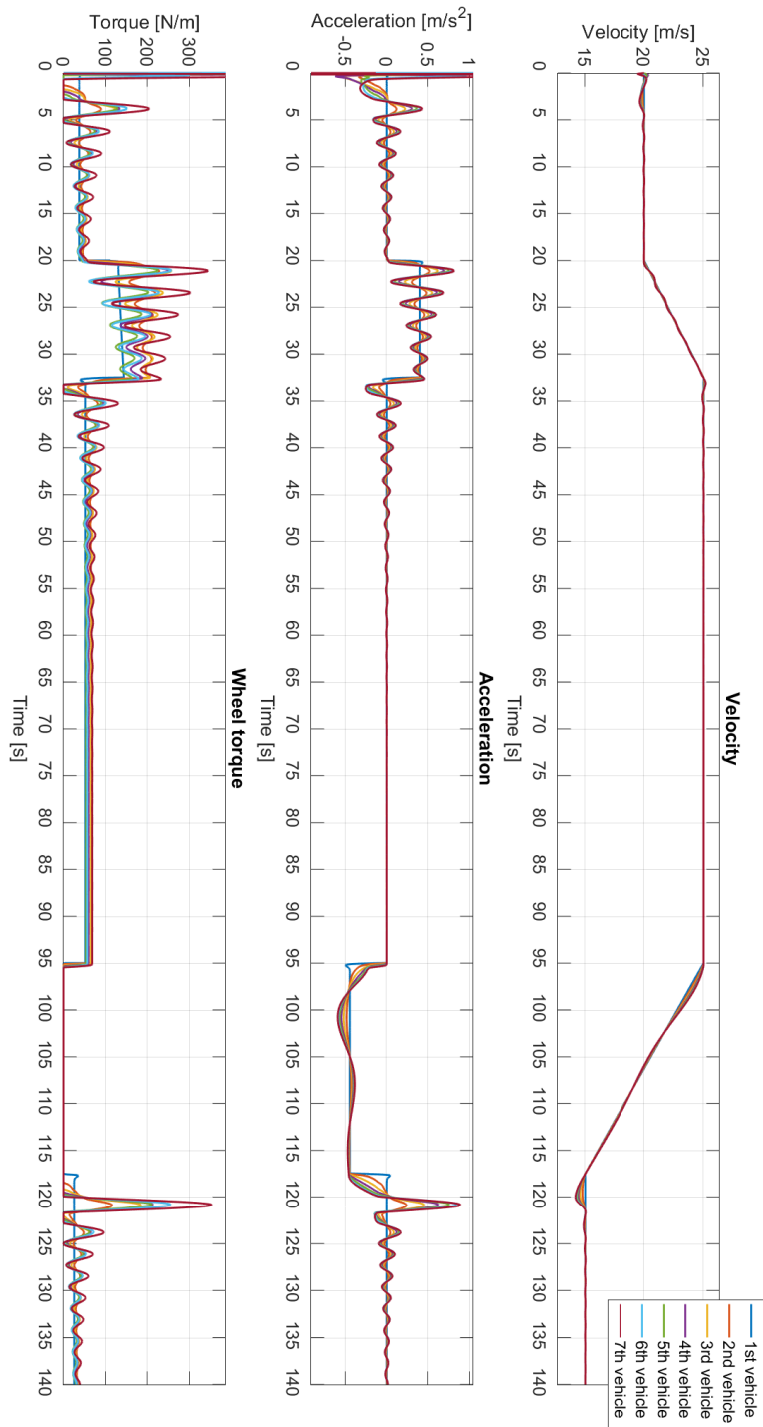


**Figure 4-28:** Delay (radar - 0.1s, wireless - 0.3s, "powertrain" - 0.2s) - vehicles velocity, acceleration and wheel torque

### 4-6-5 Simulation Results - Conclusion

In the simulations the behaviours of the heterogeneous vehicular platoon with uncertain parameters (Table 4-1) were presented. Since the reality of the experiments is an important factor, an advanced vehicle dynamics simulator Dynacar is used.

Firstly, experiments are conducted for four different scenarios, which are meant to evaluate performances of a vehicular platoon with CACC algorithm based on a continuous sliding mode control with a bidirectional communication flow topology. The mentioned scenarios are designed in such a way as to mimic the highway traffic, especially, normal highway traffic, traffic jam with low velocities and Stop and Go feature, emergency braking scenario and finally joining a platoon scenario. Later on, simulations with a headwind with three different amplitudes of wind are presented. The proposed experiment is carried on in order to check how implemented platoon controller is able to reject the external disturbances. Finally, delays are added to the vehicular system. Three simulation are conducted where it is assumed that radar system, wireless communication and a powertrain have delay.

Presented results show that the proposed CACC algorithm is able to maintain constant string stability in a sense of decreasing the relative distance toward the end of the platoon. However, with implemented controller it can be observed the it performs a certain error in relative distance during a travel with constant speed. It seems to be a steady-state error, however, as it is shown in Figure 4-29 it can be seen that this error decreases in a very slow manner.

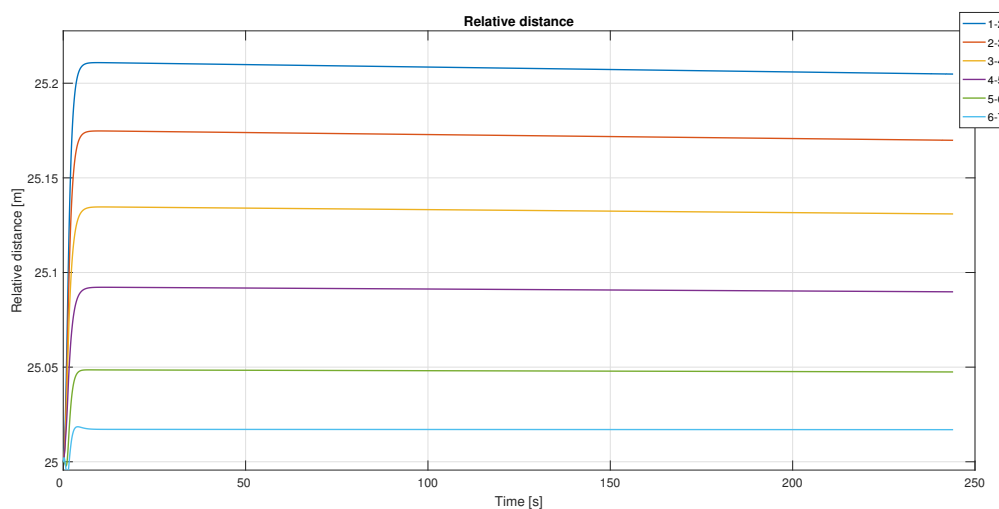


**Figure 4-29:** Decreasing relative distance error

During the evaluation of the simulated scenarios certain performance indicators are used. As a safety and comfort indicator an acceleration and deceleration procedures from ISO 22179:2009 [4] for FSRA are used. It turns out that all the scenarios, except the emergency braking scenario, which is very unusual, satisfied acceleration and deceleration limits. Additionally, a Maximum absolute Relative Velocity indicator is used, which determines the propagation of error in the platoon. It is shown that for all of the presented simulations the error is attenuated along the platoon.

In the simulations, especially in the joining the platoon scenario (4-6-2) it can be seen that in bidirectional communication flow topology the behaviour of the leading vehicles depends also on the following vehicles. It can be said that the vehicles are "merged" together.

# Conclusions and Future Works

## 5-1 Conclusions

In this work Cooperative Adaptive Cruise Control algorithm based on continuous sliding-mode control with adaptive law to estimate uncertain vehicles' parameters is designed and evaluated. It is assumed that the controllers are decentralized, hence, each vehicle computes a control action by itself. The evaluation of the proposed CACC system is conducted on a realistic vehicle model provided by Dynacar. The simulator is based on Matlab/Simulink software and allows to conduct various kinds of scenarios with varying traffic situations and with different vehicle parameters.

For the CACC algorithm the input to the system is a directly applied wheel torque. Hence, a powertrain, transmission, torque converter and brake dynamics is omitted (no low-level controller). The longitudinal platoon control is designed in such a way that provides feasibility, in sense, that the control action behaves in a realistic way. It is proven analytically that continuous control algorithm is able to attenuate disturbances and relative distance error goes to zero as time tends to infinity. String stability is checked experimentally.

Simulations are conducted for a platoon of vehicles with bidirectional information flow topology. The behaviour of the vehicular string is studied with various highway traffic scenarios. Moreover, it is also verified how the CACC system rejects the disturbances and how it deals with delays. It is shown that the proposed controller performs satisfactory in full range of speeds and accelerations. What is more, from the simulations it is observed that the platoon behaves in a string stable way and even in the case of an emergency braking scenario a rear-end collision can be avoided.

In addition, the performances of the proposed CACC system are verified using an ISO 22179:2009 standard, which specifies the system's performances for Full Speed Range Adaptive Cruise Control (FSRA). For the purpose of the experiments as safety and comfort indicators the acceleration and deceleration limits from mentioned ISO standard are used. Also a Maximum Absolute Relative Velocity (MRV) indicator is introduced, which allows to determine the propagation of the error in a vehicle platoon. For different traffic scenarios the specified

ISO and MRV performances are fulfilled, except the emergency braking scenario, where the deceleration exceeded the deceleration limits stated in ISO standard.

## 5-2 Future Works

All suggestions for future work focus mainly on the improvement of the current master project and development of the Cooperative Cruise Control system. Both analytical and experimental improvements are taken into account.

As an analytical future work, it may be beneficial to prove string stability of a vehicular platoon. In order to prove that, it needs to be proven that the sliding surface is reachable in a finite time.

Another important and interesting proof, which can be considered as a future work is to prove boundness of velocity and acceleration of each vehicle in a platoon. Having bounded those two quantities, it can be proven further that control input is bounded.

Speaking about computer simulations with Dynacar, a vehicle model with a realistic/advanced powertrain, transmission, torque converter and brake dynamics might be added. Therefore a low-level controller would need to be implemented. It would be also worth to conduct the simulations in real-time, where a leader driver would be a human.

It would be also beneficial from a realistic point of view to implement a real wireless communication network protocol. The same can be done with in-vehicle communication bus, it would be a good idea to implement a CAN protocol, in order to evaluate the performance of a CACC system.

Another way to improve the current control algorithm is to use a more complex vehicle model on which a CACC control is based. The complex model should contain more detailed vehicle dynamics features, like system's time constants and delays.

Future work should also include road scenarios, where the disturbances influence a vehicle from varying sources. Steepness of the road or changing friction coefficient of the road, for instance wet surface or bumpy road could be taken into account.

Since Cooperative Adaptive Cruise Control systems are still in the experimental phase (they are not sold commercially), it might take some time until the roads would be full of cars equipped in CACC. That is why, it would be beneficial to check how the vehicles with different cruise systems (CACC, ACC) or even without any would behave in the same platoon.

Finally, the proposed CACC algorithm should be implemented in a real vehicle platoon. It might be a costly and complicated task to perform and organize, however such an experiment would bring more detailed data and might verify whether this control approach is feasible with real vehicles. Moreover, to make it even more realistic the vehicle platoon could be heterogeneous.

---

# Chapter 6

---

## Appendix A

### 6-1 Matlab Code

```
1 % =====  
2 %  
3 % Routine created to launch Dynacar visor + Simulink model  
4 %  
5 % (c) TECNALIA (D.Cagigas, 16-June-2017)  
6 % =====  
7 %  
8 %  
9 % Pawel Krzesinski  
10 % Master Thesis - "Decentralized Controllers for CACC in platoons of  
11 % heterogenous vehicles with model uncertainties"  
12 %  
13 % Delft Center for Systems and Control  
14 % Systems and Control  
15 % TU Delft 2016/2017  
16 % =====  
17 %  
18 clear all force  
19 clc  
20 %% Vehicle model  
21 %% dd_x=(ui-ci d_x^2-fi)/Mi +deltai  
22 % Radar, wireless communication and "powertrain" delays  
23 discrete_nominator = 1;%0.09516;  
24 discrete_denominator = 1;%[1 -0.9048];  
25 discrete_nominator_wireless = 1;%0.06449;%0.03278  
26 discrete_denominator_wireless = 1;%[1 -0.9355] ;%[1 -0.9672]
```

```

27
28 % Platoon and controller parameters
29 xd = 25; % [m] desiredcc distance
30 lambda = 1; %1
31 k = 330; %500 330 7000
32 k_bar = 22; %22 22 1000
33 q = 0.95; %1
34
35 % Adaptation law gains
36 gamma_c = 10e-8;
37 gamma_f = 10e-8;
38 gamma_D = 10e-2;
39 gamma_M = 10e-4;
40 % Adaptation law - initial values
41 c_hat_initial = 0.2;
42 f_hat_initial = 0.01;
43 D_hat_initial = 2000;
44 M_hat_initial = 1600;
45
46 % VISOR:
47 % 1) Declare parameters:
48 VisorExeFile = 'VisorV30.exe';
49 VisorPath = 'C:\Dynacar\v_2_0\Visual\Visor\BatchFiles';
50 VisorBatchPathAndFilename = [VisorPath, '\
    StartSimulator_Proving_CarE_Keyboard_3Vehicles.bat'];
51 WaitTimeSecs = 45;
52
53 % 2) Check if it is already opened:
54 String = ['tasklist /FI "imagename eq ',VisorExeFile,'" /fo table /nh'];
55 [~,Answer] = system(String);
56 if isempty(strfind(Answer,VisorExeFile)) == 1
57     % If the executable is not running, launch it!
58     ActualPath = cd;
59     cd(VisorPath);
60     disp(' ');disp(['Opening visor: ',num2str(WaitTimeSecs),' secs.']);
61     dos(VisorBatchPathAndFilename);
62     % Pause and wait for the VISOR to open:
63     pause(WaitTimeSecs);
64 else
65     % If it is already opened, do nothing.
66     disp(' ');disp('Visor already opened. ');
67 end;
68
69 % SIMULINK:
70 % 1) Declare the input variables required by SimRoutine a GLOBAL:
71 global InputStruct;
72 InputStruct.MatlabPath = 'C:\Dynacar\v_2_0\Matlab';
73 InputStruct.SlxPath = [InputStruct.MatlabPath, '\TestHarness\MiL3'];
74 InputStruct.SlxName = 'Dynacar_TestHarness_MiL3';
75 InputStruct.ResultsBlockName = [{'Results1'};{'Results2'};{'Results3'};{'
    Results4'};{'Results5'};{'Results6'};{'Results7'}];
76
77 % Simulation parameters

```

```

78 InputStruct.StepTime = '0.01';
79 InputStruct.StopTime = '140';
80
81 InputStruct.SetVariablesScript = 'Dynacar_TestHarness_MiL3_SetVariables';
82 InputStruct.XmlPath = InputStruct.SlxPath;
83 InputStruct.XmlFilename = 'Dynacar_TestHarness_MiL3_Outputs.xml';
84 InputStruct.XmlChassisNodeName = 'CHASSIS';
85 InputStruct.XlsPath = [InputStruct.MatlabPath, '\OutputsXls'];
86 InputStruct.XlsFilename = 'Dynacar_Outputs.xlsx';
87 InputStruct.XlsNameCol = 3;
88 InputStruct.bLoadInputsFile = 1;
89 InputStruct.InputsFile = 'Dynacar_OpenLoopTest_Steering.mat';
90 InputStruct.bSlxClose = 0;
91 InputStruct.nOutputs = 300;
92
93 % 2) Run routine:
94 % Graphics:
95 opengl hardware;
96 % Add recursive path:
97 addpath(genpath(InputStruct.MatlabPath));
98 % Run routine:
99 cd(InputStruct.SlxPath);
100 Dynacar_TestHarness_SimRoutine;

1 % =====
  %
2 % Pawel Krzesinski
3 % Master Thesis - "Decentralized Controllers for CACC in platoons of
4 % heterogenous vehicles with model uncertainties"
5 %
6 % Delft Center for Systems and Control
7 % Systems and Control
8 % TU Delft 2016/2017
9 % =====
  %
10
11 % =====
  %
12 % This script defines the variables needed by Dynacar S-Function:
13 %
14 % Launch: .TXT file that contains the configuration of the model
15 %   - LICENSE .txt file
16 %   - VEHICLE .xml file
17 %   - GROUND .scn file
18 %   - OUTPUT .xml file
19 %   - Initial conditions [INIPOS, INIVEL]:
20 %     - The DOF for each chassis, knuckle, wheel:
21 %       - 6 DOF per Chassis (X Y Z Roll Pitch Yaw)
22 %       - 1 DOF per Knuckle (Jounce)
23 %       - 1 DOF per Wheel (Angle: It is NOT the steer angle, just the
  rotation angle)
24 %     - The same applies for speeds
25 %     - From front to rear, from right to left

```

```

26 %      - Example:
27 %      - 1 chassis
28 %      - 2 axis (Front, rear) = 4 Knuckles
29 %      - FR, FL Knuckles = 1 Wheel
30 %      - RR, RL Knuckles = 2 Wheels
31 %      - INIPOS = [ Chassis_1_X Chassis_1_Y Chassis_1_Z Chassis_1_Roll
Chassis_1_Pitch Chassis_1_Heading...
32 %      Knuckle_1_Jounce Knuckle_2_Jounce Knuckle_3_Jounce
Knuckle_4_Jounce...
33 %      Wheel_1_Angle Wheel_2_Angle ... Wheel_6_Angle]
34 %      - INIVEL = [ cc V_inicial*sin(Heading) 0 0 0 0 0 0 0 0 0 0 0 0];
35 %
36 %      (Check documentation for more details)
37 %
38 % (c) TECNALIA (D.Cagigas, 16-June-2017)
39 % =====
%
40
41 % Clear variables:
42 clear INSTANCE1 LAUNCH1 INIPOS1 INIVEL1
43 clear INSTANCE2 LAUNCH2 INIPOS2 INIVEL2
44 clear INSTANCE3 LAUNCH3 INIPOS3 INIVEL3
45 clear INSTANCE4 LAUNCH4 INIPOS4 INIVEL4
46 clear INSTANCE5 LAUNCH5 INIPOS5 INIVEL5
47 clear INSTANCE6 LAUNCH6 INIPOS6 INIVEL6
48 clear INSTANCE7 LAUNCH7 INIPOS7 INIVEL7
49
50 xd = 25; % [m] Desired inter-vehicle distance
51
52 % For each vehicle, define an instance:
53 % (0-based, 1st vehicle defined as instance = 0)
54 INSTANCE1 = 0;
55
56 % Define "Launch.txt" file:
57 ActualPath = cd;
58
59 % Define start SPEED conditions:
60 V_inicial = 20*3.6;          % Units [km/h]
61 V_inicial = V_inicial/3.6;  % Units [m/s]
62 R_wheel = 0.364;           % Units [m]
63 Heading = 0;               % Units [rad]
64
65 % IMPORTANT:
66 % =====
67 % Set-up for 1 chassis, with 4 knuckles and 1 wheel per knuckle =...
68 % 1*3(x,y,z) + 1*3(X,Y,Z) + 4*1(Compression) + 4*1(Angular position) =
[1,14]
69 % The size is defined as 28 to have enough space to define 2 chassis
70 % If this size changes in Dynacar, this length has to be updated
71 INIPOS1 = zeros([1 28]);
72 INIVEL1 = zeros([1 28]);
73
74 % Define start POSITION conditions:

```

```

75 INIPOS1(1) = 0;           % X position
76 INIPOS1(2) = -xd*6;     % Y position
77 INIPOS1(3) = 0.064;    % Z position
78 INIPOS1(6) = -1.5707963268;
79
80 W_wheel = (V_inicial*cos(Heading))/R_wheel;
81
82 INIVEL1(1) = -V_inicial*sin(Heading);
83 INIVEL1(2) = -V_inicial*cos(Heading);
84 INIVEL1(11:14) = W_wheel;
85
86 LAUNCH1 = double([ActualPath, '\Dynacar_TestHarness_MiL3_Launch1.txt']);
87 LAUNCH1 = [LAUNCH1 zeros(1,100)];
88 LAUNCH1(101:end) = [];
89 LAUNCH1 = int8(LAUNCH1);
90
91 % 2nd VEHICLE:
92 % =====
93 % Instance:
94 INSTANCE2 = 1;
95 % "Launch.txt" file:
96 LAUNCH2 = double([ActualPath, '\Dynacar_TestHarness_MiL3_Launch2.txt']);
97 LAUNCH2 = [LAUNCH2 zeros(1,100)];
98 LAUNCH2(101:end) = [];
99 LAUNCH2 = int8(LAUNCH2);
100 % INIPOS, INIVEL:
101 INIPOS2 = INIPOS1; INIPOS2(2) = INIPOS2(2) + xd;
102 INIVEL2 = INIVEL1;
103
104 % 3rd VEHICLE:
105 % =====
106 % Instance:
107 INSTANCE3 = 2;
108 % "Launch.txt" file:
109 LAUNCH3 = double([ActualPath, '\Dynacar_TestHarness_MiL3_Launch3.txt']);
110 LAUNCH3 = [LAUNCH3 zeros(1,100)];
111 LAUNCH3(101:end) = [];
112 LAUNCH3 = int8(LAUNCH3);
113 % INIPOS, INIVEL:
114 INIPOS3 = INIPOS1; INIPOS3(2) = INIPOS3(2) + 2*xd;
115 INIVEL3 = INIVEL1;
116
117 % 4th VEHICLE:
118 % =====
119 % Instance:
120 INSTANCE4 = 3;
121 % "Launch.txt" file:
122 LAUNCH4 = double([ActualPath, '\Dynacar_TestHarness_MiL3_Launch4.txt']);
123 LAUNCH4 = [LAUNCH4 zeros(1,100)];
124 LAUNCH4(101:end) = [];
125 LAUNCH4 = int8(LAUNCH4);
126 % INIPOS, INIVEL:
127 INIPOS4 = INIPOS1; INIPOS4(2) = INIPOS4(2) + 3*xd;

```

```

128 INIVEL4 = INIVEL1;
129
130 % 5th VEHICLE:
131 % =====
132 % Instance:
133 INSTANCE5 = 4;
134 % "Launch.txt" file:
135 LAUNCH5 = double([ActualPath, '\Dynacar_TestHarness_MiL3_Launch5.txt']);
136 LAUNCH5 = [LAUNCH5 zeros(1,100)];
137 LAUNCH5(101:end) = [];
138 LAUNCH5 = int8(LAUNCH5);
139 % INIPOS, INIVEL:
140 INIPOS5 = INIPOS1; INIPOS5(2) = INIPOS5(2) + 4*xd;
141 INIVEL5 = INIVEL1;
142
143 % 6th VEHICLE:
144 % =====
145 % Instance:
146 INSTANCE6 = 5;
147 % "Launch.txt" file:
148 LAUNCH6 = double([ActualPath, '\Dynacar_TestHarness_MiL3_Launch6.txt']);
149 LAUNCH6 = [LAUNCH6 zeros(1,100)];
150 LAUNCH6(101:end) = [];
151 LAUNCH6 = int8(LAUNCH6);
152 % INIPOS, INIVEL:
153 INIPOS6 = INIPOS1; INIPOS6(2) = INIPOS6(2) + 5*xd;
154 INIVEL6 = INIVEL1;
155
156 % 7th VEHICLE:
157 % =====
158
159 % Join the platoon scenario
160 % V_inicial = 36*3.6;           % Units [km/h]
161 % V_inicial = V_inicial/3.6;   % Units [m/s]
162 % R_wheel = 0.364;             % Units [m]
163 % Heading = 0;                 % Units [rad]
164 %
165 % INIVEL7 = zeros([1 28]);
166 % W_wheel = (V_inicial*cos(Heading))/R_wheel;
167 %
168 % INIVEL7(1) = -V_inicial*sin(Heading);
169 % INIVEL7(2) = -V_inicial*cos(Heading);
170 % INIVEL7(11:14) = W_wheel;
171 INSTANCE7 = 6;
172 % "Launch.txt" file:
173 LAUNCH7 = double([ActualPath, '\Dynacar_TestHarness_MiL3_Launch7.txt']);
174 LAUNCH7 = [LAUNCH7 zeros(1,100)];
175 LAUNCH7(101:end) = [];
176 LAUNCH7 = int8(LAUNCH7);
177 % INIPOS, INIVEL:
178 INIPOS7 = INIPOS1; INIPOS7(2) = INIPOS7(2) + 6*xd;
179 INIVEL7 = INIVEL1;

```

---

## Chapter 7

---

# Appendix B

### 7-1 Simulink Overview

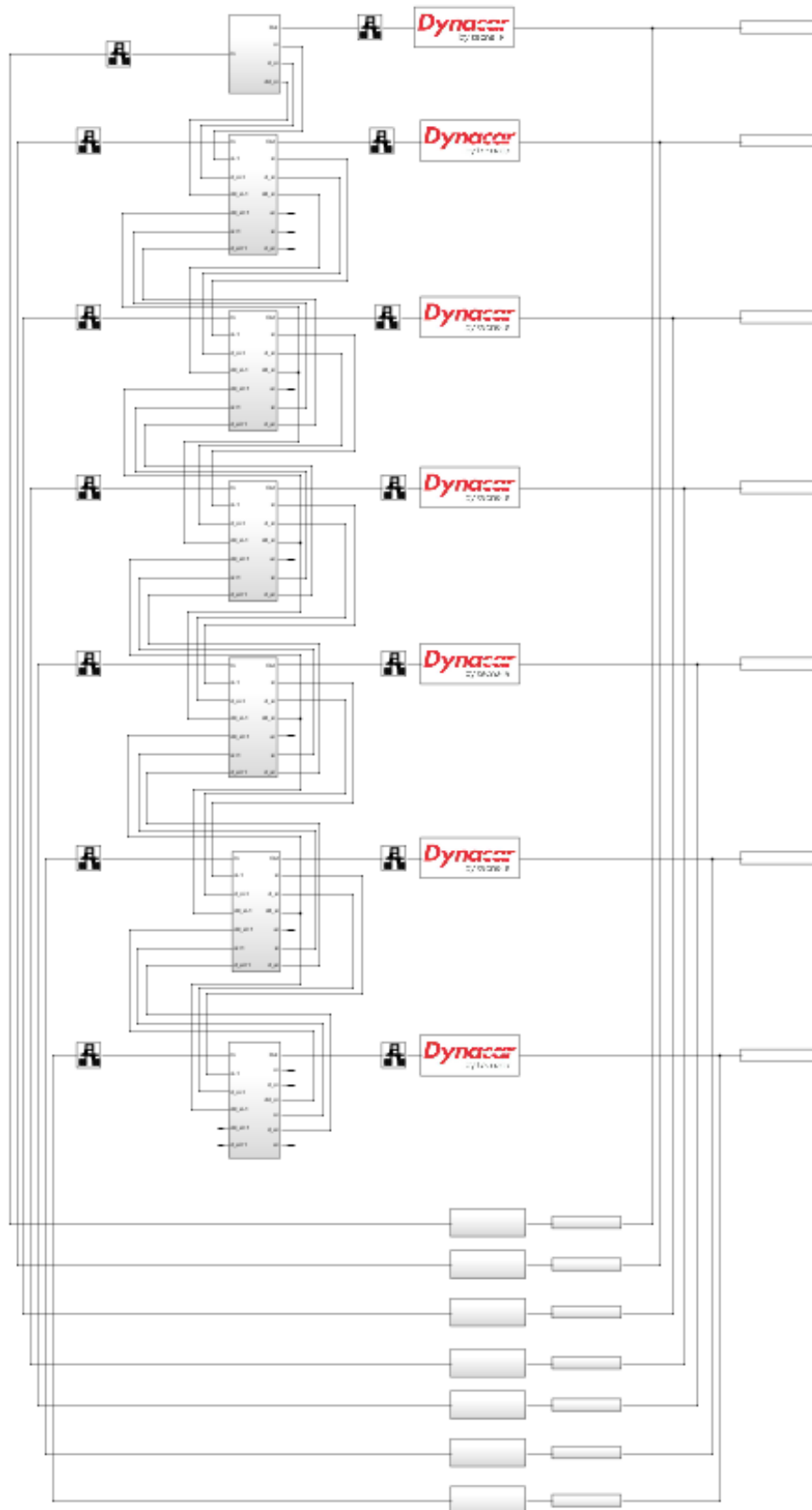


Figure 7-1: Simulink - vehicle platoon overview

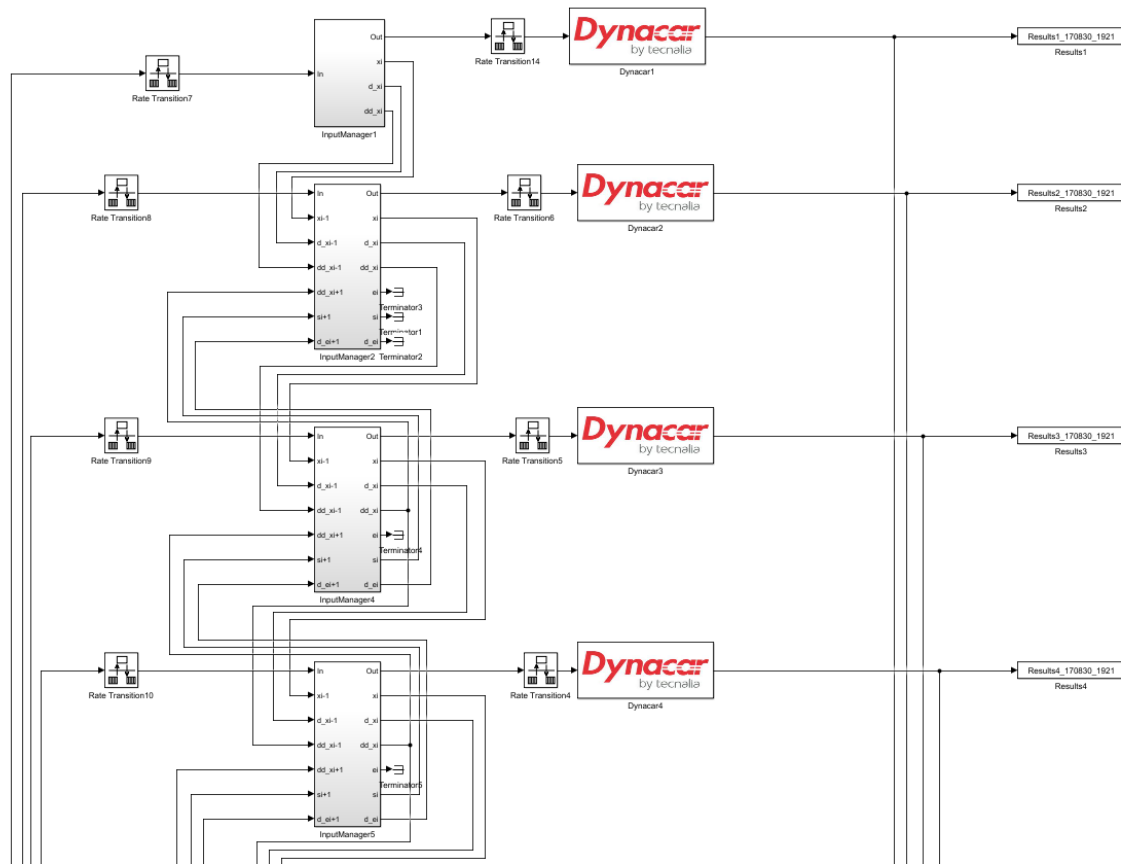


Figure 7-2: Simulink - vehicle platoon overview (zoomed)

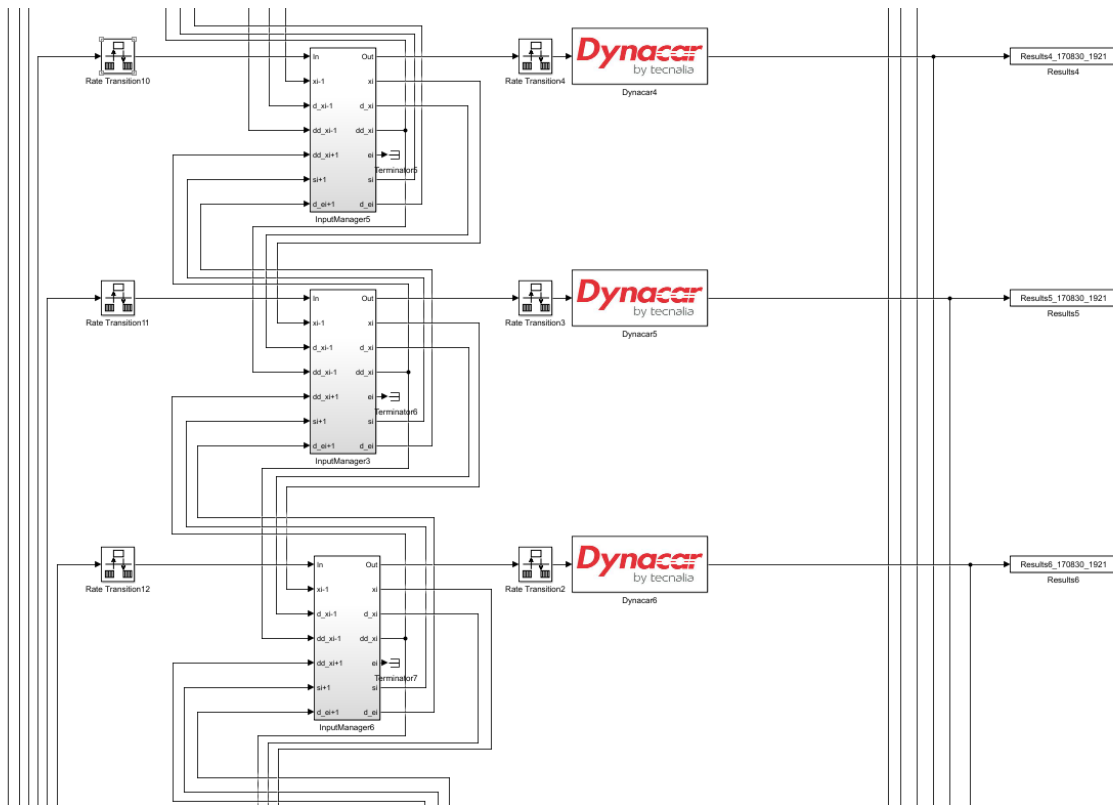


Figure 7-3: Simulink - vehicle platoon overview (zoomed)

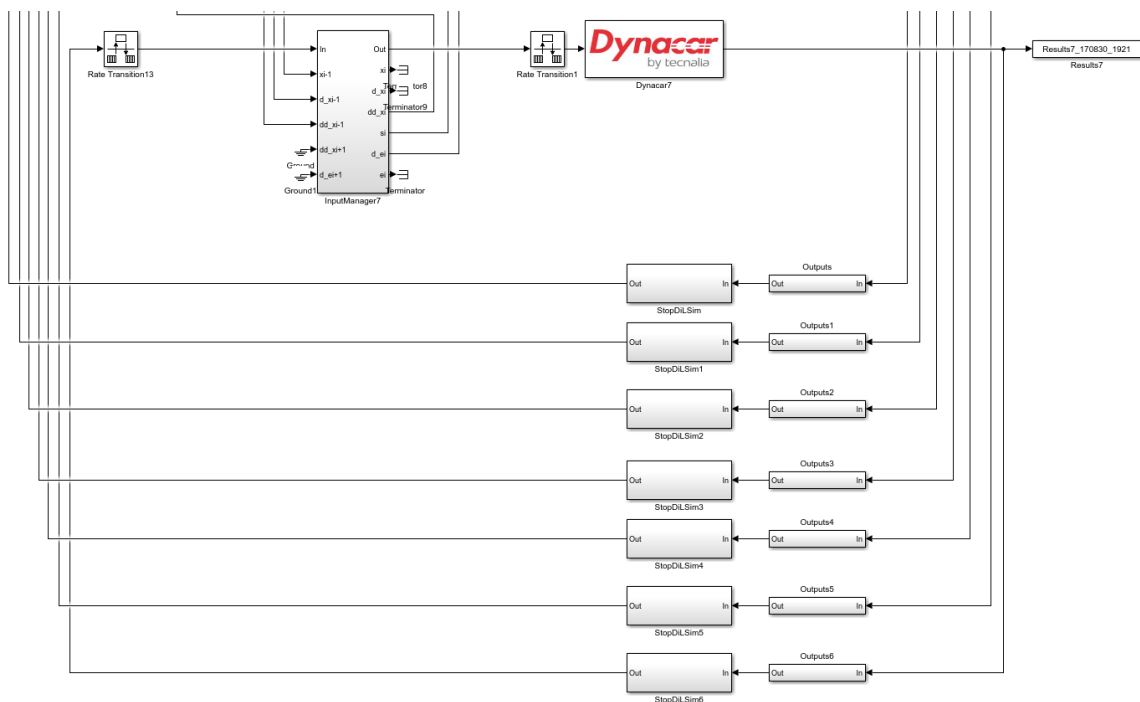


Figure 7-4: Simulink - vehicle platoon overview (zoomed)

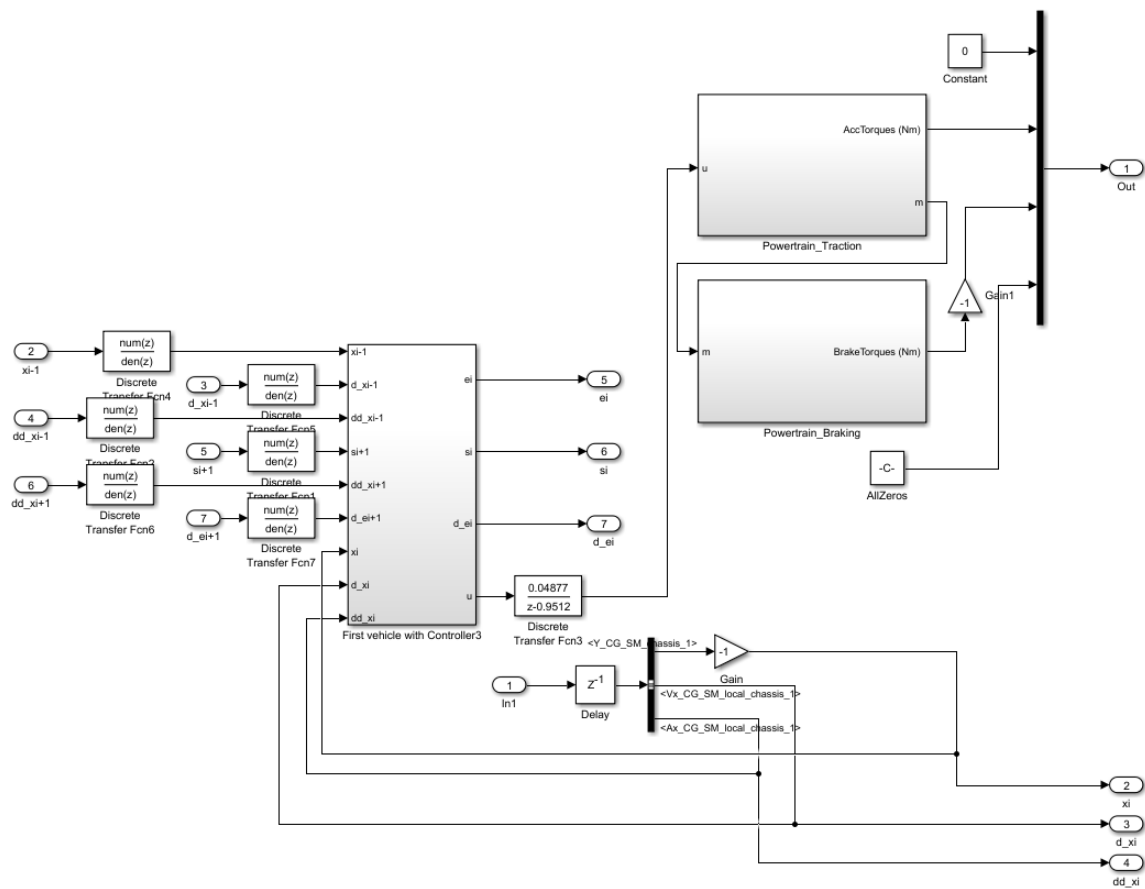


Figure 7-5: Simulink - Control and Torque blocks overview

Front wheel torque block

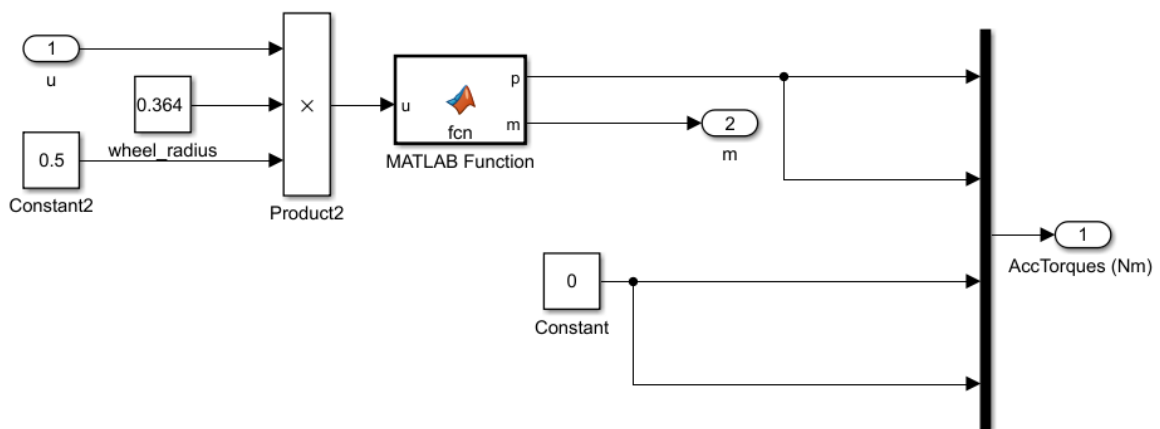


Figure 7-6: Simulink - torque applied to wheels block

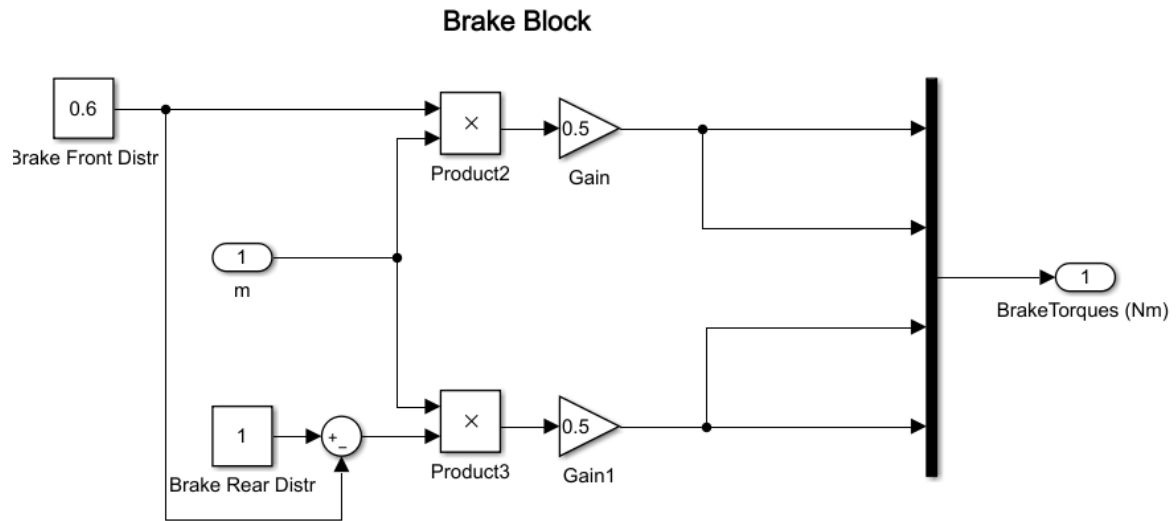


Figure 7-7: Simulink - brake torque applied to wheels block

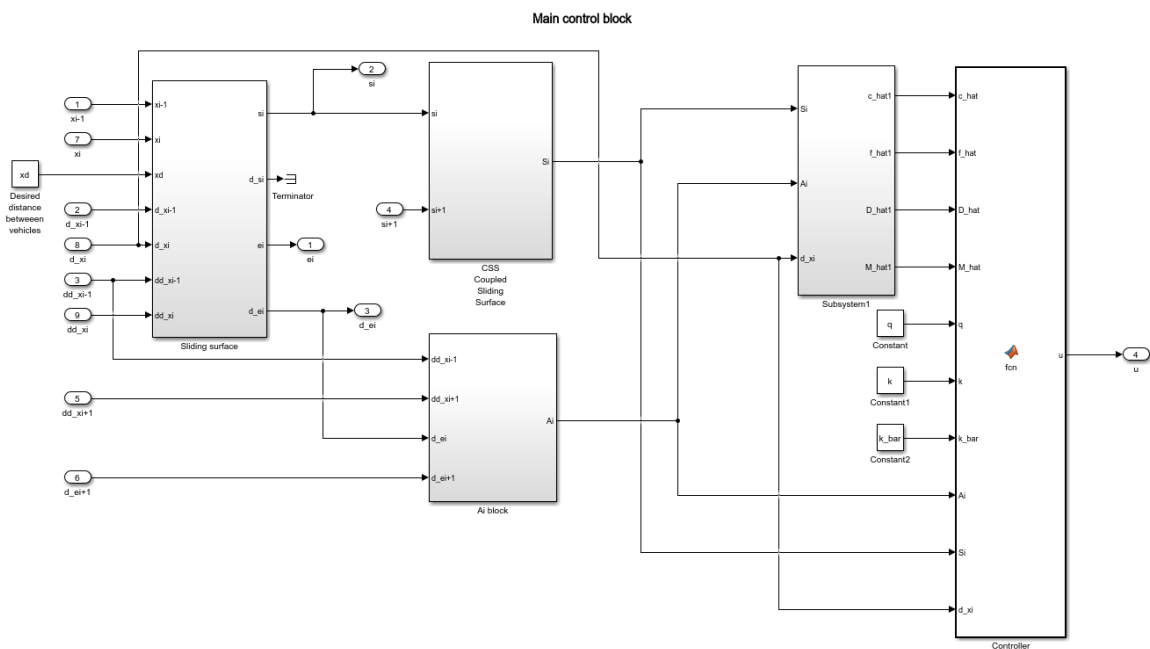
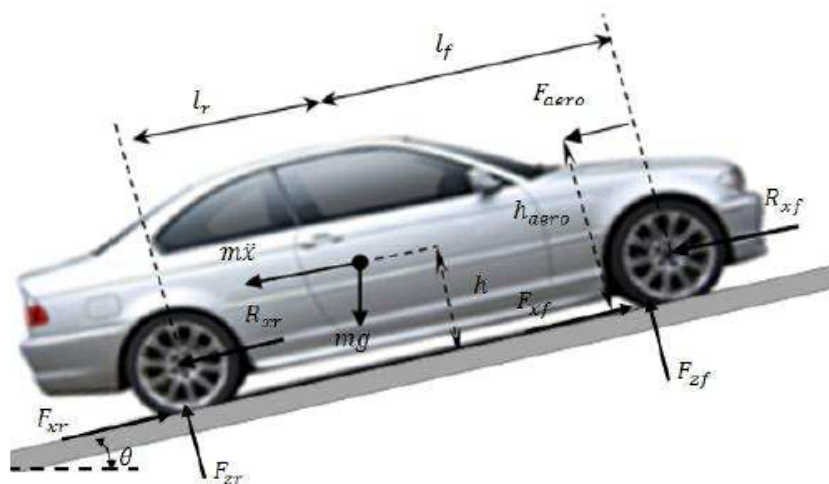


Figure 7-8: Simulink - control block overview

### 8-1 Longitudinal Forces

When the overview of the Dynacar's vehicle model is known, it is worth to mention the forces, which are act on a vehicle. Basically, there are a lot of exerting forces from different directions and sources. However, there are a few main forces, which influence a vehicle behaviour significantly.



**Figure 8-1:** Forces acting on a vehicle, [6]

In Figure 8-1 the longitudinal forces are presented, all the presented forces are balanced in the following way:

$$m\ddot{x} = F_{xf} + F_{xfr} - F_{aero} - R_{xf} - R_{xr} \pm mgsin(\theta) \quad (8-1)$$

where  $F_{xf}$  and  $F_{xr}$  stand for longitudinal traction force generated by the wheels,  $F_{aero}$  is a aerodynamic force opposite to direction of movement,  $R_{xf}$  and  $R_{xr}$  are the rolling resistance forces generated by tires. In (8-1) the inclination of the road is also included,  $\theta$  is a road inclination angle, where  $\theta$  is positive when a vehicle is "climbing" a hill and negative, when a car is moving downhill. Respectively, the sign in (8-1) is minus (-) for positive angle and plus (+) for negative  $\theta$ . The other parameters  $m$  and  $g$  are vehicle's mass and gravitational acceleration, respectively.

## 8-2 Aerodynamic Drag Force

An important force acting on a moving vehicle is an aerodynamic force, which can be represented as follows:

$$F_{aero} = \frac{1}{2}\rho AC_d(v_x - v_{wind})^2 \quad (8-2)$$

where  $\rho$  is the air density,  $A$  is a maximal vehicle's frontal cross area,  $C_d$  stands for a drag coefficient, which depends on the shape of a vehicle,  $v_x$  is a longitudinal velocity and  $v_{wind}$  is a velocity of the wind. A headwind is expressed as a positive and for tailwind as a negative coefficient.

The air density depends on atmospheric conditions, which can affect an aerodynamic drag. A value of  $\rho$  depends on the temperature and a barometric pressure. For the purpose of the simulation experiments  $\rho = 1.206 \text{ kg/m}^3$ .

According to [35], the frontal area  $A$  can be approximated with a relationship of a vehicle mass. Equation 8-3 is suitable for the passenger cars in the mass range of 800 – 2000  $kg$ . The passenger cars' drag coefficient is between 0.2 – 0.4 and it depends significantly on the vehicle shape.

$$A = 1.6 + 0.00056(m - 765) \quad (8-3)$$

Since the vehicles in a platoon in this master project are assumed to be a passenger cars the equation (8-3) is used to calculate a frontal cross area of the vehicles in a string.

In the Dynacar simulator it is possible to adjust the aerodynamic parameters. The aero force coefficients, aero moment coefficient, reference center of the point where the aerodynamic force is applied and the frontal area can be changed. It gives a huge possibility to make each vehicle in a platoon different. In addition, a constant wind blow can be added.

## 8-3 Suspension Model

The vertical wheel load is a very important force and is one of the main inputs of the tire model. Therefore, a suspension model is required from which a calculation of the vertical load on each of the wheels is possible. The calculation needs to be precise. Generally speaking, there are three suspension modelling approaches. The first one and the simplest is a

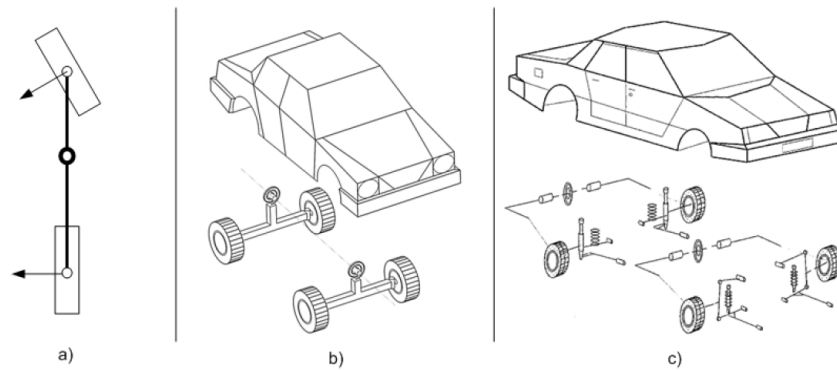


**Figure 8-2:** Suspension models: a) bicycle model, b) "roll stiffness", c) multi-body, [7]

bicycle model, then a "roll stiffness" model is an option and finally a multi-body model of the suspension can be used.

The first presented model in Figure 8-2 is a huge simplification of a vehicle. In this model it is assumed that each axis has only one wheel, hence the lateral weight transfer is impossible to calculate. In the "roll stiffness" approach a vehicle is assumed to be a rigid mass on a single axis. The forces and momentum acting onto a rigid mass are translated to front and rear suspension. With this method it is possible to obtain a precise weight distribution.

In the Dynacar's vehicle model the third suspension model is used. Multi-body approach provides precise information about the vertical forces acting on a wheel, however the design process is complicated and requires a detailed knowledge of the geometry model of the suspension (Figure 8-3). On the other hand, weight distribution and directly related normal forces are very important factors of a vehicle's longitudinal dynamics. In order to achieve a realistic vehicle behaviour, it is crucial to have precise information about those forces both during a drive with constant velocity but also during accelerating or decelerating.

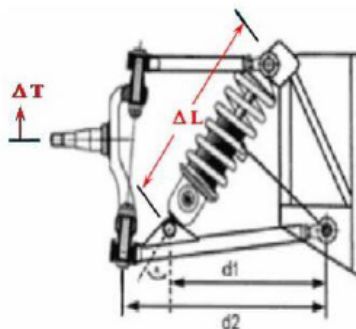


**Figure 8-3:** Multi-body suspension design, [5]

## 8-4 Tire Model

The tire itself is one of the most crucial elements in the entire wheeled vehicle, since it is the only component, which keeps the vehicle in contact with the road. Through those contact

points all the power and torque generated by an engine is transferred into the road-tire forces. There are three main forces generated between a road and a tire, which causes the movement of a vehicle. Longitudinal force ( $F_x$ ), which "pushes" a vehicle during acceleration and slows it down while braking. The next one is a lateral force ( $F_y$ ), which is generated during cornering causing a moment around yaw axis, which makes a car turn. The last, normal force ( $F_z$ ) acts in a vertical plain and as mentioned, it is highly influenced by a vehicle's weight transfer.

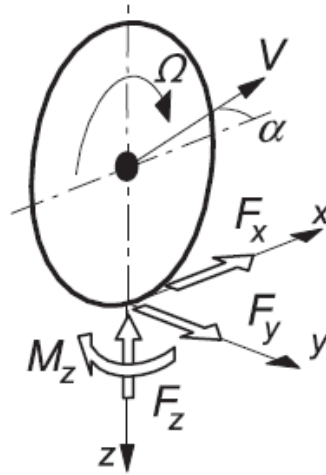


**Figure 8-4:** Tire-road forces, [8]

Since the tire is a very important component in a vehicle, during the last decades vast research has been done regarding modeling of its behaviour. Hence, a few different modeling approaches of a tire have been introduced. Generally, the tire models can be divided into those completely empirical and theoretical. As an example of an empirical approach modeling, a Magic Formula tire model can be mentioned. Such a model is based on experimental data only and the model is developed by trying to fit full scale tire data by regression techniques [8]. On the other hand, theoretical method of modeling a tire is focused on complex physical modeling, often using finite element methods. However, for simulation purposes the empirical approach is more suitable due to its compact form and simplicity of application.

The tire model used in Dynacar vehicle simulator is the model called "Magic Formula" based on published formulation and developed by Prof. H.B. Pacejka. The model is based on a set of mathematical equations, which mimic the behaviour of the tire.

In (8-4) the general form of the Magic Formula equation is given. It is an empirical equation based on four fitting coefficients.

$$y = D \sin[C \tan^{-1}\{Bx - E(Bx - \tan^{-1}(Bx))\}] \quad (8-4)$$

where  $y$  is a tire force or torque,  $x$  stands for either the slip angle or slip ratio variable,  $B$ ,  $C$ ,  $D$  and  $E$  are the factors, which define the characteristic of a tire.

Magic Formula tire model calculates the forces and momentum acting on a tire (output) based on the input parameters, which are slip angle ( $\alpha$ ), longitudinal slip ratio ( $\kappa$ ), camber angle ( $\gamma$ ) and a normal force ( $F_z$ ) acting on a wheel. A schematic overview of the Magic formula is presented in Figure 8-5.

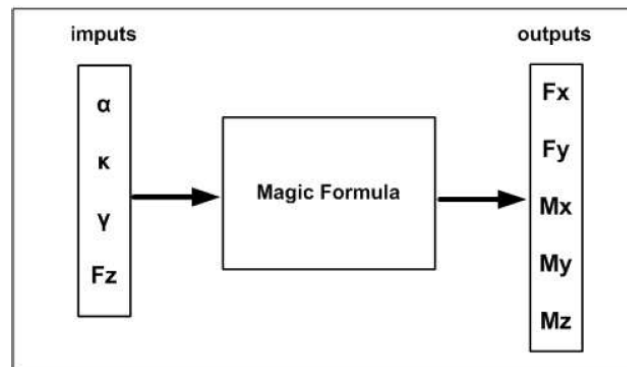


**Figure 8-5:** Inputs and outputs of the Magic Formula tire model, [7]

In a platoon simulation it is assumed that each vehicle has the same set of tires. The tire model used in the simulations corresponds to passenger tires (205-60-R15).

### Rolling resistance

Speaking about tires it is also important to mention tire rolling resistance, which is always present in realistic environment. Due to elasticity of the tire, a deflection is produced, caused by a rotation on a much stiffer, than the tire, road. Because of the wheel's rotation the new piece of a tire's rubber is constantly entering a contact patch, which is vertically deflected by the normal load. The elastic material, which goes through the contact point is sprung back to its original shape, however, because of the internal tire's damping a loss of energy occurs. This loss of energy is represented by a force, which exerts to oppose the motion of the vehicle. Next to it, due to non-symmetric distribution of the normal tire force over the contact patch, the energy is lost as well. The force exerted by those two factors is called the rolling resistance [12].

The rolling resistance depends on many parameters, which are for instance, tire shoulder temperature, ambient temperature, diameter of the tire, road condition, inflation pressure and the tire type [35].



---

# Bibliography

- [1] R. Happee, "Lecture notes - automation technology ii, support automation," *TU Delft - ME1100, Automated Driving, Automotive Human Factors Safety*, 2016.
- [2] A. Firooznia, "Controller design for string stability of infinite vehicle strings," Master's thesis, Eindhoven University of Technology, 2012.
- [3] R. P. A. Vugts, "String-stable cacc design and experimental validation," *TU/e Master's Thesis*, 2010.
- [4] "Intelligent transport systems – full speed range adaptive cruise control (fsra) systems – performance requirements and test procedures," standard, 2009.
- [5] "Dynacar v2.0 - release notes." Tecnia, 2017.
- [6] P. Shakouri, A. Ordys, M. Askari, and D. S. Laila, "Longitudinal vehicle dynamics using simulink/matlab," *UKACC International Conference on Control 2010*, pp. 1–6, 2010.
- [7] "Dynacar - model overview." <http://www.dynacar.es/en/home.php>, 2015.
- [8] H. B. Pacejka, *Tyre and vehicle dynamics*. 2006.
- [9] F. Gao, Y. Zheng, S. E. Li, and D. Kum, "Robust control of heterogeneous vehicular platoon with uncertain dynamics and communication delay," *IET Intelligent Transport Systems*, vol. 10, no. 7, pp. 503–513, 2016.
- [10] "European Road Safety Observatory, European Commission," 2016.
- [11] B. W. Smith, "Human error as a cause of vehicle crashes." <http://cyberlaw.stanford.edu/blog/2013/12/human-error-cause-vehicle-crashes>, 2013.
- [12] R. Rajamani, *Vehicle dynamics and control*. New York :: Springer, second edition. ed., 2012.
- [13] A. Eskandarian, *Handbook of intelligent vehicles*. London: Springer, 2012.

- [14] “Intelligent transport systems – adaptive cruise control systems – performance requirements and test procedures,” standard, 2010.
- [15] Fanping Bu, Han-Shue Tan, Jihua Huang, “Design and field testing of a cooperative adaptive cruise control system,” 2010.
- [16] M. M. J. Piao, “Advanced driver assistance systems from autonomous to cooperative approach,” *Transport Reviews*, vol. 28, no. 5, pp. 659–684, 2008.
- [17] G. J. L. Naus, R. P. A. Vugts, J. Ploeg, M. J. G. van de Molengraft, and M. Steinbuch, “String-stable cacc design and experimental validation: A frequency-domain approach,” *IEEE Transactions on Vehicular Technology*, vol. 59, no. 9, pp. 4268–4279, 2010.
- [18] X.-Y. L. Steven E. Shladover, Dongyan Su, “Impacts of cooperative adaptive cruise control on freeway traffic flow,” *Transportation Research Board*, 2012.
- [19] J. Huang, Q. Huang, Y. Deng, and Y.-H. Chen, “Toward robust vehicle platooning with bounded spacing error,” *IEEE Transactions on Computer-Aided Design of Integrated Circuits and Systems*, pp. 1–1, 2016.
- [20] J. W. Kwon and D. Chwa, “Adaptive bidirectional platoon control using a coupled sliding mode control method,” *IEEE Transactions on Intelligent Transportation Systems*, vol. 15, no. 5, pp. 2040–2048, 2014.
- [21] <http://www.dynacar.es/en/home.php>.
- [22] V. Milanés, S. E. Shladover, J. Spring, C. Nowakowski, H. Kawazoe, and M. Nakamura, “Cooperative adaptive cruise control in real traffic situations,” *IEEE Transactions on Intelligent Transportation Systems*, vol. 15, no. 1, pp. 296–305, 2014.
- [23] J. Ploeg, D. P. Shukla, N. v. d. Wouw, and H. Nijmeijer, “Controller synthesis for string stability of vehicle platoons,” *IEEE Transactions on Intelligent Transportation Systems*, vol. 15, no. 2, pp. 854–865, 2014.
- [24] J. Ploeg, N. van de Wouw, and H. Nijmeijer, “Lp string stability of cascaded systems: Application to vehicle platooning,” *IEEE Transactions on Control Systems Technology*, vol. 22, no. 2, pp. 786–793, 2014.
- [25] S. B. C. Darbha Swaroop, J. Karl. Hedrick, “Direct adaptive longitudinal control of vehicle platoons,” 2001.
- [26] D. Swaroop and J. K. Hedrick, “Constant spacing strategies for platooning in automated highway systems,” *Journal of Dynamic Systems, Measurement, and Control*, vol. 121, no. 3, pp. 462–470, 1999.
- [27] S. E. Li, Y. Zheng, K. Li, and J. Wang, “An overview of vehicular platoon control under the four-component framework,” in *2015 IEEE Intelligent Vehicles Symposium (IV)*, pp. 286–291.
- [28] L. Xiao and F. Gao, “Practical string stability of platoon of adaptive cruise control vehicles,” *IEEE Transactions on Intelligent Transportation Systems*, vol. 12, no. 4, pp. 1184–1194, 2011.

- 
- [29] X. Y. Lu, S. Shladover, and J. K. Hedrick, "Heavy-duty truck control: short inter-vehicle distance following," in *Proceedings of the 2004 American Control Conference*, vol. 5, pp. 4722–4727 vol.5.
- [30] P. Seiler, A. Pant, and K. Hedrick, "Disturbance propagation in vehicle strings," *IEEE Transactions on Automatic Control*, vol. 49, no. 10, pp. 1835–1842, 2004.
- [31] A. Rivas, "Stability and string stability analysis of formation control architectures for platooning." A dissertation submitted for the degree of doctor of philosophy, Hamilton Institute, Maynooth University, Maynooth, 2015.
- [32] F. A. Mullakkal-Babu, M. Wang, B. v. Arem, and R. Happee, "Design and analysis of full range adaptive cruise control with integrated collision a voidance strategy," in *2016 IEEE 19th International Conference on Intelligent Transportation Systems (ITSC)*, pp. 308–315.
- [33] X. Guo, J. Wang, F. Liao, and R. S. H. Teo, "Distributed adaptive integrated-sliding-mode controller synthesis for string stability of vehicle platoons," 2016.
- [34] G. Guo and W. Yue, "Hierarchical platoon control with heterogeneous information feedback," *IET Control Theory Applications*, vol. 5, no. 15, pp. 1766–1781, 2011.
- [35] J. Y. Wang, *Theory of ground vehicles*. New York, N.Y. :: J. Wiley, 3rd ed. ed., 2001.

